WATER VAPOR TRANSPORT THROUGH AN OPENING IN A WALL BETWEEN TWO AIR SPACES AT DIFFERENT TEMPERATURES

by

JEAN PAUL STEELE

B.S., Kansas State University, 1979

A THESIS

submitted in partial fulfillment of the

requirements for the degree

MASTER OF SCIENCE

Department of Mechanical Engineering

KANSAS STATE UNIVERSITY
Manhattan, Kansas

1981

Approved by:

Major Professor

ILLEGIBLE

THE FOLLOWING DOCUMENT (S) IS ILLEGIBLE DUE TO THE PRINTING ON THE ORIGINAL BEING CUT OFF

ILLEGIBLE

TABLE OF CONTENTS

LIST OF TABLES

LIST OF FIGURES

CHAPTER I

INTRODUCTION

1.1 Statement of the Problem

A problem which frequently occurs in air conditioning applications is the desired temperature to which air is to be cooled has a corresponding water vapor saturation pressure less than the water vapor pressure in the air prior to cooling. This means that if the air is to be cooled to the desired temperature some of the water vapor contained within it must be removed. The phenomenon that occurs as air is cooled beyond the point where it becomes saturated with water vapor is familiar as condensation. As air with a constant humidity ratio is cooled, the temperature at which the air becomes saturated, so that condensation occurs upon further cooling, is known as the dewpoint temperature.

Because, as it condenses, water vapor in air is undergoing a phase change, from vapor to liquid or in situations below freezing from vapor to solid, a great deal more energy must be expended to cool air saturated with water vapor than must be expended in cooling air which is not saturated. The portion of a refrigeration cooling load due to condensation of water vapor is referred to as the latent load and the portion of the cooling load that actually causes the temperature of the air to change is called the sensible cooling load. In certain situations the magnitude of the latent load may exceed the magnitude of the sensible load.

Often, because of uncontrolable circumstances, an opening in the wall of a refrigerated air space is unavoidable so that a means of predicting the magnitude of latent load, from air interchange and or vapor diffusion, is desireable. Unavoidable openings may be doors or hatches, which are only used periodically, or continuous openings such as those through which conveyer belts pass, constant access doorways or openings through which ventilation air flows.

This paper develops a model of the air interchange occurring at a rectangular opening in a vertical wall between two air spaces at different temperatures. The model is based on a simple consideration of the driving forces believed to exist and cause convection to occur. Experimental data measuring water vapor transfer between the two air spaces generally supports the simple model theory. Data taken for both natural and combined natural and forced convection through the opening is presented on a normalized set of graphical coordinates designed to establish the actual relationship between the net bulk flow of air through the opening, from forced convection, and the reverse component of flow moving in the opposite direction of the net bulk due to thermally driven natural convection. Test results are presented from six different opening geometries; 6x6x0, 6x12x0, 12x12x0, 12x6x0, 6x6x12 and 12x12x12 inches where the dimensions given are width x height x length. Test results from a variety of conditions, bulk mass flowrates from 0 to 80 lbm/hr, temperature differences across the opening ranging from 0 to 65 °F; typically from 30 to 50 °F; and humidity ratio differences ranging from .0042 to .0090 lbm/lbm, typically .0062 lbm/lbm. Based on the assumption that diffusion, movement of water vapor independent of air movement, is neglible compared with the transport of water vapor from air circulation, this paper seeks to establish a fairly accurate description of the convection occurring at the opening through the experimental water vapor transfer measurments made.

1.2 Review of Previous Work

In an early publication discussing latent refrigeration loads McDermott[1] identified the three basic mechanisms of moisture migration; movement of total volumes, diffusion and hygroscopic action. For water vapor transport by movement of total volumes to occur an interchange of air, infiltration and exfiltration

in which there is an associated humidity difference, must be present somewhere at the boundary of an environemntally controlled space, generally at one or more openings, so water vapor is carried by the movement of air. Diffusion of water vapor occurs because, within the total mixture of air molecules, water vapor molecules randomly collide and migrate due to the kinetic energy they possess. Moisture transfer by diffusion is driven by differences in the concentrations of water vapor molecules within air and can occur in the absence, as well as the presence, of any gross air motion. Hygroscopic action is generally associated with some solid, usually porus, media through which moisture migrates possibly involving adsorption and or absorption by the solid. Frequently all three means of transport occur simultaneously and the presence of the three mechanisms are interrelated. Of these three basic physical mechanisms of vapor transport only two, movement by total volumes and diffusion, are usually significant in the transport of moisture into cold storage spaces the walls of which are generally constructed from or lined with an impermeable material.

Several experimental and analytical studies have been made concerning moisture transfer by pure diffusion and these give rough indications of the expected magnitude of diffusion for certain situations. However it is not possible to isolate the mechanism of vapor transport by air movement alone and there is some controversy as to what conditions must exist for the magnitude of diffusion transport to be neglible compared with transport by air interchange. The development of a physical model describing the process of vapor transport by the combined action of diffusion and air movement is extremely complicated and has yet to be accomplished successfully. Transport of vapor, through openings, by diffusion is believed to become less and less significant, compared with transport by air movement; as air velocities are increased or, for natural convection, as opening size is increased or as the temperature difference between

inside and outside air is increased. The means of moisture transfer believed to be predominant in building spaces with openings of practical size is that by movement of total volumes or infiltration.

In both heating and cooling situations it is desireable to limit, as much as possible, the infiltration of outside air into a controlled environment because of the resulting sensible load, due to a temperature difference between inside and outside air, and because of the latent load, due to a difference in the humidity of inside and outside air. Minimization of vapor infiltration as well as diffusion, in construction, is accomplished by sealing all potential leaks and using water vapor barriers in conjunction with insulation in walls.

As part of an investigation into the effectiveness of vapor barrier material, used as overlapping or near overlapping sheets in building walls, Babbit[2] conducted a study of diffusion of water vapor through a slit in an impermeable membrane. This included experimental data taken using aluminum foil sheets sandwiched between reinforcement to prevent any air interchange and insure the moisture transfer measured was by pure diffusion. Experimental measurements were made similar to building material permeability tests with opening test specimens mounted on glass crystalizing dishes and kept in a humidity chamber for some measured period of time. Results relating diffusion rate to opening dimensions revealed that the length of perimeter of the opening tested was a greater influencing factor than the opening's area in connection with the rate of diffusion through the opening. The theory developed dealt with diffusion path lengths, humidity concentration gradients and three dimensional lines of flow.

Queer and McLauglin[3] investigated, with limited experimental measurements, the transient moisture transfer, under isothermal conditions, into a sealed low humidity room through very small holes from higher humidity surroundings. Because

no temperature difference or net air exchange existed and because of the opening's size the moisture transport was assumed to be due entirely to diffusion. Using a mathematical model differential equation the diffusion rate was solved for as a function of time based on two or more known differences in vapor pressure as boundary conditions. From the developed model estimates were made of the time required to establish humidity equilibrium as well as the necessary net flow of air from the sealed space to suppress any inflow of water vapor. However, no experimental verification of the latter assertion was made and the validity of results is questionable for larger openings or where a temperature difference exists.

Wilson and Novak[4] investigated experimentally the transport of water vapor, by convection and diffusion, as it applied to the problem of condensation between double pane windows. The openings involved, multiple openings with sizes up to 1/4 inch diameter, were for venting and were small enough that, depending on their size and location, vapor transport by diffusion was found to be significant compared with vapor transport by infiltration. The amount of infiltration, or convection, present was found to depend upon the vertical location of the openings relative to each other and relative to the horizontal line of neutral pressure in the space between the two window panes. The study includes measurements of moisture transfer using a mass balance and in some cases a net flow of air through the openings but the main objective was the determination of venting requirements to prevent condensation and not the characteristics of vapor transport through the openings.

In an attempt to determine the extent to which diffusion of water vapor could exist up a moving air stream Davis[5] made an experimental study of humidity conditions in a duct type opening around one foot square. Test results showed that for a flow of air with a velocity of 50 ft/min no significant upstream

moisture migration could be detected. Moisture transfer was not measured directly but was inferred from wet bulb temperature measurements. Complications developed in maintaining low enough air velocities to observe diffusion yet high enough to insure the adiabatic saturation of air in the immediate vicinity of the wet bulb thus making test results somewhat inconclusive.

Investigations of the thermally driven natural convection phenomenon occurring at a rectangular opening between two air spaces at different temperatures[6] and of the heat and moisture transfer occurring as a result of convection interchange through a rectangular opening between two air spaces[7] have been conducted by Brown et al. Convective water vapor mass transfer, depending on humidity difference, was given a consideration analgous to convective heat transfer, depending on temperature difference, but only experimental measurements of heat transfer were undertaken. As a preliminary to these publications a description of the experimental apparatus used to measure heat transfer,[8] an insulated box with two air spaces sharing a common wall and each containing a guarded heat exchanger, was published by Solvason.

The convection study[6] employed emperical development of equations based on the coefficient of convective heat transfer, h_q. Heat transfer correlations were made using dimensionless ratios; the Nusselt number, the Prandtl number and the Grashof number based on density difference. Equations of flow, involving the dimensionless groups, for air interchange through the opening were assumed to be somewhere near the extreme case of frictionless flow, neglecting effects of viscosity, so that $Nu = K\ (Gr)^{\frac{1}{2}}\ Pr$, where $1/3 \leq K \leq 1$. Depending on the values of the Grashof number and the thickness to height ratio for specific situations, slight variations on the equation relating the dimensionless groups were made to give a better fit to the heat transfer data collected. Vapor transfer correlations were assumed to take on a similar form based on the coefficient of

convective water vapor mass transfer, h_m, and using the dimensionless groups; the Sherwood number, the Schmitt number and Grashof number based on density difference. The convective coefficient of mass transfer is related to the convective coefficient of heat transfer, h_q, by the simple expression $h_m = h_q / C_p$ thus $Sh = K (Gr)^{\frac{1}{2}} Pr$.

The study of heat and moisture transfer, due to convection, by Brown et al.[7] through a continuation of the experimental work, measuring heat transfer, in Brown's convection study developed, in graphical and empirical form, ways of determining the convection coefficient of heat transfer sufficiently simple and accurate for use in engineering applications similar to the experimental test conditions for openings in both vertical and horizontal partitions. The equations developed are applicable to natural convection alone with no net airflow through the opening tested although some forced convection data, with air flowing horizontally and parallel to the wall with the opening, was included for comparison. Both publications by Brown, [6] and [7], were based on experimental tests on openings with width and height dimensions of 3x3, 6x6, 6x12, 9x9 and 12x12 inches and values of depth to height ratios of 0.19, 0.25, 0.38 and 0.75. Temperature differences across the openings ranged from 15 to 85 °F and Grashof numbers, calculated with consideration of air temperature and humidity difference, ranging from 10^6 to 10^8. For the conditions in these studies heat transfer through the air by conduction and vapor transfer by diffusion were presumed to be neglible.

In a recent publication Shaw[9] investigated the convection interchange occurring through a large rectangular opening in a vertical partition by both natural convection alone and combined natural and forced convection with a net flow of air passing through the opening by making heat transfer measurments. He extended the work of Brown by introducing a coefficient of discharge that

appeared in the heat transfer equation relating the dimensionless groups as a proportionality constant to adjust the Bernoulli equation for natural and forced convection air velocities through the opening. To correlate the combined interchange of air through the opening due to thermally driven natural convection and a forced convection flow he proposed that two separate discharge coefficient factors be used, the product of which make up the total coefficient of discharge, C, so that $Nu = C/3\ (Gr)^{\frac{1}{2}}\ Pr$ where $C = C_t\ C_v$.

The temperature coefficient, C_t, for the portion of interchange due to natural convection was assumed to vary as a function of the temperature difference across the opening and was determined experimentally from data for natural convection alone since in the absence of a forced air flow the velocity coefficient is constant, $C_v = 1$. The velocity coefficient for interchange due to forced convection flow through the opening could not be experimentally evaluated independently because it was found to vary with both the bulk air velocity through the opening and the temperature difference across the opening. Values of C_t are presented graphically with the temperature difference across the opening as the independent variable and values of C_v are graphed, for various temperature differences and consequently assumed values of C_t, with the bulk velocity through the opening as the independent variable. Experimental measurements of heat transfer and some opening velocity profile measurements were made using two adjoining rooms connected by a door 6.73 feet high with width varied from 3.94 to 35.43 inches and a thickness to height ratio of 0.05. Temperature differences from 0 to 21.6°F were used giving Grashof numbers in the range from 10^8 to 1.3×10^{10} and bulk volumetric flows through the opening ranged from 0 to 11 cfm.

1.3 Scope of Experimental Work in this Study

The primary emphasis of this study was to experimentally determine the effects of various influencing parameters upon the water vapor transport through a rectangular opening in a vertical wall. Variables believed to influence an opening's water vapor transfer characteristics are the temperature and humidity difference across the opening as well as the opening's geometry and the net airflow passing through. Data was taken using a sealed chamber as an open system with the opening being tested and an exit section as locations where air could cross the system's boundaries. Previous work that dealt with heat and mass transfer by convection through openings in walls, by experimentally measuring the heat transfer through an opening, provided the inspiration for a study of opening convection theory by experimentally measuring the water vapor transfer through an opening. The vapor transfer occurring through the opening in the sealed chamber wall was determined by using a mass balance to account for all water crossing the boundaries of the chamber. Measurments of the magnitude of water vapor contained in the air on either side of the opening, as well as in the exit section, were made using an electronic dewpoint measuring device and the net volume of air water vapor mixture passing into the chamber, through the opening, and out of the chamber, through the exit section, was determined with a flowmeter in the exit section.

In order to reduce the data taken; temperatures, dewpoint temperatures, pressure drop through the flowmeter and the humidity generator water consumption rate; to a useable form where a judgment of reasonableness could be made, a unique reduction scheme was devised and is explained in detail in chapter 2. Because the main intention of this study was to make experimental measurements of water vapor transport and the correlation and comparison of data taken using

previously developed reduction techniques was initially considered of secondary importance this method of reducing and delivering data, Chapter 2, was adopted rather than using the conventional dimensionless groups. A physical meaning is generally attached to the classically defined dimensionless ratios; for example Re = inertia forces/ viscous forces, Nu = convected heat transfer/ conducted heat transfer; however, the combinations of dimensionless groups found to correlate data well in previous work have no readily apparant significance in terms of the convection phenomenon that is physically occuring. A comparison of the data taken in this study to the equations involving dimensionless groups is delayed until Chapter 4.

CHAPTER II

THE THEORY FOR DEVELOPMENT OF DATA REDUCTION

An equation is given in the 1977 ASHRAE Fundamentals manual applying to a consideration of two isolated spaces, both containing air but at different temperatures. The spaces separated by a vertical wall and the pressure drop across the wall due to the thermally driven chimney effect.[10] The development of this equation is based on the assumptions that the density or air can be calculated by treating it as an ideal gas and that the air density within each air space at different heights remains constant so the pressure varies linearly with vertical level. These are reasonably valid assumptions for situations where some type of heating or air conditioning is desired in buildings.

The reference level where the pressure difference across the wall is zero is called the neutral pressure line and the absolute pressure at this level, P_n, can generally be assumed to be standard barometric pressure. Figure 1a and 1b show plots of the pressures and pressure difference of two spaces with positively increasing height, h, where the density in space 1 is greater than the density in space 2.

The equations for the pressures within the two spaces as well as the pressure difference can be expressed as follows.

$$P_1 = P_n - h\,\rho_1\,\frac{g}{g_c}$$

$$P_2 = P_n - h\,\rho_2\,\frac{g}{g_c}$$

$$P_2 - P_1 = h\,(\rho_1 - \rho_2)\,\frac{g}{g_c} \qquad (1)$$

where g is the acceleration due to gravity, g_c is a proportionality constant for the units of g and ρ is the density of air.

If the partition separating the two sealed spaces has one or more openings in it an interchange of air between the spaces can occur however if densities within the two spaces remain constant then the net mass transfer of air between the spaces will be zero, $\dot{m}_1 = \dot{m}_2$.

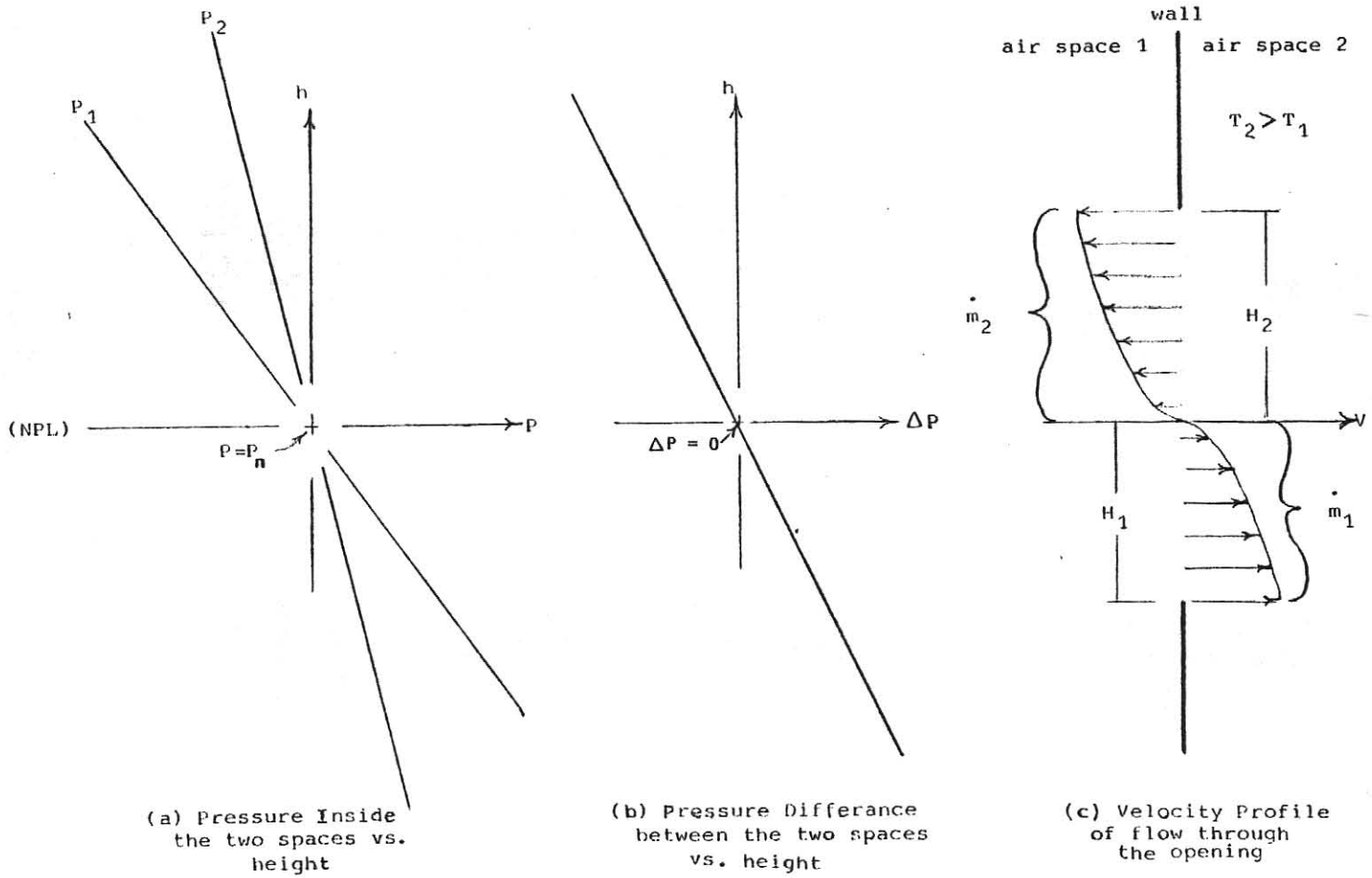

Figure 1

View of Opening's Vertical Profile

From the assumption that the air can be treated as an ideal gas the densities within the two spaces will be inversely proportional to the absolute temperatures within the spaces.

$$\rho_1 = \frac{P}{R T_1} \qquad \rho_2 = \frac{P}{R T_2} \qquad (2)$$

Two qualifying factors necessary for this ideal gas assumption are; (1) within both spaces only small pressure difference exist so the pressures, P, in the density expressions are always near P_n, (2) the effects of changing fractions of water vapor mixed with the air have neglible effects upon the value of R, the ideal gas constant.

From the form of the ideal gas equations used, equation (2), it is implied that the effects upon the air density of different mass fractions of water vapor (different humidity ratios) are neglible compared with the effects, upon the air density, of thermal expansion from the differences of temperatures of the two spaces. A precise accounting of the possible changes in density due to air humidity content that might influence convection transport, as well as the water vapor transport due to diffusion driven by water concentration gradients has not been undertaken due to the added complexity of such an analysis and the negligible increase in accuracy for commonly encountered air conditions.

For a rectangular opening in the vertical partition, (figure 1), if the air exiting space 1 has density ρ_1 and the air exiting space 2 has density ρ_2, where $\rho_1 > \rho_2$, and the net mass transfer between the two sealed spaces is zero then the neutral pressure line, NPL, will fall slightly below the opening's horizontal centerline (figures 1b and 1c). Because of the very small variations of density encountered in reasonable air temperature differences, relative to absolute mean density, and because, for the two air spaces at different humidities zero net mass transfer is an ideal situation, the NPL can essentially be assumed to fall on the opening's horizontal centerline.

By substituting equations (2) into (1) the pressure drop across the wall is obtained in terms of the height, h, and the absolute temperatures in the two spaces, T_1 and T_2.

$$\Delta P(h) = h \frac{g}{g_c} \frac{P_{atm}}{R} \left(\frac{1}{T_1} - \frac{1}{T_2}\right) \qquad (3)$$

By using the Bernoulli steady flow energy equation an ideal air velocity, V, through the opening due to the pressure drop can be expressed.

$$V = \sqrt{\frac{2\, g_c \Delta P}{\rho}} \qquad (4)$$

For actual flow through orifices a coefficient of discharge, C, is frequently included. Substituting an expression for ideal gas density, similar to equation (2), and equation (3) into equation (4) the velocity of air flow through the opening at vertical levels relative to the NPL becomes.

$$V(h) = \sqrt{2\, h\, g\, T \left(\frac{1}{T_1} - \frac{1}{T_2}\right)} \qquad (5)$$

The velocity is positive in the direction from space 1 to space 2 and to avoid complications under the radical sign only the magnitude of h, the distance from NPL, is used. A velocity profile that varies with $\sqrt{h}$ results. (figure 1c)

A determination of the volume of flow occurring above and below the NPL requires integration of the velocity density product for the range of height, h, involved. For a single opening of uniform width and assuming constant density for the range of h the flow above the NPL from air space 2, the hot side, to air space 1, the cold side, is,

$$\dot{m}_2 = W \rho \int_0^{H_2} V dh \qquad (6)$$

where H_2 is the distance from the NPL to the top of the opening.

Substituting equation (5) for velocity as a function of h into this expression.

$$\dot{m}_2 = W\rho\sqrt{2\,g\,T\,(\frac{1}{T_1} - \frac{1}{T_2})} \int_0^{H_2} h^{(1/2)}\,dh$$

$$\dot{m}_2 = W\rho\sqrt{2\,g\,T\,(\frac{1}{T_1} - \frac{1}{T_2})} \left.\frac{2}{3}\,h^{(3/2)}\right|_0^{H_2}$$

$$\dot{m}_2 = \frac{2}{3}\,W\rho\sqrt{2\,g\,T\,(\frac{1}{T_1} - \frac{1}{T_2})\,(H_2)^3} \qquad (7)$$

In a likewise manner the flow below the NPL, from air space 1 to air space 2, can be calculated to obtain.

$$\dot{m}_1 = \frac{2}{3}\,W\rho\sqrt{2\,g\,T\,(\frac{1}{T_1} - \frac{1}{T_2})\,(H_1)^3} \qquad (8)$$

Assuming the air leaving the hot side, above the NPL, has temperature T_2 and density ρ_2 and that the air leaving the cool side, below the NPL, has properties T_1 and ρ_1 the T and ρ in equation (7) would be subscripted with a 2 and in equation (8) they would be subscripted with a 1. In reality some dilution of air of the two extreme densities might be occurring at or very near the opening so the density may even lie in the range between ρ_1 and ρ_2 in the plane of the wall as some algebraically expressible function of h. As a simplifying assumption in this data reduction scheme the average density was used for the entire opening.

For the range of air properties investigated in this study generally the difference in densities encountered were small compared with the mean density so probably only small errors resulted in using the average values of ρ and T, $\bar{\rho}$ and $\bar{T}$.

$$\bar{T} = \frac{T_1 + T_2}{2}$$

$$\bar{\rho} = \left(\frac{P_{atm} - \bar{P}_0}{53.35} + \frac{\bar{P}_0}{85.76} \right) \frac{1}{\bar{T}}$$

$\bar{P}_0$ is the mean vapor pressure averaged from the vapor pressures on both sides of the opening.

$$\bar{P}_0 = \frac{P_{01} + P_{02}}{2}$$

The use of $\bar{\rho}$ and $\bar{T}$ in equations (7) and (8) provide for the definition of a common normalizing factor $\dot{m}'$ to be used for flow both above and below the NPL.

$$\dot{m}' = \frac{2}{3} W \bar{\rho} \sqrt{2 g H^3 \bar{T} \left(\frac{1}{T_1} - \frac{1}{T_2} \right)} \qquad (9)$$

Attention is now directed at situations where a bulk flow of air is made to pass through the opening. If no net mass of air is transferred through the opening, $\dot{m}_1 = \dot{m}_2$, (figure 1c) the NPL is located along the horizontal centerline of the rectangular opening. The effect of forcing a bulk flow through the opening would be the same as shifting the NPL, and consequently the velocity profile, vertically.

As constructed the environmental chamber used in this study was equipped with an exit section with an Annubar flow meter and humidity exit air sample system on the hot side of the partition, in space 2, so that a net bulk flow could be made to occur from air space 1 to air space 2, $\dot{m}_1 > \dot{m}_2$. Since it was assumed previously that $T_2 > T_1$ superimposing a bulk flow upon the natural convection interchange occurring at the opening causes the location of the NPL to shift upward, H_1 increases and H_2 decreases.

If bulk flow from space 1 to space 2 is conventionalized to be positive, same as positive pressure drop, the net bulk flow is the difference between $\dot{m}_1$, equation (8), and $\dot{m}_2$, equation (7).

$$\dot{m}_b = \dot{m}_1 - \dot{m}_2$$

$$\dot{m}_b = \frac{2}{3} W \bar{\rho} \sqrt{2\, g\, \bar{T} \left(\frac{1}{\bar{T}_1} - \frac{1}{\bar{T}_2}\right) \left(H_1^3 - H_2^3\right)} \qquad (10)$$

For a negative flow or if $H_2 > H_1$ this equation loses meaningfulness. The portion of flow that occurs above the NPL from space 2 to space 1 is defined as the reverse flow, equation (8) repeated.

$$\dot{m}_r = \frac{2}{3} W \bar{\rho} \sqrt{2\, g\, \bar{T} \left(\frac{1}{\bar{T}_1} - \frac{1}{\bar{T}_2}\right) H_2^3} \qquad (11)$$

Equation (11) only applies to situations where the shifted NPL remains in the same range of height as the opening. If the NPL is shifted upward until it no longer crosses the opening the water vapor transfer problem is reduced to simple bulk flow, $\dot{m}_r = 0$.

By using the previously defined factor $\dot{m}'$ (9) the normalized bulk flow from equation (10) is

$$\frac{\dot{m}_b}{\dot{m}'} = \frac{\dot{m}_1 - \dot{m}_2}{\dot{m}'} = \sqrt{\frac{H_1^3}{H^3}} - \sqrt{\frac{H_2^3}{H^3}} \qquad (12)$$

and the normalized reverse flow from equation (11) is

$$\frac{\dot{m}_r}{\dot{m}'} = \sqrt{\frac{H_2^3}{H^3}}$$

this can be rearranged to give H_2 in terms of $\dot{m}_r$.

$$H_2 = \left(\frac{\dot{m}_r}{\dot{m}'}\right)^{(2/3)} H \qquad (13)$$

Also for the opening by the constraints of geometry

$$H = H_1 + H_2$$

therefore rearranging and substituting for H_2 from equation (13).

$$H_1 = H - H_2 = H \left(1 - \frac{\dot{m}_r}{\dot{m}'} \right)^{(2/3)} \qquad (14)$$

Equations (13) and (14) can be substituted into (12) to eliminate the H terms and obtain the normalized bulk flow as a function of the normalized reverse flow.

$$\frac{\dot{m}_b}{\dot{m}'} = \left[1 - \left(\frac{\dot{m}_r}{\dot{m}'} \right)^{(2/3)} \right]^{(3/2)} - \frac{\dot{m}_r}{\dot{m}'} \qquad (15)$$

Equation (15) expresses the relationship of $\dot{m}_b$ to $\dot{m}_r$, unfortunately it can not be explicitly solved for an exact expression of $\dot{m}_r$. However the function can be plotted (figure 2), and is relatively simple in the range of interest, $\dot{m}_b \geq 0$ and $\dot{m}_r \geq 0$.

Thus far the equations developed have dealt with the mass flow of air in general. With these natural convection and bulk flow terms and the introduction of humidity ratio w, dimensionless in units pounds mass of water vapor per pound mass of dry air, similar conclusions regarding moisture transfer through the opening due to mass interchange of the air can be drawn. The net moisture transfer through the opening from air flow driven by temperature difference in a development analogous to (10).

$$\dot{m}_{H_2O \text{ net}} = \dot{m}_1 \, w_1/(1 + w_1) - \dot{m}_2 \, w_2/(1 + w_2) \qquad (16)$$

If there was no difference in the temperature of the two spaces and only a bulk flow of air was forced through the opening the moisture transfer would be.

$$\dot{m}_{H_2O \text{ bulk}} = \dot{m}_{da} w_1 \qquad (17)$$

If both the convection phenomenon from temperature difference and a bulk flow are occurring simultaneously then a reverse moisture flow term can be

$$\frac{\dot{m}_b}{\dot{m}'} = \left[1 - \left(\frac{\dot{m}_r}{\dot{m}'}\right)^{(2/3)}\right]^{(3/2)} - \frac{\dot{m}_r}{\dot{m}'}$$

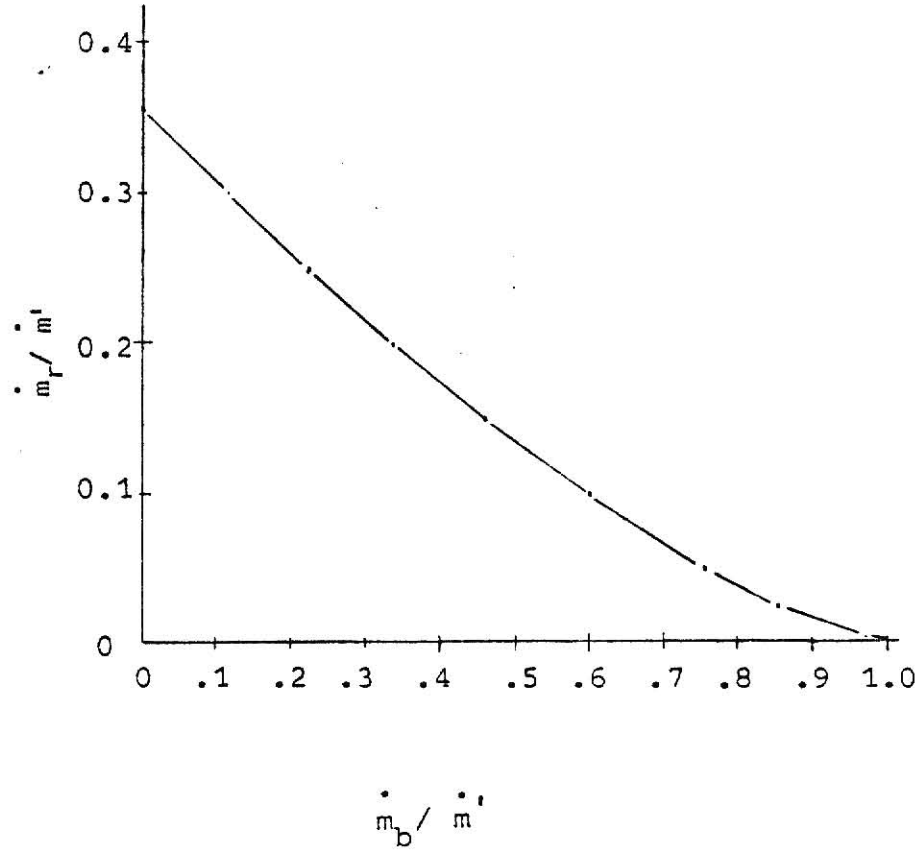

Figure 2

Plot of Normalized Reverse Flow
vs Normalized Bulk Flow

determined using (16) and (17).

$$\dot{m}_{H_2O\ r} = \dot{m}_{H_2O\ b} - \dot{m}_{H_2O\ net}$$

$$\dot{m}_{H_2O\ r} = [\dot{m}_1/(1 + w_1) - \dot{m}_2/(1 + w_2)]w_1 - \dot{m}_1 w_1/(1 + w_1) + \dot{m}_2 w_2/(1 + w_1)$$

$$\dot{m}_{H_2O\ r} = \dot{m}_2(w_2 - w_1)/(1 + w_1) \qquad (18)$$

Since, by nature, warmer air is capable of possessing a higher humidity ratio than cool air, $w_2 > w_1$, the humidity ratio difference is defined, $\Delta w = w_2 - w_1$, similar to the temperature difference used in heat transfer calculations, for moisture transfer calculations. Also since $\dot{m}_2 = \dot{m}_r$ rearrangment of (18) gives.

$$\frac{\dot{m}_{H_2O\ r}\ (1 + w_1)}{\Delta w} = \dot{m}_r \qquad (19)$$

Thus equation (15) may be rewritten as

$$\frac{\dot{m}_b}{\dot{m}'} = \left[1 - \left(\frac{\dot{m}_{H_2O\ r}\ (1 + w_2)}{\dot{m}'\ \Delta w}\right)^{(2/3)}\right]^{(3/2)} - \frac{\dot{m}_{H_2O\ r}\ (1 + w_2)}{\dot{m}'\ \Delta w} \qquad (20)$$

and figure 2 is still applicable.

This relationship describes an ideal moisture situation which predicts moisture flow on a basis of simple bulk air flow.

In this study the reverse flow term was calculated using

$$\frac{\dot{m}_r}{\dot{m}'} = \frac{\dot{m}_{H_2O\ r}}{\dot{m}'\ \Delta w}$$

for the experimental conditions resulting in a constant error of 1 % since w_2 was typically 0.01 lbm/lbm.

CHAPTER III

EXPERIMENTAL APPARATUS

3.1 The Test Chamber

In order to collect data related to moisture transfer and the various factors believed to influence it a sealed test chamber 6 x 12 feet and 6 feet tall was constructed. (figure 3) The data taken using the chamber and accompanying instrumentation was reduced to graphical form using the analysis scheme given in chapter 2.

The chamber was constructed using 1/2 inch plywood and 2 x 4 studs spaced 4 feet apart. To allow access to all parts of the chamber it was erected on legs 20 inches above the floor and both of the six foot square ends were made into bolt on doors. The legs and framework were made reasonably sturdy so that the chamber was capable of supporting in excess of 1000 pounds of metal and humanity as a distributed static load.

To prevent any leakage through seams or penetration or absorption through permeable wood building materials the chamber was lined with 24 gauge galvinized steel sheets with folded over and soldered seams and soldered at all points nailed to the wood. To divide the chamber into two 6 foot cubical spaces strips of sheet metal with 90° folds were soldered to the walls ceiling and floor along which the side panels of the partition, two 2' by 6' sheets of steel, were soldered leaving a 2' by 6' doorway through the center of the partition (illustration 1). The threshold of the doorway in the partition was reinforced with more folded strips of sheet metal soldered to the wall panels. This door frame was later closed off by adhering 2' wide panels of sheet metal, including a panel with the opening to be tested, to it with silicon rubber sealant. The center partition, at all metal union corners, was tin soldered and any welded areas suspected of being a potential leak, generally where warping had occurred, were sealed with silicon rubber from the dry side of the partition.

Two 6 foot square 2.5 inch deep baffles, made from 2 rows of offset 4 inch

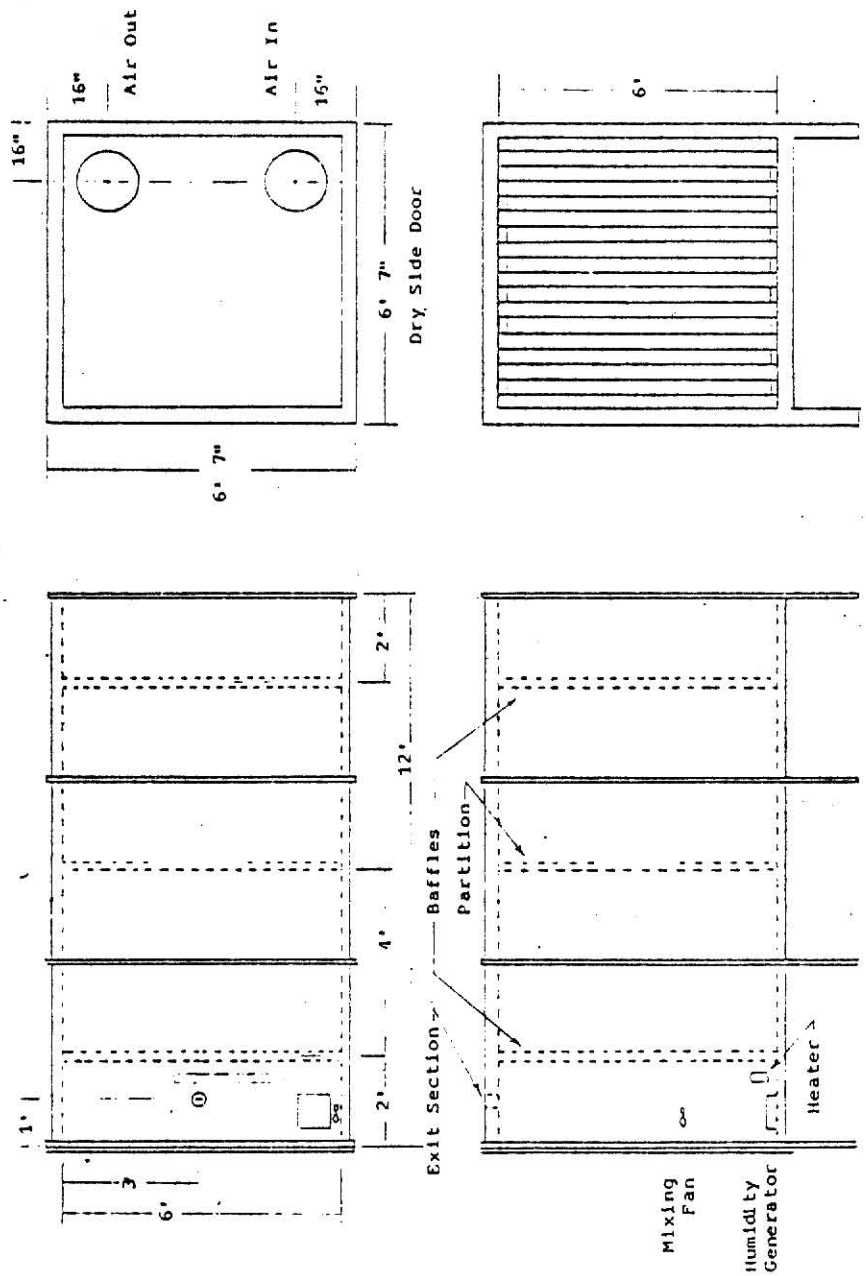

Figure 3

Experimental Chamber Detail

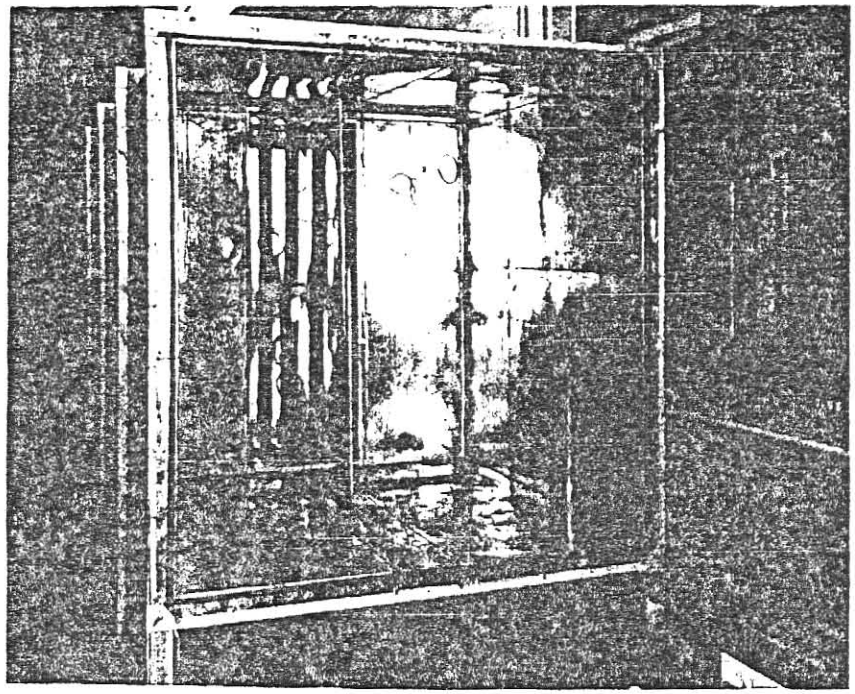

Illustration 1

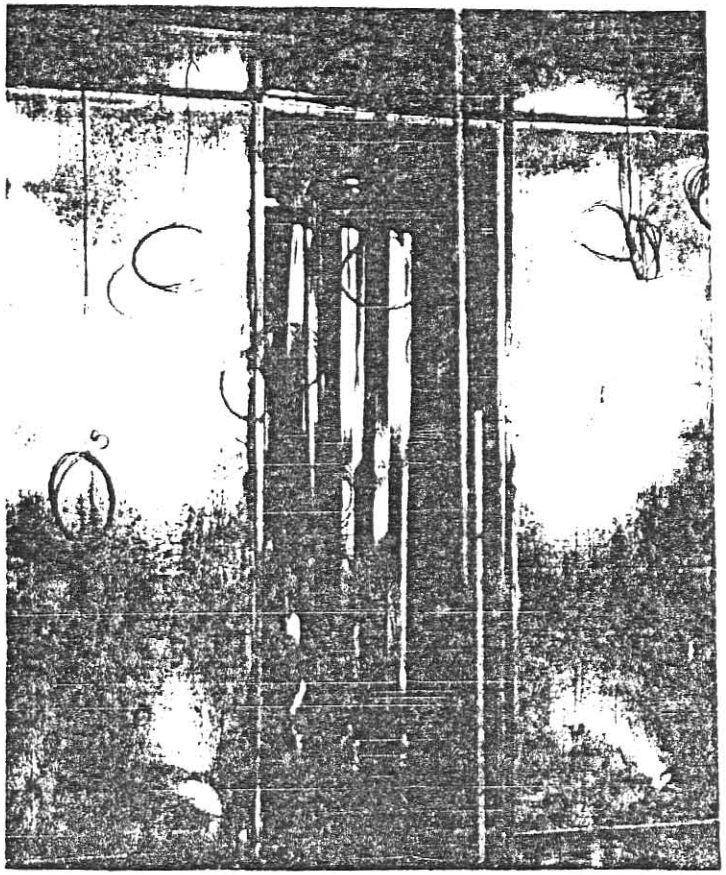

Illustration 2

Photos of the interior of the cool/dry side of the chamber without opening panels or cool/dry side baffle in position. Coils of thermocouple wire are visible prior to potentiometer switchbox connection.

wide strips of sheet metal 6 feet long and spaced on 7 inch centers, were mounted two feet from the doors on both sides of the partition (1 baffle visible in illustrations 1 and 2 through partition doorway). The baffles were used to prevent direct jets of air from impinging on the measuring devices or opening, so a more evenly distributed homogeneous air water vapor mixture was maintained on the warm humid side of the inner partition and in general to minimumize any possible external turbulent or gusty air movement effects upon the phenomenon being measured. Because the baffles needed to be removed to provide periodic access to the partition, brackets that the baffles were bolted onto, were soldered to the sheet metal lining on the ceiling.

The use of any material capable of absorbing water was avoided, whenever possible, on the humid side of the partition because of the critical nature of the mass balance measurements to any unaccounted leakage or water consumption within. Both of the 6' square doors were lined with sheet metal and the chamber door frames were weather stripped with 1/4 by 3/4 inch black foam rubber, (illustration 1.) After all apparatus on the warm humid side of the partition was in place the bolts attaching that door were cinched up so that a visual inspection within revealed no paths for leakage.

The exterior walls floor and roof as well as the sheet metal inside on the dry side of the partition were insulated with 2 inch thick polystyrene foam to limit the heat loss conducted through these areas and prevent condensation that could occur on surfaces cooler than the dewpoint of air. The insulation immediately adjacent to the opening in the partition was beveled at a 45° angle to prevent any thickness effects for openings which were desired to have zero thickness. For those openings where thickness was desired posterboard panels held in place with duct tape were situated as squarely as possible symmetrically with respect to the plane of the partition wall inside the opening. In preliminary

experiments the use of sheet metal panels for opening thickness was found to produce erratic results. Posterboard was selected over metal because of the complicated heat conduction and condensation problem that was believed to be occurring on metal panels of the duct causing erroneous values of the reverse flow to be indicated in the water mass balance determination.

Several holes were drilled through the tin lined plywood walls through which air sampling lines and the humidity generator water line passed (1/4 inch O D copper tube soldered into wall and floor) and where wires for thermocouples of power for the heater, boiler, inside fan and humidity control system sample line pump (1/2 inch O D copper tube soldered into sheet metal and stopped up with caps and silicon rubber sealant). Within the chamber 1/4 inch I D flexible clear aquarium tubing that slid over the copper tubing passing through the floor was used to make positioning and movement of the humidity sample inlets easier. The samples were pulled through the dewpoint instruments using aquarium pumps which were sealed into airtight metal containers. Outside the chamber the 1/4 O D copper tube sampling lines leading to and from the hot side, for both the humidity control and humidity measurement systems, were provided with electric heat tapes and insulation to prevent their walls from becoming cooler than the dewpoint of the sample flowing inside the lines and cause condensation from the sample to occur.

For measurement conditions where a bulk flow of air was to pass through the opening an exit section was installed through the roof of the humid side of the chamber in the space between the baffle and the door. In order to calculate the amount of water that was carried out with the bulk flow of air exiting through the section a dewpoint temperature sampling line, channel 1 on the humidity measurement system line selector, tapped off of the exit section.

The temperature within the hot side of the chamber and, later on, the

temperature difference between the hot and cold side of the partition was maintained using a 3 setting floor space convection heater whose power was regulated using an on-off controller the input to which was provided by thermocouple output. Initially the heater was controlled relative to a constant temperature reservoir external to the chamber, the thermocouple reference junctions in a constant temperature ice or water bath, in tests where the humid half of the chamber was sealed up completely and the air within was brought up to warm and humid conditions to determine the magnitude of unavoidable leakage present. The ease of achieving nearly steady state conditions as well as the desireability of a nearly constant temperature difference between the two sides of the chamber made control relative to the temperature difference appealing. The temperature difference was measured by placing the thermocouple reference junctions inside the cool and dry side of the chamber and stringing the measuring junctions through the opening to the hot side. In this configuration the temperature on the cool and dry side was controlled by regulating the air supply loop temperature output and the temperature in the hot and dry side was controlled by setting the desired magnitude of temperature difference on the heater controller.

The humidity control system used a Cambridge model 990 dewpoint hygrometer which measured the dewpoint of a sample of the air within the humid side of the chamber and displayed, with a meter, the dewpoint temperature in degrees C or F. For this application and the range of dewpoint temperatures anticipated the accuracy of the instrument was given as ± 1° C and the response time as 0.5° C/sec. However the output signal to the instrument's meter, proportional to the measured dewpoint temperature, was tapped and amplified to give a millivolt input for the on-off controller and damping in the form of a capacitor was installed to smooth out oscillations of the humidity system that probably affected these specifications.

The humidity generator consisted of an electric skillet thermostatically

controlled and set to 350° F which had water piped to it from a gallon jug reservoir the flow from which was regulated by a solenoid valve activated by the humidity on-off controller. To prevent a humidity build up in areas immediately adjacent to the generator a small mixing fan was installed on the wall above the skillet.

3.2 The Air Supply

The air supply loop (figure 4) was designed as a source of air at constant temperature and with constant water vapor pressure. It was used to maintain cool and dry air conditions within half of the experimental chamber. As used for this study the supply loop was in an open configuration since the air exiting the experimental chamber was dumped directly out to the atmosphere rather than being returned to the fan intake. Upstream of the loop's primary air mover a venetian blind type air regulator was installed to aid in controlling the flow of air to the fan. After passing through the shutter the air was drawn to an 18 inch diameter duct at the fan's inlet. The air flow through the loop was moved by a centrifical airfoil blower with a 16 inch diameter rotor and powered by a 115 volt induction motor rated at 1/3 Hp at 1785 rpm. Prior to exiting the blower the air flowed through a transition duct from 16x18 inches to 15.5x22 inches which comprised the length of the loop's horizontal ductwork and was sized to directly fit the evaporators. After exiting the transition the air was passed vertically through the loop's primary refrigeration system evaporator through a 90° rectangular elbow and through a variac controlled 6.7 kw duct heater.

The primary refrigeration evaporator was located in the supply loop to facilitate rehumidification of the cooled supply to achieve a higher degree of control over air conditions as well as provide a large cooling capacity for extreme cold or dry conditions. However the primary system was not used in this study because of complications in the plumbing and separate compressor and

All dimensions in inches.

Scale: 1 foot = 3/8 inch

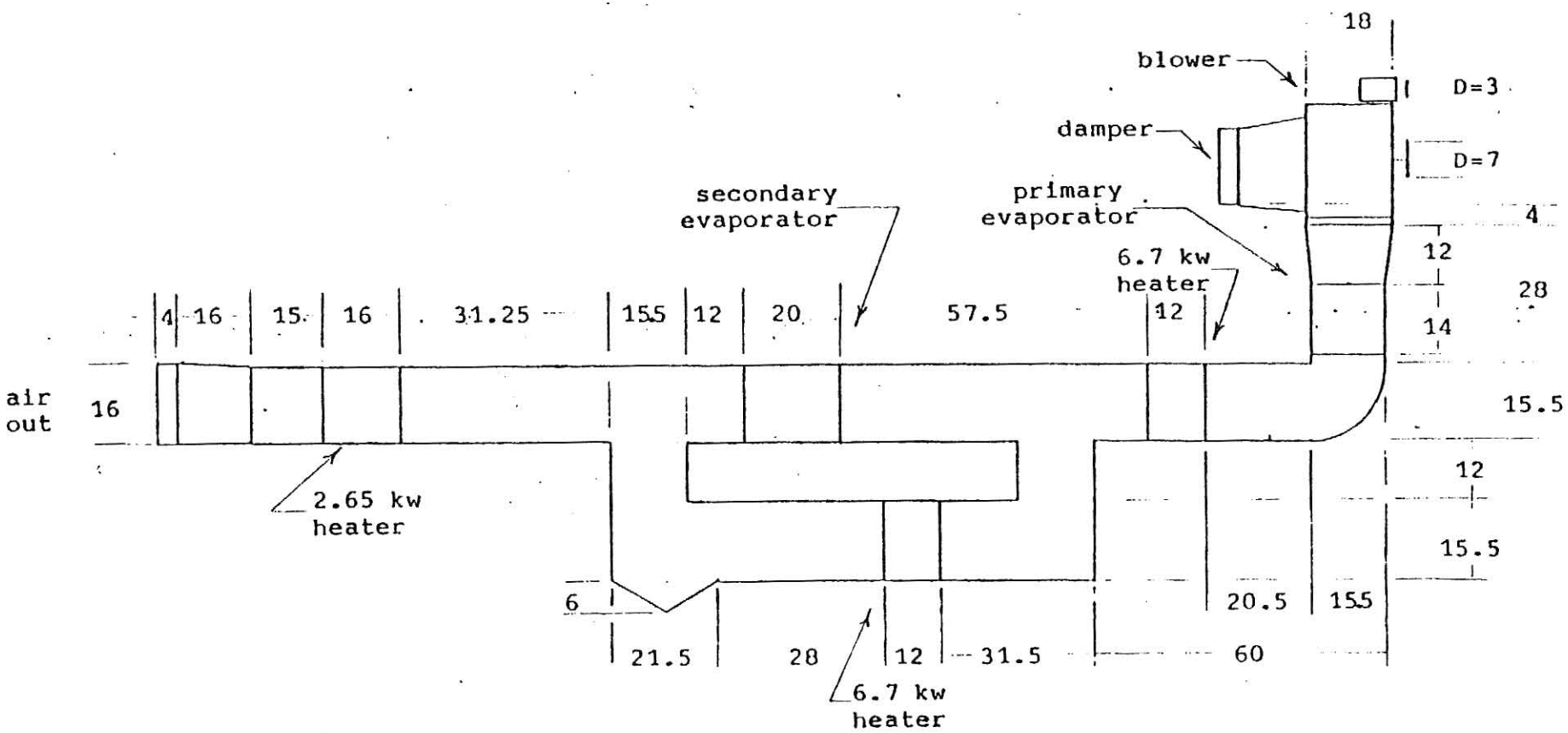

Figure 4

The Air Supply Loop

because a secondary refrigeration unit, the evaporator for which was located down stream from the rehumidification bypass intake, was installed and made operative.

The secondary refrigeration unit was driven by a 46,231 Btu/h Tecumseh compressor unit with the electric motor hermetically sealed inside. The system rejected heat to utility water supply which was drained to the sewer. This refrigeration system had sufficient capacity to maintain desired temperature conditions for this study (around 1000 cfm and 40F) and, in fact, required a hot gas bypass to prevent underloading due to low air flow at the evaporator. Because of the arrangement of the secondary cooling unit and the rehumidification section (figure 4) in situations where the ambient air dewpoint temperature was below the refrigeration evaporator temperature, direct control of supply air humidity was not possible. Whenever this problem occurred it was usually overcome by opening windows for fresh supply of relative constant humidity outside air.

To maintain constant supply outlet temperature and to accomplish any further reheating desired a 2.67 kw duct heater with a proportional controller was installed in the last stage of the supply loop. Specifications for the RFL Model 760 temperature controller claim an accuracy of ± 0.1° C although on certain occasions the downstream air temperature seemed to drift away from the set value.

To deliver the supply air to the test chamber a 16 inch diameter fiberglass insulated flexible duct was attached with a transition to the supply loop and the other end to the chamber inlet so that no rigid connections constrained access to the dry side chamber entrance. To help regulate the flow and attempt to limit turbulent conditions within the chamber adjustable dampers were installed at the delivery and exhaust ports on the dry side of the chamber.

3.3 Data Measurement

The amount of water that was consumed by the humidity control system in maintaining the air conditions within the humid half of the chamber was measured by hand with a 100 ml graduated cylinder as the glass gallon jug reservoir, fixed to the chamber with supply line to humidity generator, was refilled to the same level as when time measurements originated.

To more precisely determine the interval of time involved in the calculation of the rate of water consumption instants of time were recorded just as the solenoid water valve was activated, at the low point of the oscillation of the dewpoint conditions within the chamber.

To some extent the magnitude of the oscillation of dewpoint conditions within the chamber, and the length of time the water solenoid valve remained activated, could be controlled by regulating the flow rate that occurred instantaneously through the water feed line, when it was open, with a needle valve installed in the line. If the instantaneous flow rate through the needle valve dropped below the consumption rate necessary to maintain conditions within the chamber the solenoid valve would never shut off and conditions would not be maintained.

In a likewise manner the frequency of oscillation of switching of the temperature difference controller could be limited by lowering the amount of power to the heater with the three position, 500, 100 and 1500 watts, switch but the power input could not fall below the heat input necessary to maintain temperature conditions.

In order to measure the variables believed to influence the moisture transfer through the opening, the air temperature in the spaces on either side of the opening and consequently the air temperature difference across the opening, T_1 T_2 and ΔT, the humidity of the air in the spaces on either side of the opening and consequently the humidity difference across the opening, w_1 w_2 and Δw, as

well as the net airflow through the opening, m_b , measuring devices were located at various points in and on the test chamber.

Air temperatures within both sides of the chamber were measured with arrays of 8 copper constantan thermocouples located centrally in a plane one foot away from the partition, figure 5. Thermocouple voltages were measured with a Leeds and Northrup millivolt potentiometer with reference junction compensation using a mercury in glass thermometer.

Dewpoint measurements were made with a digital readout E G and G chilled mirror dewpoint testor. Eight sampling line intakes were located at various points on both sides of the partition to determine the dewpoint of air on the hot and cold sides of the partition as well as the dewpoint of the air exiting the hot side for bulk flow cases (figure 5 where H's preceding numbers signify humidity sample locations.) The 8 dewpoint sample lines were routed through a channel selector system prior to the single line into the testor. Because the sampling lines were relatively long the time constant for the humidity measurement system to respond to a change in sampling lines was too long to allow a sufficient determination of every line thus the data collected in this study contains humidity samples from the exit section, channel 1, and along the chamber's lengthwise axis of symmetry 2 feet away from the opening on the humid side of the partition, channel 3, and on the dry side of the partition, channel 7 (figure 5).

The volume of flow through the exit section and, as a consequence, the mass of the bulk flow through the opening in the partition were measured with a 1.049 inch Annubar flowmeter and a micromanometer. The annubar was calibrated with a bell prover, calibration data Appendix B and figure 19. Errors that occurred in measurement of the bulk flow lowered the accuracy of results of correlations made for a net bulk flow through the opening, however no alternative means of measurement were available.

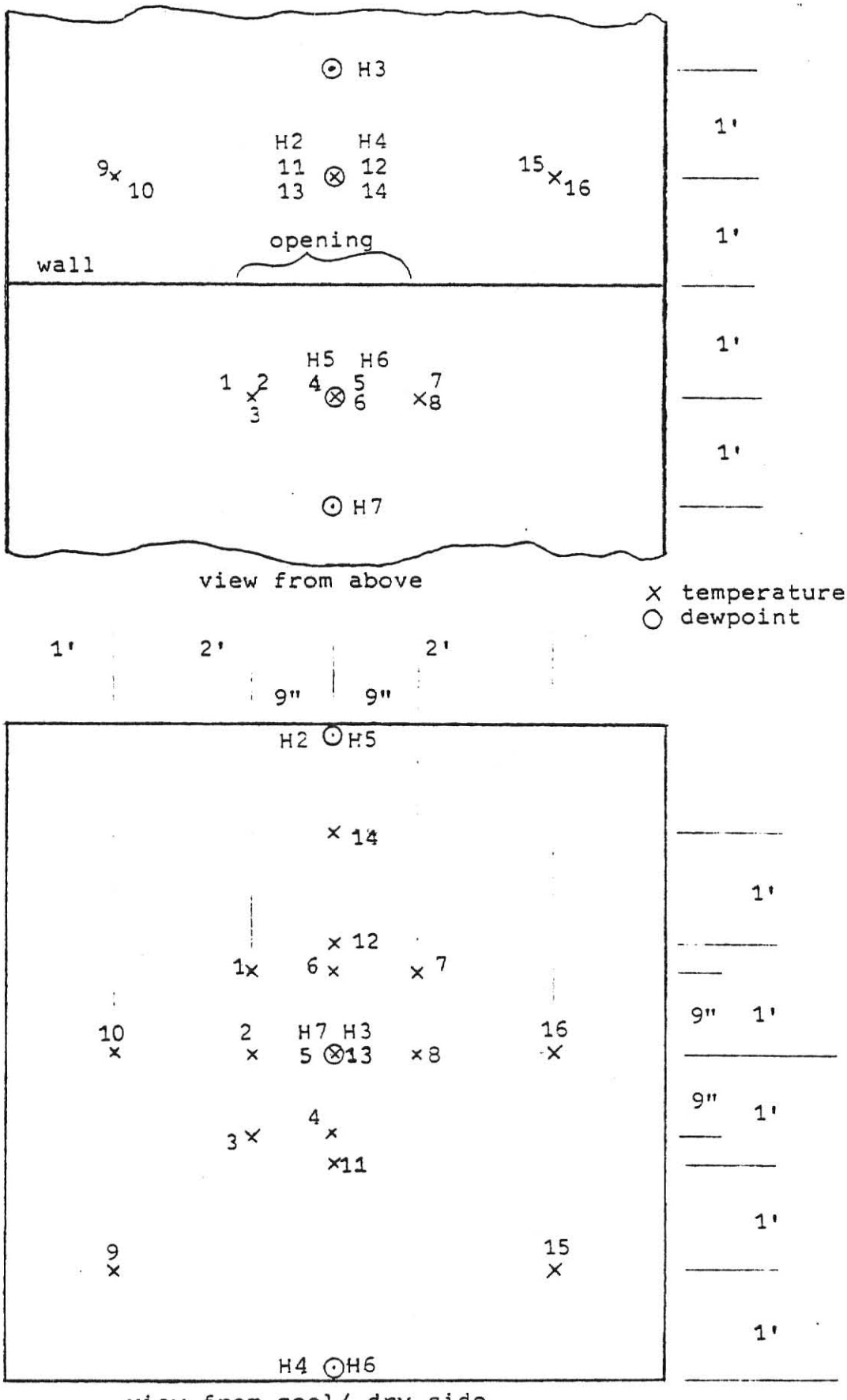

Figure 5
Instrumentation Location

After preliminary testing with a bulk flow through the opening, it was observed that the partition wall flexed easily and that flow through the opening pushed by the supply loop blower required pressurization of the chamber and exhibited some pulsating effects, a small centrifical fan to draw the air from the hot side through the exit section and flowmeter was installed. The flow through the exit section and flowmeter was regulated with a damper in the air line and by varying the looseness of the connections to the fan intake downstream of the flowmeter. Addition of the downstream fan gave greater bulk flow capacity, needed for larger openings, as well as having a steadying effect upon the air flow and the pressure drop registered on the micromanometer.

To try to determine how much variation in turbulent air velocities was occurring within the chamber adjacent to the opening for different test conditions, an anemometer was mounted 18 inches away from the opening on the lengthwise axis of symmetry on the dry side. The anemometer was positioned on one of the aluminum racks which held the thermocouples and dewpoint sampling lines in place and it was oriented so it would measure vertical air velocities.

3.4 Data Procedure

Prior to taking data the chamber required a sufficient time to come to steady state conditions on both sides of the partition. To bring the temperature within the warm and cold sides of the chamber to levels to achieve the desired temperature conditions and then maintain these temperatures fairly constantly the chamber heater, supply loop refrigeration system and duct reheater with sensor and control were all used to whatever extent was necessary. Depending on the temperatures involved both sides of the chamber could take as long as 2 hours to come to thermal equilibrium. The establishment of humidity conditions within the chamber did not require this much time but it was necessary to follow a start up procedure to prevent an unstable response by the humidity control system.

The first step in starting up the humidity control system was turning on power to the electric skillet and the dewpoint hygrometer as well as the bread-board for amplification of the controller input. After the dewpoint hygrometer was warmed up and the sample line pump for the control system turned on, the water line valve controller could be switched on although humidification could only take place if the skillet surface had reached boiling temperature usually taking about five minutes. In addition the heat tapes warming the humidity control sample lines needed to be turned on.

After the temperature difference and humidity conditions were reasonably well established, data collection could begin by recording the time at which the water valve was activated if prior to its activation the water reservoir had been filled to the reference level. The water consumption rate was periodically checked throughout the test by measuring the volume necessary to refill the water reservoir to the level at which time measurement originated and recording the time at which the water valve was activated. These checks helped assure a reasonably uniform rate of consumption. A typical set of data on the standard format sheet as well as the accompanying reduction is given in table 1.

The dewpoint temperatures from the humid side and the dry side of the opening were monitored from channels 3 and 7, respectively, and for data with a bulk flow leaving the humid side of the chamber through the exit section channel 1 was also monitored. Because of the time lag involved in switching channels and because of the oscillatory nature of humidity conditions each individual measurement required anywhere from 5 to 30 minutes to establish during which time other data measurements could be made. Using a strip chart recorder on the output of the humidity measuring system it was determined that the oscillations of conditions within the chamber were fairly regular and repeatable if sufficient time was provided between sample line switchings to purge effects of the previous

sample. The amount of time necessary for this depended somewhat on the difference between the currently and previously measured dewpoints. Generally for each humidity check made 3 dewpoints, 2 extremes and a representative value were recorded. Ultimately for the reduced data point the dewpoints for the entire test period were averaged for an effective value. These effective average dewpoints (saturation temperatures) were used with the steam tables to find the partial pressure of water vapor and with knowledge of total atmospheric pressure the humidity ration could be determined using ideal gas laws. The humidity ratios in the air on both sides of the opening as well as of air leaving through the exit section were used in the mass balance calculations.

Initially, for temperature measurements, a thermocouple strip chart recorder with constant voltage source was used, capable of monitoring all 16 junctions, that took readings systematically enough to establish that temperature oscillations within the chamber, due to switching of the on-off controller, were of neglible magnitude and that only periodic temperature measurements were necessary. Later the thermocouple strip chart recorder was abandoned because of the difficulty in calibration and random drift oscillations taking place perhaps due to electrical noise from devices within range of the thermocouple wire. Since the conversion of thermocouple millivolt outputs to temperature scale took place using a table and the measurements from each junction stayed within a fairly small range the millivolt outputs for each separate location were averaged over the several periods of time and then these average millivolt values were converted to temperatures. The average temperature on the cold side of the chamber was determined as the average of junctions 1 through 8 however because of close proximity effects of the opening to junctions on the warm side of the chamber, a cool draft of air from flow through the opening upon junctions centrally located, the average hot side temperature was determined as the average

of the temperatures of junctions 14, 15, and 16 only (figure 5). These temperatures were used to compute air densities in the hot and cold side of the chamber.

At least twice during the period of data collection the anemometer was turned on and balanced and observed long enough to obtain rough maximum and minimum and a representative value of the randomly occuring velocities being measured. Generally these values never exceeded 30 fpm and in most cases were in the upper teens to lower twenties. A direct correlation of anemometer readings made to vapor transport has not been made although intuitively turbulent air movement inside the chamber should have some effect on the convection and water vapor transport at the opening and by limiting the magnitude of its presence some further insight into the significance of the results obtained might be gained.

The pressure drop through the flow meter and the temperature of air passing through the flowmeter were recorded at intervals between other data acquisitions. The micromanometer was zeroed at the beginning and end of each test whenever possible and the temperature, taken with an electronic temperature sensor, was used to determine the density of the air passing through the flowmeter. The barometric pressure was determined at least once each day and often once for each test if it was observed to be changing rapidly.

Table 1
Typical Data Sheet

Test Section: 6" x 12" x 0 mid Date: Jan 9, 1981 Initials:

	273.7	275.7	270.4		P_0	Total/Avg	
Time	11:44:39	12:33:06	1:15:58	1:50:22	273.5=	0.60236 $^{ibm}/_{hr}$	
H_2O		221	197	155			ibm
$T_{dp\ 1}$	13.8 - 15.5 14.8	13.6 - 15.1 14.7	13.7 - 15.4 14.8	13.7 - 15.3 14.5	34.653	58.235	F
3	14.4 - 15.2 14.8	14.0 - 15.1 14.7	13.9 - 15.1 14.7	14.0 - 15.0 14.6	34.77	58.235	F
7	2.4-3.3/2.9	2.5 - 3.5 3.0	2.5 - 3.6 3.0	2.6 - 3.5 3.1	15.823	37.385	F
T1	.385	.308	.370	.380	.37875	49.620	F
2	.375	.380	.370	.380	.375	49.620	F
3	.395	.400	.385	.385	.39125	49.364	F
4	.395	.400	.385	.385	.39125	50.102	F
5	.390	.400	.385	.380	.38875	50.102	F
6	.390	.390	.380	.380	.385	49.989	F
7	.390	.395	.380	.390	.38875	49.818	F
8	.415	.420	.405	.410	.4125	49.989	F
9	1.545	1.575	1.550	1.530	1.550	51.068	F
10	1.780	1.815	1.790	1.785	1.7525	101.43	F
11	1.785	1.830	1.820	1.785	1.805	111.77	F
12	1.540	1.555	1.580	1.535	1.5525	112.30	F
13	1.755	1.780	1.785	1.765	1.77125	101.54	F
14	1.815	1.840	1.840	1.835	1.8325	110.99	F
15	1.575	1.585	1.605	1.560	1.58125	113.48	F
16	1.755	1.755	1.780	1.800	1.7725	102.76	F
T meter ^0C	39.6	40.1	40.2	40.0	39.925	110.99	F
(Delta) P (in H_2O)	1.207	1.203	1.201	1.202	1.20325	103.96	F

$P_{atm:}$	29.33	in. V turbulence	11-21/17 fpm.		(Delta)T set	4.7	mv.
^{T} cold	50.014	F	^{T} hot 09.08	F	(Delta) T	59.06	F
510.014		R	569.08	R			

Typical Data Sheet Reduction

Table 1
(continued)

The water consumption rate for the entire test, $\dot{m}_{H_2O}$.

$$\dot{m}_{H_2O} = \frac{573 \text{ ml}}{2.095 \text{ hr} \times 454 \text{ ml/lbm}} = 0.60236 \text{ lbm/hr}$$

The atmospheric pressure, P_{atm}.

$$P_{atm} = \frac{29.33}{29} \times 2051 = 2074.34 \text{ lbf/ft}^2$$

For the air passing through the flowmeter $T_{meter} = 563.96\ ^\circ R$

$$\rho_{meter} = \left(\frac{2074 - 34.65}{53.35} + \frac{34.65}{85.76}\right) \frac{1}{564} = 0.0685 \text{ (lbm/ft}^3\text{)}$$

$$w_{meter} = \frac{34.65}{2074 - 34.65} \times 0.6234 = 0.01059 \text{ (lbm w v/lbm da)}$$

With an average $\triangle P = 1.203$ from the flowmeter calibration graph an effective value of c = 0.0605 is determined so the mass flowrate of dry air passing in through the opening and out through the meter is

$$\dot{m}_{da} = \frac{((.0685)\ 1.203/\ .0605)^{\frac{1}{2}}}{1 + .01059} = 1.155 \text{ (lbm/min)}.$$

The 2 humidity ratios and the humidity ratio difference are

$$w_1 = \frac{15.82}{2074 - 15.82} \times .06234 = .00479$$

$$w_2 = \frac{34.77}{2074 - 34.77} \times .06234 = .01063$$

$$\triangle w = w_2 - w_1 = .00584 \text{ (lbm w v/lbm da)}.$$

The reverse flow of water through the opening

$$\dot{m}_{H_2O\ r} = .60236 - 1.155(.01059 - .00479)60 = .20042 \frac{\text{lbm}}{\text{hr}}$$

Typical Data Reduction

Table 1
(continued)

The bulk flow through the opening, $\dot{m}_b$, is

$$\dot{m}_b = 1.155(1 + .00479)60 = 69.632 \text{ (lbm/hr)}$$

For the opening the average temperature and vapor pressure are

$$\bar{T} = \frac{569.08 + 510.01}{2} = 539.55 \ ^\circ R$$

$$\bar{P}_0 = \frac{15.82 + 34.77}{2} = 25.30 \text{ lbf/ft}^2$$

The average density and $\dot{m}'$ are

$$\bar{\rho} = \frac{2074 - 25.30}{53.35} + \frac{25.30}{85.76} \quad \frac{1}{539.55} = 0.07172 \text{ lbm/ft}^3$$

$$\dot{m}' = \frac{2}{3}(0.5 \text{ ft})(.07172)\sqrt{64.4(539.6)1^3\left(\frac{1}{510.01} - \frac{1}{569.08}\right)}$$

$$\dot{m}' = 228.88 \text{ lbm/hr}$$

The normalized flow parameters are;

$$\frac{\dot{m}_b}{\dot{m}'} = \frac{69.632}{228.88} = 0.3042$$

$$\frac{\dot{m}_{H_2O\ r}}{\Delta w\ \dot{m}'} = \frac{.20042}{(.00584)(228.88)} = 0.150$$

$$\frac{\dot{m}_{H_2O\ r}}{\dot{m}_{H_2O\ b\ open}} = \frac{.20042(1/60)}{(1.155)(.00479)} = .6036$$

$$\frac{\dot{m}_{H_2O\ r}}{\dot{m}_{H_2O\ b\ meter}} = \frac{.20042(1/60)}{1.155(.01059)} = .2731$$

CHAPTER IV

PRESENTATION OF DATA

4.1 Graphical Presentation of Experimental Data

The detection of any significant trends resulting in changes of the variables believed to effect water vapor transport, from the data taken, was not an entirely straight forward process. A means of reducing the data to a graphable form which took into consideration some of the different measurable influencing factors became desireable. The reduction scheme employed was derived by a fairly simple consideration of the convection transport phenomenon occurring at the opening, Chapter 2.

The sizes of openings used were chosen as convenient, all dimensions either 6 or 12 inches. The effect of the opening's size upon the amount of bulk air flow that was necessary to be drawn out through the flowmeter by the exhaust fan was not predetermined. After several tests had been made a modification of the fan equipment in the exit section was made to extend the range of bulk flow available, necessary for openings larger than 6x6 inches. After this modification was made there was not sufficient time to reinstall each opening to be retested but all zero length openings appear to have results that compare fairly favorable in the low to mid range of bulk air mass flowrate.

After the data reduction described in Appendix A was performed on each test, a graph of the data points obtained was made for each opening. These standard format graph sheets with identical scales of the ideal normalized bulk, $\dot{m}_b / \dot{m}'$, and reverse, $\dot{m}_r / \dot{m}'$, flow relationship (Chapter 2 equation (15)) and the openings' actual data points plotted with values of ΔT for reference along with supplemental graphs with enlarged scales for the two openings tested with length are given in figures 6 through 13 where the opening dimensioning convention used is WxHxL. A plot of the data from all zero length openings is shown in figure 14 and again in figure 16 with a curve showing the expected

magnitude of the limit of error possible in $\dot{m}_r/\dot{m}'$ as a function of $\dot{m}_b/\dot{m}'$ the value of which is added to, and subtracted from, an experimental data point's value of $\dot{m}_r/\dot{m}'$ with the same corresponding $\dot{m}_b/\dot{m}'$. Plots of the limit of error curves determined for the two openings with length, the 6x6x12 and 12x12x12 inch openings, are shown separately in figures 17 and 18.

4.2 Conclusions and Observations from Graphical Reduction

In the test proceedure each opening was given a zero or very low net air flow test to establish the magnitude of $\dot{m}_r/\dot{m}'$ at $\dot{m}_b/\dot{m}' = 0$ for two different values of ΔT. Generally, for all openings with zero length but with different width and height dimensions, both values of ΔT gave very similar values of intercept locations, average $\dot{m}_r/\dot{m}' = 0.25$ and all within roughly 15 percent of this. Tests with a bulk flow through the opening for data points with low values of $\dot{m}_b/\dot{m}'$, below 0.35, were made until the maximum value obtainable, because of airflow limitations or opening size, was reached. For the preliminary tests, before the exhaust fan was modified, higher values of $\dot{m}_b/\dot{m}'$ were achieveable for the 6x6 inch opening because of its reduced area compared with other openings.

By increasing the bulk flow through the opening the reverse flow is made smaller and by increasing the temperature difference across the opening the potential for reverse flow, through increased natural convection, is made larger. For openings with zero length, figures 6-9 and 14, the graphs for rectangular and square openings appear nearly to coincide on a curve paralleling the plotted ideal. This gives an encouraging impression of the situation described in Chapter 2 and the $\dot{m}'$ model developed with a consideration of $H^{3/2}$ and $\sqrt{1/T_1 - 1/T_2}$. An actual curve visualized in the vicinity of experimental data points is conservative compared with the ideal curve, the actual $\dot{m}_r/\dot{m}'$ are less than ideal for particular $\dot{m}_b/\dot{m}'$. This is probably due to, in the

ideal curve development, the neglect of viscosity effects of the flow moving immediately adjacent to the opening's boundaries and the neglect of mixing effects where the flows in both directions are immediately adjacent to each other.

From plots of the data for 12x6x0 and 12x12x12 inch openings alone it appears that some data points with higher values of ΔT lie closer to the ideal case curve, with larger $\dot{m}_r / \dot{m}'$, than points with smaller ΔT. For the large part the randomness of the locations of points with large and small values of ΔT indicates that the model developed fairly effectively compensates for different ΔT and that the scatter of actual data points is caused by something else. From the error analysis, Appendix B, the largest contributions to the expected error in the reverse flow are due to the uncertainties in the magnitude of the bulk flow and in the two humidity ratio differences involved. The scatter apparant in the general zero length curve of data points seems reasonable in light of the error analysis results however both openings with thickness, length, display considerable scatter at low $\dot{m}_b / \dot{m}'$ and suggest that some contribution in their error analysis might have been overlooked.

As part of the study an investigation of the effects of length added to openings with ratios of length to height or length to width other than zero was conducted. The predominant observable trend that results in length addition is the significant reduction in the magnitude of the reverse flow, figures 10 and 12. The distance from the actual curve to the ideal curve, for the graph of $\dot{m}_r / \dot{m}'$ versus $\dot{m}_b / \dot{m}'$, is increased and some distortion of the curve slope appears to take place with increasing length to height ratios. Comparing the square openings with and without length in no net bulk flow situations, $\dot{m}_b / \dot{m}' = 0$, for the 12x12x12 inch opening the magnitude of $\dot{m}_r / \dot{m}'$ is roughly 1/2 the magnitude of the 12x12x0 inch opening with an increase in L/H from 0 to 1 and for the 6x6x12 inch opening the magnitude of $\dot{m}_r / \dot{m}'$ is

around 40 percent of the magnitude of the 6x6x0 inch opening with an increase in L/H from 0 to 2.

Although data for different opening geometries with length is scant, one observation about the use of length in an opening to reduce reverse flow can be made. The length to height ratio, L/H, of the 6x6x12 and 12x12x12 inch openings are 2 and 1 respectively but the increased reduction in reverse flow for the increase in L/H is not linear since the curve on the graph for the 6x6x12 inch opening, figure 10, is not 1/2 the magnitude of the curve for the 12x12x12 inch opening, figure 12. This might suggest that in using length to reduce reverse flow in practical applications a point of diminishing marginal return is reached for increasing L/H. The results for openings with length are incomplete and inconclusive until further study of other geometries can be made.

The data taken for the 6x6x12 inch opening has data points of $\dot{m}_b / \dot{m}'$ greater than 0.2 that appear to have increasing values of $\dot{m}_r / \dot{m}'$. This is believed to have occurred because the panels used as the duct walls to give the opening length were made from sheet metal and heat conduction through these panels was allowing condensation of water vapor from air in the hot/humid chamber to occur. This prompted a change to be made in the material used for adding length to openings to posterboard since using metal panels added the restriction of keeping the dewpoint temperature on the humid side below the temperature on the cool side of the opening.

In some practical application problems involving an opening in a wall of an environmentally controlled, refrigerated, air space it might be necessary to, given air and opening conditions, either estimate the expected amount of flow into the space through the opening, the reverse flow, or determine the amount of bulk flow, out of the space through the opening, necessary to suppress the occurance of any inward, reverse, flow. The parameter $\dot{m}'$ can

be calculated, equation (9), for openings in actual occurring situations if the temperature and humidity conditions on both sides of the opening and the opening's dimensions are known. By determining the value of $\dot{m}'$, for an applicable opening, it would be possible to use equation (15), or some modified variation fitted to actual data points taken, as a prediction technique for an expected reverse flow given a specific value of bulk flow or to predict the amount of bulk flow needed in a given situation to prevent any reverse flow. Equation (15) relating the ideal normalized bulk to reverse flow could be altered to fit actual data points using some sort of correction factors, fractional constants or difference shift scheme however because of the difficulty in manipulating the exponentiation involved the simplest means of prediction appears to be a graphical plot of, or extrapolation from, actual data points obtained, ideally for a tested opening similar to the one whose flow characteristics are being predicted.

The results, in terms of $\dot{m}_b/\dot{m}'$ and $\dot{m}_r/\dot{m}'$, for all openings of zero length tested are plotted together in figure 14 to give a curve for the general zero length case. The general zero length curve appears to be parallel to, but offset from, the ideal curve developed in Chapter 2. Because of the reasonable consistancy of the curve of actual data points for all openings of zero length and the appearance of graphs of openings with length, figures 10 and 12, the similarity of the length to height ratios would probably be sufficient for a graph of a tested opening to predict the characteristics on an untested opening.

By expressing the fraction of total opening height (vertical distance) in terms of the normalized reverse flow, $\dot{m}_r/\dot{m}'$, it is possible to calculate, using actual measured values of $\dot{m}_r/\dot{m}'$, effective values of opening height. From equations (13) and (14);

$$(H_1 + H_2)/H = (1 - \dot{m}_r/\dot{m}')^{2/3} + (\dot{m}_r/\dot{m}')^{2/3}$$

For actual zero length data the value of $(H_1 + H_2)/ H$ is greater than one increasing slightly with increasing $\dot{m}_r/ \dot{m}'$. For openings with length the effective $(H_1 + H_2)/ H$ is less than 1 but this is not a good indicator of the deviation of actual data from the predicted ideal since it does not involve $\dot{m}_b/ \dot{m}'$.

Another means of comparing trends in the actual data taken to the predicted ideal involves rearrangement of equation (15) to give;

$$\left(\frac{\dot{m}_r}{\dot{m}'} + \frac{\dot{m}_b}{\dot{m}'}\right)^{2/3} + \left(\frac{\dot{m}_r}{\dot{m}'}\right)^{2/3} = \emptyset$$

Actual effective values of $(\dot{m}_r/ \dot{m}' + \dot{m}_b/ \dot{m}')^{2/3} + (\dot{m}_r/ \dot{m}')^{2/3}$ are listed in the last column of table 2. They are less than one increasing with increasing values of $\dot{m}_r/ \dot{m}'$ and decreasing with increasing L/H.

Finally because the graph of the curve of actual data points for zero length openings is fairly near the ideal curve some conclusions about untested zero length or near zero length openings can be generalized. It could be assumed that all reverse flow is suppressed when $\dot{m}_b/ \dot{m}' = 1$ or when $\dot{m}_b = \dot{m}'$. This statement might even be true since the ideal and actual curves appear to converge slightly, on graphs with equal scales on both axes, as $\dot{m}_b/ \dot{m}'$ approaches 1. Also worst case values of the reverse flow could be estimated for zero or near zero length openings using the ideal curve relationship. The expected accuracy of a prediction scheme, using calculated values of $\dot{m}'$ and the ideal curve graph, seems fairly reasonable in light of most engineering applications since the developed ideal model gives conservative estimates (high compared with actual) of the reverse flow and since the influence of temperature humidity and geometry variables is taken into account.

Table 2

Presentation of Data
In Reduced Form

Opening Geometry 6" x 6" 0 mid D_h = 0.5 ft.

Δw $\times 10^3$	$\bar{T}$ (^oR)	$\bar{\rho}$ $\left(\frac{lbm}{ft^3}\right)$	ΔT (^oF)	$\dot{m}'$ $\left(\frac{lbm}{sec}\right)$	$\frac{\dot{m}_b}{\dot{m}'}$	$\frac{\dot{m}_{H_2O\ r}}{\Delta w\ \dot{m}'}$	$\frac{\dot{m}_{H_2O\ r}}{\dot{m}_{H_2O\ b\ opening}}$	$\frac{\dot{m}_{H_2O\ r}}{\dot{m}_{H_2O\ b\ meter}}$	Re $\times 10^{-5}$	Rs $\times 10^{-5}$	Gr $\times 10^{-7}$	Sw $\times 10^{-E}$	E	$\frac{Nu}{Pr}$	ϕ *
7.81	554.5	.06914	39.5	62.8	.90904	-.00857	-.00640	-.02198	99.03	99.03	1.498	6.482	13	-2761	
6.55	529.7	.07239	43.1	70.2	0	0.23086	∞	∞	0	.08205	1.683	4.103	3	781.5	0.753
8.56	531.5	.07386	31.4	61.0	0	0.230	∞	∞	0	.07116	1.266	3.558	3	672.9	0.751
6.01	531.9	.07288	43.3	70.8	0.63	0.029	0.060	0.025	77.37	77.37	1.676	2.764	13	-2016	0.852
5.98	531.7	.07291	43.1	71.9	0.42	0.070	0.21	0.09	52.38	52.38	1.670	8.606	12	-1196	0.791
6.03	545.4	.06995	52.9	74.2	0.395	0.096	7.14	0.13	50.84	50.84	1.985	6.620	12	-1057	0.832
5.77	540.5	.07088	34.1	60.5	0.49	0.063	0.156	0.060	51.42	51.42	1.324	1.027	13	-1220	0.832
5.55	536.7	.07148	39.2	65.7	0.49	0.049	0.114	0.052	55.84	55.84	1.506	1.156	13	-1366	0.796
6.19	529.4	.07316	34.16	63.2	0.47	0.060	0.166	0.071	51.53	51.52	1.345	1.017	13	-1240	0.808
6.37	536.6	.07163	53.4	76.9	0.275	0.134	0.656	0.276	36.68	36.68	2.038	2.422	12	-464.5	0.813
6.26	536.7	.07135	42.8	68.5	0.426	0.0735	0.226	0.096	50.62	50.62	1.645	7.884	12	-1149	0.805
4.68	557.0	.06885	0	2.48	0	1.3261	∞	∞	0	0	.05511	0		125.5	2.41

* Defined on page 45.

Table 2 (continued)

Opening Geometry 12" x 12" x 0 mid D_h = 1 ft.

Δw $\times 10^{3}$	$\bar{T}$ (^{o}R)	$\bar{\rho}$ ($\frac{lbm}{ft^3}$)	ΔT (^{o}F)	$\dot{m}'$ ($\frac{lbm}{sec}$)	$\frac{\dot{m}_b}{\dot{m}'}$	$\frac{\dot{m}_{H_2O\ r}}{\Delta w\ \dot{m}'}$	$\frac{\dot{m}_{H_2O\ r}}{\dot{m}_{H_2O\ b\ opening}}$	$\frac{\dot{m}_{H_2O\ r}}{\dot{m}_{H_2O\ b\ meter}}$	Re $\times 10^{-5}$	Rs $\times 10^{-5}$	Gr $\times 10^{-7}$	Sw $\times 10^{-E}$	E	$\frac{Nu}{Pr}$	ϕ
5.59	543.6	.07056	14.79	223.85	.3112	.09944	.33132	.15480	60.42	60.42	4.820	4.576	12	-1130	0.767
6.92	549.8	.07089	26.76	300.80	.2354	.15540	1.1497	.41544	61.41	61.41	8.331	2.780	12	-572.6	0.824
7.43	553.5	.07031	32.53	327.91	.2053	.17494	1.7015	.56638	58.39	58.39	9.974	1.996	12	-232.4	0.838
7.29	554.3	.07021	33.21	330.60	.1323	.21046	3.1552	1.0461	37.93	37.93	10.14	5.383	11	632.5	0.844
7.40	539.0	.07214	48.83	417.93	.1612	.19848	2.5137	.81239	58.43	58.43	14.99	1.331	12	384.2	0.846
6.85	539.6	.07189	50.59	423.75	.1109	.22929	3.4709	1.2768	40.76	40.76	15.44	4.385	11	1222	0.862
7.52	539.0	.07197	49.67	420.61	.0954	.23318	4.9326	4.6521	34.80	34.80	15.25	2.764	11	1402	0.855
7.55	540.4	.07080	52.87	426.37	.01691	.27219	30.827	10.539	6.253	6.252	16.15	1.513	9	2625	0.857
7.29	534.4	.07168	44.19	396.70	.02770	.26314	18.363	6.0023	9.530	9.530	13.74	6.299	9	2257	0.850
6.87	540.5	.07075	55.41	436.19	0	.27428	∞	∞	0	.1297	16.82	1.297	4	2877	0.844
6.77	537.0	.07109	37.38	362.32	0	.25558	∞	∞	0	.1082	11.71	1.082	4	2231	0.805

Table 2 (continued)

Opening Geometry 12" x 6" x 0 D_h = 0.667 ft.

Δw $\times 10^3$	$\bar{T}$ (^oR)	$\bar{\rho}$ ($\frac{lbm}{ft^3}$)	ΔT (^oF)	$\dot{m}'$ ($\frac{lbm}{sec}$)	$\frac{\dot{m}_b}{\dot{m}'}$	$\frac{\dot{m}_{H_2O\ r}}{\Delta w\ \dot{m}'}$	$\frac{\dot{m}_{H_2O\ r}}{\dot{m}_{H_2O\ b}}$ opening	$\frac{\dot{m}_{H_2O\ r}}{\dot{m}_{H_2O\ b}}$ meter	Re $\times 10^{-5}$	Rs $\times 10^{-5}$	Gr $\times 10^{-7}$	Sw $\times 10^{-E}$	E	$\frac{Nu}{Pr}$	ϕ
6.63	539.3	.07088	56.41	156.057	.10178	.24055	3.329	1.343	18.37	18.37	2.141	1.221	11	526.0	0.876
6.31	547.7	.07017	26.77	105.5	.5627	.06383	.1537	.06338	68.65	68.65	1.038	1.315	13	-1263	0.892
6.45	530.8	.07279	43.73	142.15	.4214	.09827	.3258	.13157	69.27	69.27	1.701	8.244	12	-1099	0.859
7.11	538.9	.07161	56.60	156.61	.1846	.17540	1.589	.60059	33.43	33.43	2.119	7.438	11	-29.60	0.819
6.49	537.0	.07185	55.09	156.64	.3773	.11719	.43410	.17990	68.34	68.34	2.100	6.413	12	-971.5	0.865
6.89	536.3	.07280	53.72	156.82	.2931	.14892	.86862	.31482	53.15	53.15	2.057	3.080	12	-536.3	0.861
5.92	536.7	.07212	53.78	155.41	.3087	.16561	.67609	.28281	55.48	55.48	2.046	3.521	12	-525.0	0.910
7.12	533.2	.07323	43.36	142.31	.3176	.13784	.80892	.27409	52.27	52.27	1.725	3.493	12	-607.6	0.859
6.33	533.1	.07263	46.31	145.68	0	.24727	∞	∞	0	.005638	1.788	4.229	3	867.9	0.788
6.69	539.2	.07176	57.56	159.633	0	.27073	∞	∞	0	.006231	2.184	4.674	3	1041	0.837

Table 2 (continued)

Opening Geometry 6" x 12" x 0 mid D_h = 0.667 ft.

Δw $\times 10^3$	$\bar{T}$ (^oR)	$\bar{\rho}$ ($\frac{lbm}{ft^3}$)	ΔT (^oF)	$\dot{m}'$ ($\frac{lbm}{sec}$)	$\frac{\dot{m}_b}{\dot{m}'}$	$\frac{\dot{m}_{H_2O\ r}}{\Delta w\ \dot{m}'}$	$\frac{\dot{m}_{H_2O\ r}}{\dot{m}_{H_2O\ b\ opening}}$	$\frac{\dot{m}_{H_2O\ r}}{\dot{m}_{H_2O\ b\ meter}}$	Re $\times 10^{-5}$	Rs $\times 10^{-5}$	Gr $\times 10^{-7}$	Sw $\times 10^{-E}$	E	$\frac{Nu}{Pr}$	ϕ
6.15	539.7	.0710	45	197.5	.01607	.25380	20.375	8.775	3.670	3.669	13.8	1.208	9	2264	0.818
6.13	542	.0708	58.61	224.3	0.01950	.25206	16.7086	7.209	5.058	5.057	17.6	2.480	9	2516	0.818
5.83	540	.0718	59.06	228.88	.30423	.15010	.60357	.27309	80.52	80.52	17.8	9.899	12	-1684	0.873
6.23	540	.0712	55.15	219.032	.18392	.18911	1.32086	.57874	46.59	46.58	16.7	2.043	12	73.91	0.848
5.69	535	.0715	47.32	204.616	.19711	.17720	1.02994	.46982	46.64	46.64	14.5	2.361	12	-176.4	0.835
6.08	538.9	.0718	45.0	199.78	.35076	.12653	.46493	.20225	81.10	81.03	13.7	1.311	13	-2143	0.863
6.30	553.2	.0690	34.45	165.66	.41146	.12808	.44757	.17988	78.82	78.82	10.4	1.589	13	-2241	0.917
5.90	551.2	.0693	31.54	159.4	.44986	.08099	.22736	.09622	82.92	82.92	9.59	2.007	13	-2817	0.843

Table 2 (continued)

Opening Geometry 6" x 6" x 12" mid D_h = 0.5 ft.

Δw $\times 10^3$	$\bar{T}$ (^oR)	$\bar{\rho}$ ($\frac{lbm}{ft^3}$)	ΔT (^oF)	$\dot{m}'$ ($\frac{lbm}{sec}$)	$\frac{\dot{m}_b}{\dot{m}'}$	$\frac{\dot{m}_{H_2O\ r}}{\Delta w\ \dot{m}'}$	$\frac{\dot{m}_{H_2O\ r}}{\dot{m}_{H_2O\ b}\ opening}$	$\frac{\dot{m}_{H_2O\ r}}{\dot{m}_{H_2O\ b}\ meter}$	Re $\times 10^{-5}$	Rs $\times 10^{-5}$	Gr $\times 10^{-7}$	Sw $\times 10^{-E}$	E	$\frac{Nu}{Pr}$	Ø
6.87	544.2	.07040	46.83	70.26	.07127	.03471	.29963	.07868	8.686	8.685	1.778	3.685	10	-121.1	0.330
7.12	542.1	.07098	44.82	69.45	.09453	.03850	.76147	.27098	11.39	11.39	1.715	8.611	10	-233.0	0.375
7.86	540.8	.07120	42.69	68.05	.08209	.02830	.78465	.23624	9.690	9.690	1.650	5.514	10	-173.6	0.323
8.38	546.7	.07076	28.22	54.66	.05196	.09274	5.3348	1.3065	4.927	4.926	1.117	1.070	10	108.8	0.481
9.05	537.7	.07199	57.98	80.48	.05296	.06591	4.4863	0.9837	7.254	7.393	2.234	1.809	10	50.80	0.405
7.87	538.7	.07183	58.47	80.58	.09317	.02874	.80222	.21621	19.56	13.02	2.241	9.855	10	-246.7	0.340
6.92	538.1	.07211	58.44	80.89	.13995	.01801	.21584	.08064	19.64	19.64	2.223	3.406	11	-470.1	0.361
4.63	545.1	.07041	24.29	50.51	1.3873	.12160	.08139	.03657	121.6	121.5	.9325	1.926	14	-3064	1.561
6.14	533.0	.07428	42.77	69.19	.86738	.08104	.12067	.05104	104.1	103.7	1.651	6.749	13	-2586	1.153
6.64	538.1	.07109	56.82	78.63	.7540	.07931	.15209	.06325	102.8	102.8	2.161	5.033	13	-2535	1.070
6.02	531.5	.07199	42.73	69.44	.34715	.04490	.16791	.07205	41.82	41.81	1.657	4.413	12	-1007	0.662
6.53	538.1	.07109	56.51	78.42	.30620	.03162	.14651	.06114	41.65	41.65	2.148	3.364	12	-1033	0.585
6.60	538.9	.07131	67.62	79.38	.1677	.01284	.10988	.04433	23.09	23.09	2.187	5.630	11	300.8	0.373
6.36	533.6	.07149	42.65	68.76	0	0.08439	∞	∞	0	.04063	1.651	4.064	3	279.6	0.385
7.03	538.8	.07082	58.19	79.24	0	0.072374	∞	∞	0	.04704	2.213	4.704	3	276.3	0.347

Table 2 (continued)

Opening Geometry 12" x 12" x 12" D_h = 1 ft.

Δw $\times 10^3$	$\bar{T}$ ($^\circ R$)	$\bar{\rho}$ ($\frac{lbm}{ft^3}$)	ΔT ($^\circ F$)	$\dot{m}'$ ($\frac{lbm}{sec}$)	$\frac{\dot{m}_b}{\dot{m}'}$	$\frac{\dot{m}_{H_2O\ r}}{\Delta w\ \dot{m}'}$	$\frac{\dot{m}_{H_2O\ r}}{\dot{m}_{H_2O\ b\ opening}}$	$\frac{\dot{m}_{H_2O\ r}}{\dot{m}_{H_2O\ b\ meter}}$	Re $\times 10^{-5}$	Rs $\times 10^{-5}$	Gr $\times 10^{-7}$	Sw $\times 10^{-E}$	E	$\frac{Nu}{Pr}$	$\emptyset$
7.25	543.5	.06980	61.31	451.57	.02199	.11404	7.05292	2.9243	8.612	8.611	18.41	3.469	9	1007	0.500
5.97	540.5	.06997	40.45	368.33	.02646	.10855	5.01123	2.1307	8.453	8.452	12.37	4.881	9	733.6	0.491
6.80	540.3	.07099	55.17	436.80	0	.12490	∞	∞	0	.1294	16.75	1.294	4	1362	0.500
6.43	535.8	.07126	41.04	380.70	0	.12594	∞	∞	0	.1127	12.69	1.127	4	1155	0.980
6.86	539.5	.07094	49.77	414.77	.07712	.09416	1.99626	0.74233	27.74	27.74	15.20	1.405	11	177.9	0.515
6.10	553.1	.06924	33.57	328.2	.18118	.02733	.20145	.08148	51.57	51.57	10.15	1.351	12	-1182	0.442
6.05	553.1	.06930	31.66	318.99	.14297	.03686	.35643	.14156	39.55	39.55	9.603	6.444	11	-808.9	0.429
6.14	553.9	.06871	31.73	316.40	.11072	.04564	.52870	.22355	30.38	30.38	9.168	2.916	11	-488.1	0.418
6.85	543.2	.07008	64.10	463.77	.08139	.09423	1.9443	.72047	32.74	32.74	19.27	1.821	11	151.7	0.521
6.98	543.2	.07015	62.41	457.99	.04921	.10597	3.8064	1.3596	19.55	19.55	18.79	3.974	10	631.2	0.513
4.46	551.7	.06926	31.32	317.46	.9243	.05346	.41238	.23410	254.5	254.5	9.376	1.758	14	-290.1	1.127
5.23	547.7	.06971	67.90	472.85	.20545	.01537	.06993	.0355	84.26	84.26	20.05	2.983	12	-2147	0.427
4.17	554.4	.06878	31.01	312.89	.05010	.08132	1.0414	.61312	13.60	13.60	9.218	2.726	10	250.0	0.446
6.60	547.4	.07013	66.27	470.08	.13991	.05186	.52796	.21802	57.04	57.04	19.73	9.401	11	-988.4	0.472
5.45	553.6	.06878	30.24	309.24	.01348	.08377	5.6092	2.8952	3.615	3.614	9.132	5.170	8	525.0	0.403
7.16	546.8	.06972	62.76	454.95	.12980	.06808	.86162	.32501	51.22	51.22	18.78	7.154	11	-668.7	0.506
6.25	544.9	.06985	63.77	460.35	.16476	.05702	.42497	.18667	65.78	65.78	19.06	1.494	12	-1186	0.515

4.3 Comparison of Experimental Data Taken with Previous Work

In previous work by Brown [6], [7] and Shaw [9], where the natural convection and combined natural and forced convection at an opening were examined experimentally from heat transfer data, equations relating dimensionless groups were used to fit prediction curves or compare theory to actual data taken. To compare the experimental results obtained in this study with previous work, dealing with convection at an opening, relevant dimensionless ratios have been computed and are listed in Table 2 along with the results of the normalizing data reduction scheme.

For both the heat and water vapor transfer occurring through an opening between two air spaces the physical cause of transfer is convective air interchange. From the reasonably valid assumptions that for heat transfer pure conduction is neglible and for mass transfer diffusion of vapor is neglible an analgous development of heat and water vapor transfer, both due to air mass interchange through an opening, lead to a direct relationship between the convective coefficient of heat transfer, h_q, and the convective coefficient of water vapor transfer, h_m. Theoretically experimental data presented in reduced form, dimensionless ratios, describes the convective air mass interchange and it does not matter if the raw data taken involved heat transfer measurments o water vapor transfer measurments. Because the classically used dimensionless groups for water vapor transfer involve the term D, the diffusion coefficient, and because previously developed emperical and semi emperical formulas are expressed in terms of heat transfer groups the data taken in this study has been reduced to dimensionless heat transfer groups. In manipulating the terms within the dimensionless groups for heat transfer to obtain an expression for the convective coefficient of heat transfer, h_q, the conductivity k, and viscosity, μ, terms cancel out. In manipulating the terms within the

dimensionless water vapor transfer groups to obtain an expression for the convective coefficient of water vapor transfer, h_m, the coefficient of diffusion, D, cancels out.

The definition of the convective coefficient of water vapor transfer involves the net mass flowrate of water vapor through the opening, $\dot{m}_{H_2O\ net}$, $h_m = \dot{m}_{H_2O\ net} / W\ H\ \Delta w$. In terms of mass flowrates defined in Chapter 2

$$\dot{m}_{H_2O\ net} = \dot{m}_{H_2O\ r} - \dot{m}_{da}(w_2 - w_1) = \dot{m}_{H_2O} - \dot{m}_{da}(w_{meter} + w_2 - 2w_1).$$

For test situations where no bulk flow was made to pass through the opening $\dot{m}_{da} = 0$, $\dot{m}_{H_2O\ net} = \dot{m}_{H_2O}$. This is the type of situation dealt with by Brown, for natural convection alone.

In the publication by Brown [7] two equations, one theoretical and one semi emperical, are presented that express a relationship between heat transfer dimensionless groups applicable to a rectangular opening in a vertical wall.

$Nu/Pr = 1/3\ (Gr)^{1/2}$ for small values of L/H.

$Nu/Pr = 0.343\ (Gr)^{1/2}(1 - 0.498\ L/H)$ determined for $.19 \leq L/H \leq .38$.

From data taken in this study there are 11 tests with zero bulk flow. Table 3 lists the values of Nu/Pr calculated using the first equation for all 11 applicable tests, a value of L is calculated using the second equation for all 11 and a value of Nu/Pr is calculated using the second equation for the 4 applicable tests with length.

Since the so called zero length openings in this study were made by beveling 2 inch thick polystyrene insulation at a 45 ° angle so the actual length at the opening threshold was the thickness of the metal panel some length effects might have been present for zero length openings however it is unlikely that these effects were as large as those calculated, table 3. The equation used to calculate the L values was derived for a different range

Table 3

Comparison of Data with Previous Correlations

Opening Dimensions (inches)	Nu/Pr actual	Nu/Pr theory	L (ft) emp. eqn.	Nu/Pr emp. eqn.	$K = Nu/Pr\ (Gr)^{-1/2}$
6x6x0	781.5	1367	.446		0.190
6x6x0	672.9	1186	.450		0.189
6x6x0	125.5	247.5	.509		0.169
12x12x0	2877	4323	.709		0.222
12x12x0	2231	3607	.801		0.206
12x6x0	867.9	1409	.403		0.205
12x6x0	1041	1558	.352		0.223
6x6x12	279.6	1354	.803	5.575	0.0688
6x6x12	276.3	1568	.823	6.45	0.0587
12x12x12	1362	4314	1.39	2229	0.105
12x12x12	1155	3755	1.41	2123	0.102

of L/H however if some length effects were present for the so called zero length openings they might explain slight discontinuities in the curve of actual data points on figure 14 since the data from the 4 opening geometries would have been for 2 different ratios of L/H.

The paper by Shaw [9] makes several conflicting or at least confusing statements, that presumably come from proofreading errors, so that an interpretation of his work in comparison with the data taken in this study required some assumptions to be made. For combined natural and forced convection Shaw implied an equivalent velocity, in this paper called V_s, was to be used to determine the Reynolds number used in the correlations. Somewhat unclear in the publication was the exact definition of this velocity, now believed to be $V_s = (V_b^2 - g \frac{\Delta\rho}{\rho} H)^{1/2}$, which gives values of Reynolds numbers, column labled Rs Table 2, very close to the values of Reynolds numbers based upon the bulk velocity alone, column labled Re Table 2, for all data collected in this study. The equations for combined forced and natural convection give rise to an original dimensionless group $Sw = \frac{Rs^3 H^3}{Gr D_h^3}$ where the theoretical equation for heat transfer is Nu = C/3 Pr Sw, and for water vapor transfer Sh = C/3 Sm Sw.

Because of a fundamental difference in the experimental setup for Shaw's work and the work in this study, the bulk flow imposed upon the natural convection in his study was from the hot to cold air space rather than from the cold to hot, a direct comparison of results was not possible. However the value of the dimensionless group Sw, henceforth called the Shaw number, was calculated for the data taken in this study and is listed in Table 2. Figure 15 shows all the data taken in this study plotted as Nu/Pr versus Sw, the value of Nu/Pr calculated indirectly from water vapor transfer data, decreases for increasing Sw. This trend is opposite of data taken by Shaw so conclusions he made can not be applied to this situation however a functional relationship

could be developed from the data graphed on figure 15 using the coordinate system he developed. The plot was not made on log-log coordinates, as done by Shaw, because the value of Nu/Pr has both negative and positive values and because the log-log plot he made did not appear as a straight line anyway.

In interpreting the results expressed as dimensionless heat transfer ratios at first impression it seems unbelievable that Nu/Pr could take on negative values, indicating heat transfer through the opening from the cold air space to the hot air space. For water vapor transfer this represents a situation where more water vapor is being carried in the opening to the hot space from the cool space by natural and forced convection than is being carried out of the opening from the hot side by the reverse flow. The fact that a negative value of Nu/Pr exists for this situation follows from the definitions of the convective heat and water vapor transfer coefficients and thus, however unlikely it may seem, heat is being transfered through the opening from the cold air space to the hot air space by the bulk flow of air passing through the opening.

From observations made using the experimental apparatus in this study the definitions of temperature and velocity flow coefficients by Shaw, for natural convection alone and combined natural and forced convection, become somewhat questionable. Prior to gathering experimental data in this study preliminary tests were conducted varying the air supply loop flowrate and consequently the turbulent random air velocity conditions on the cool dry side of the opening. The flow coefficient for natural convection alone, which Shaw plotted as a function of temperature difference, appeared also to depend upon the free air movement within the air space adjacent to the opening so that the flow coefficient values he determined might only apply to conditions similar to those used in their determination.

From figure 15 on the dimensionless ratio coordinate system the data

points for zero length openings with different geometries do not appear to compare all that well although the trend for increasing L/H ratios, towards lower asymptotic values of Nu/Pr as Sw approaches zero, can be observed. In general more data for openings with and without length as well as data with very low bulk flow or large air density differences, so that $Re \neq Rs$ and $10^5 \leq Sw \leq 10^9$, would be desireable to formulate functional equations involving these dimensionless groups.

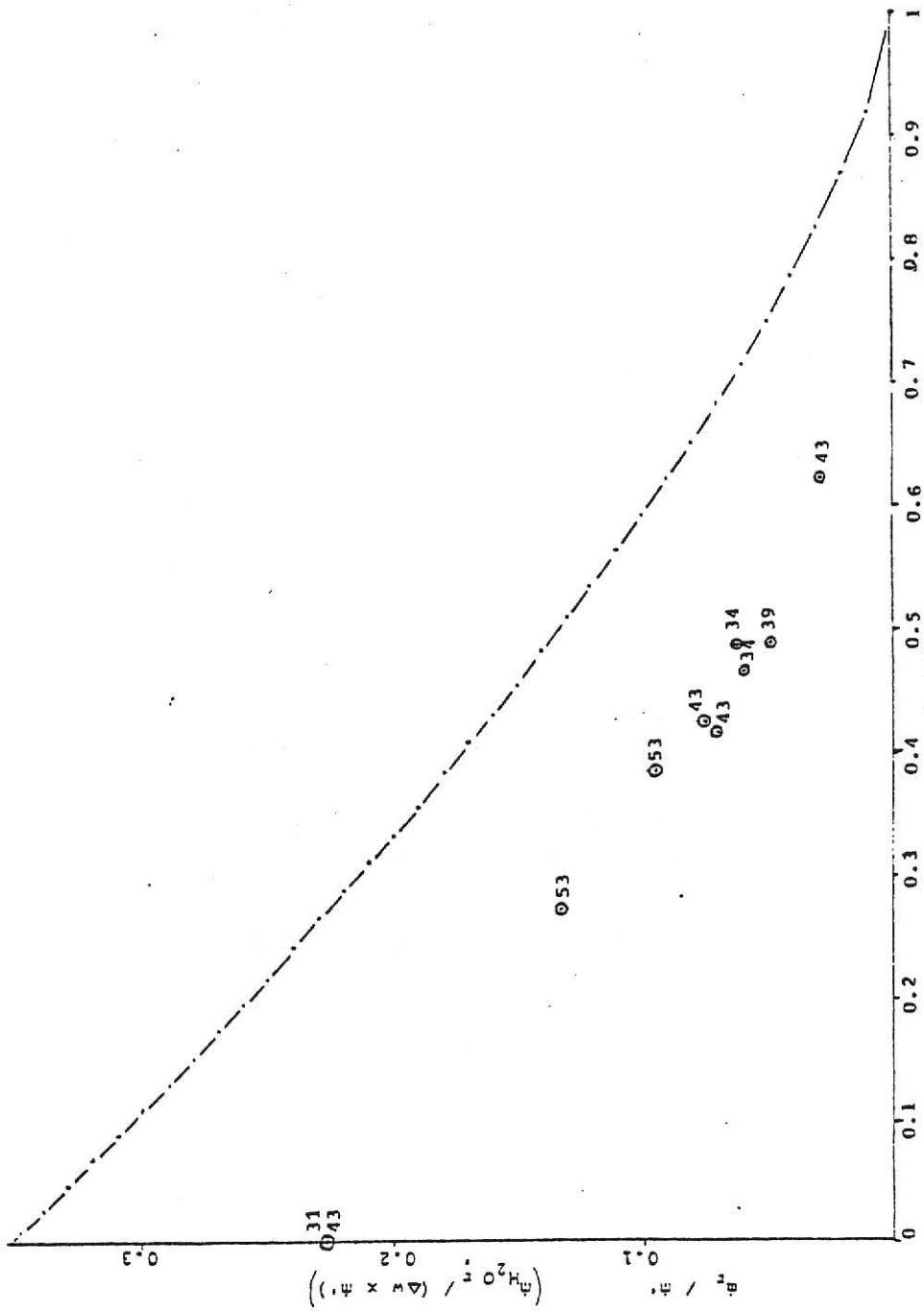

Figure 6

6x6 inch opening zero length

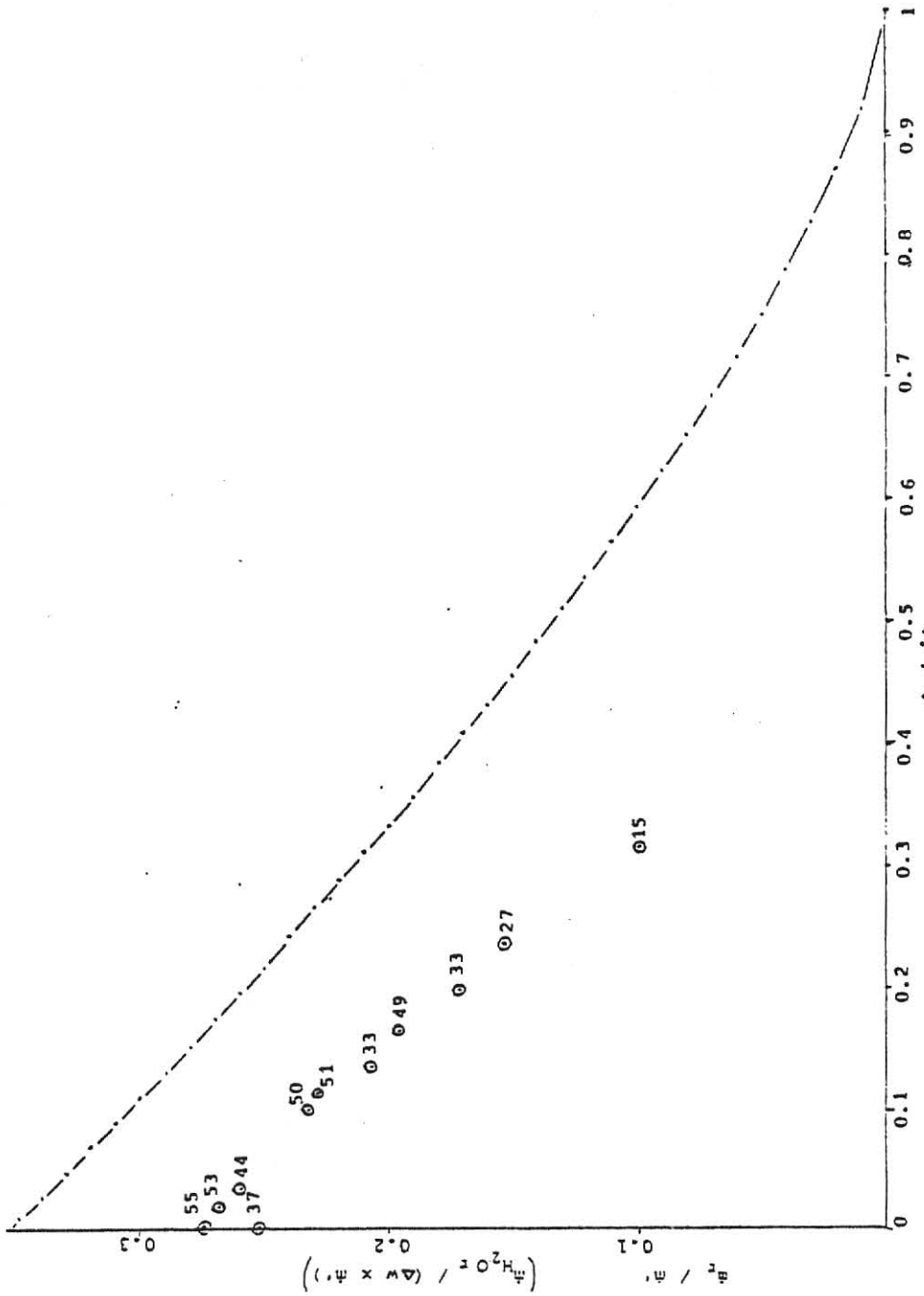

Figure 7

12x12 inch opening zero length

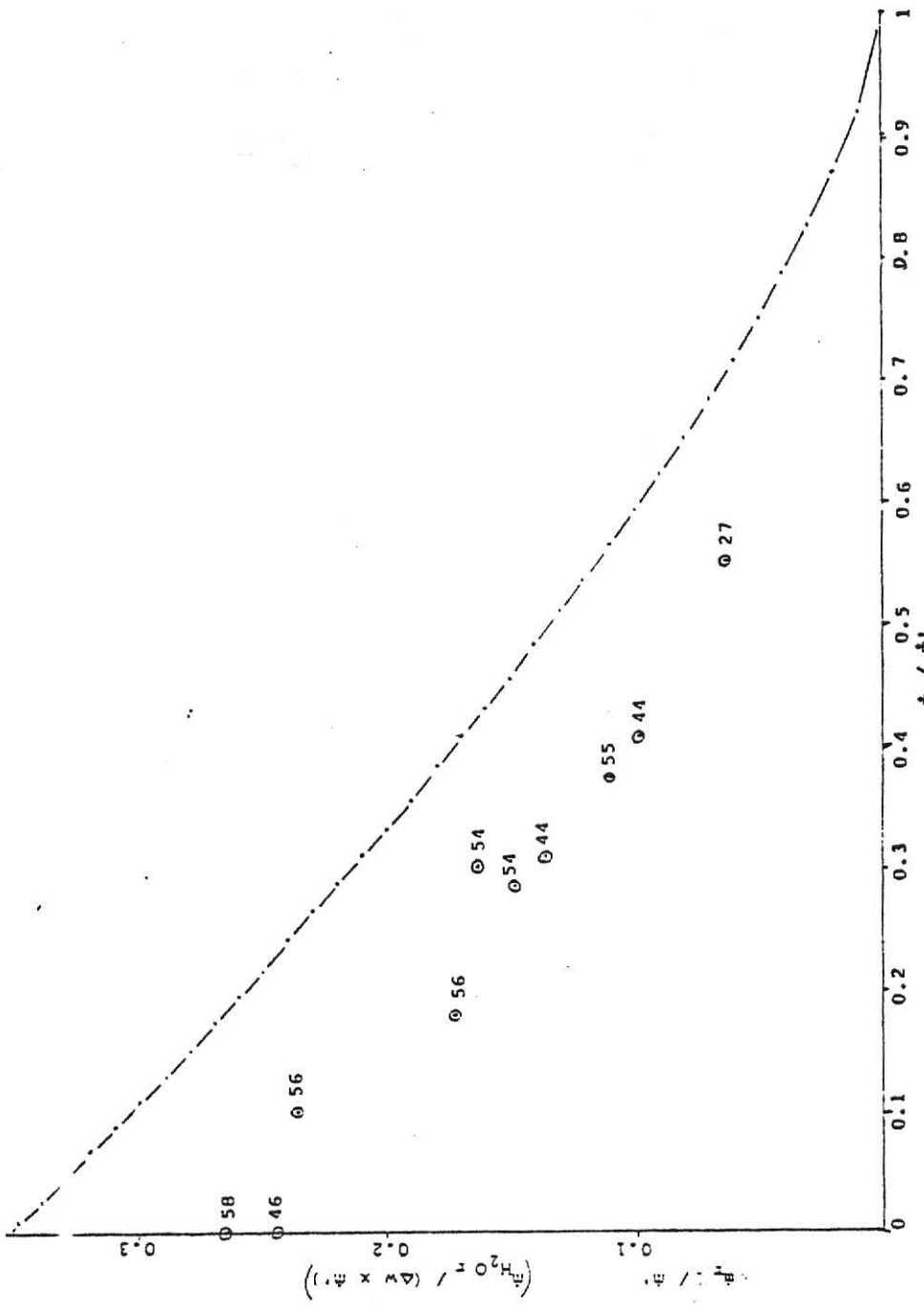

Figure 8

12x6 inch opening zero length

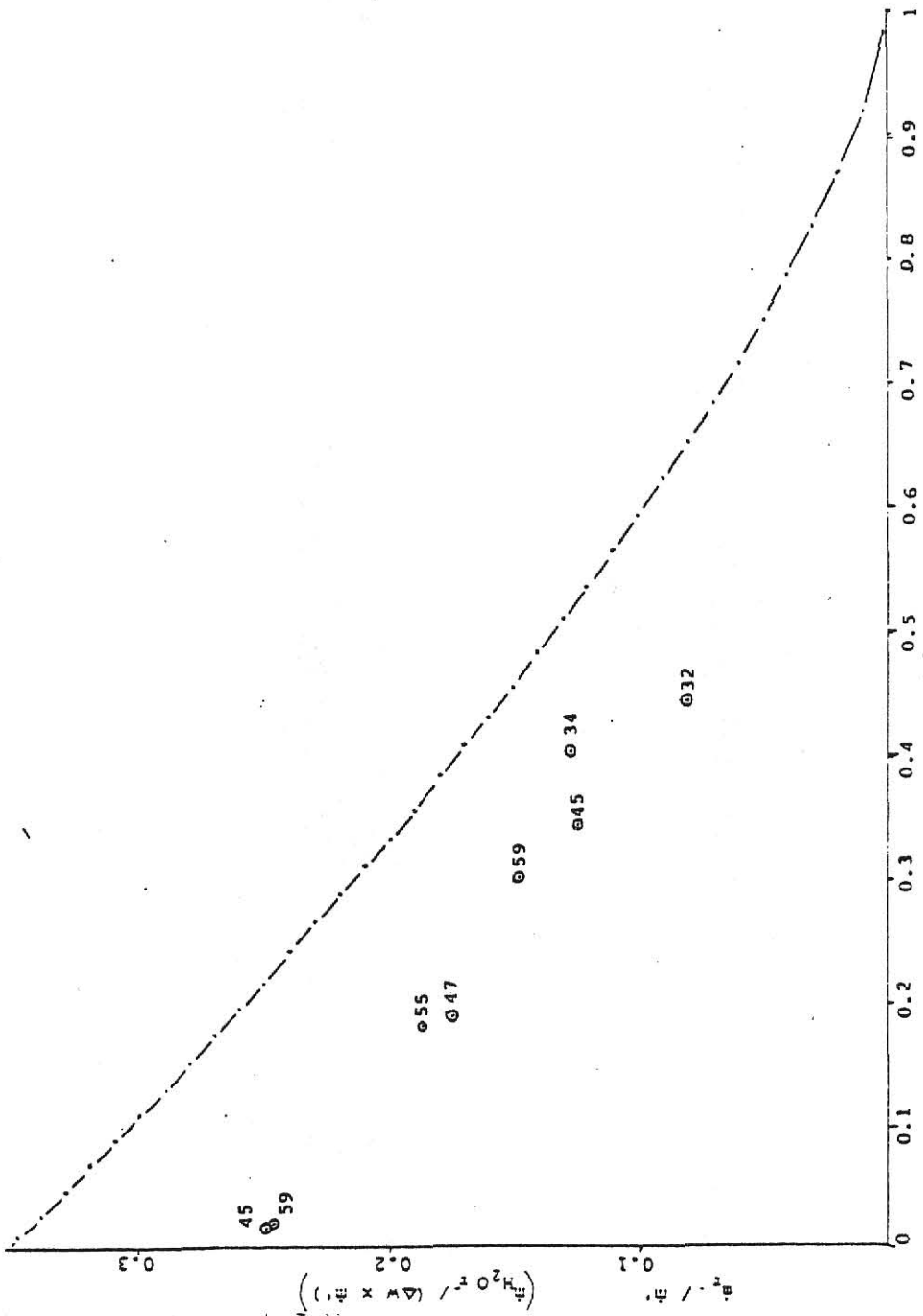

Figure 9

6x12 inch opening zero length

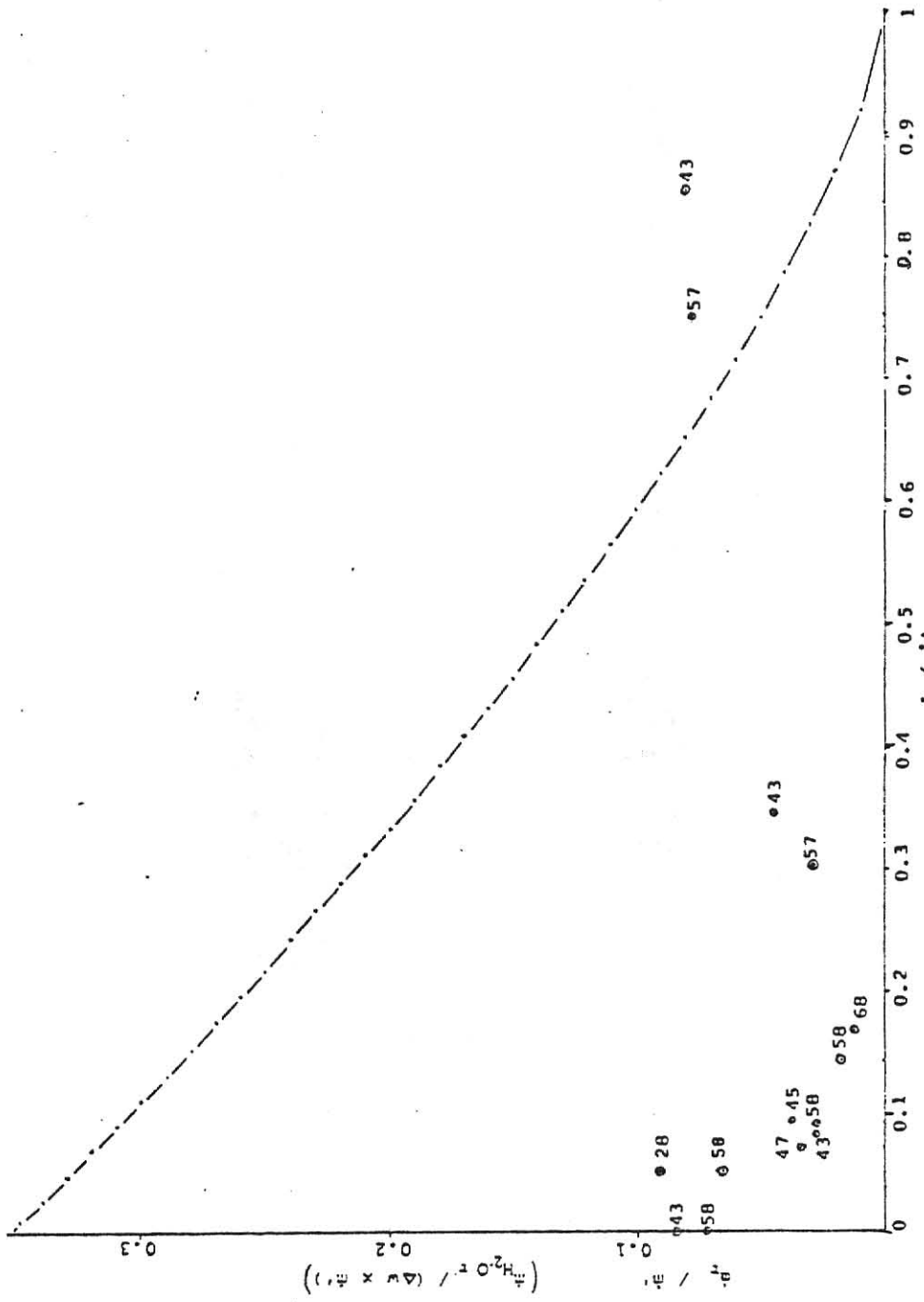

Figure 10

6x6x12 inch opening

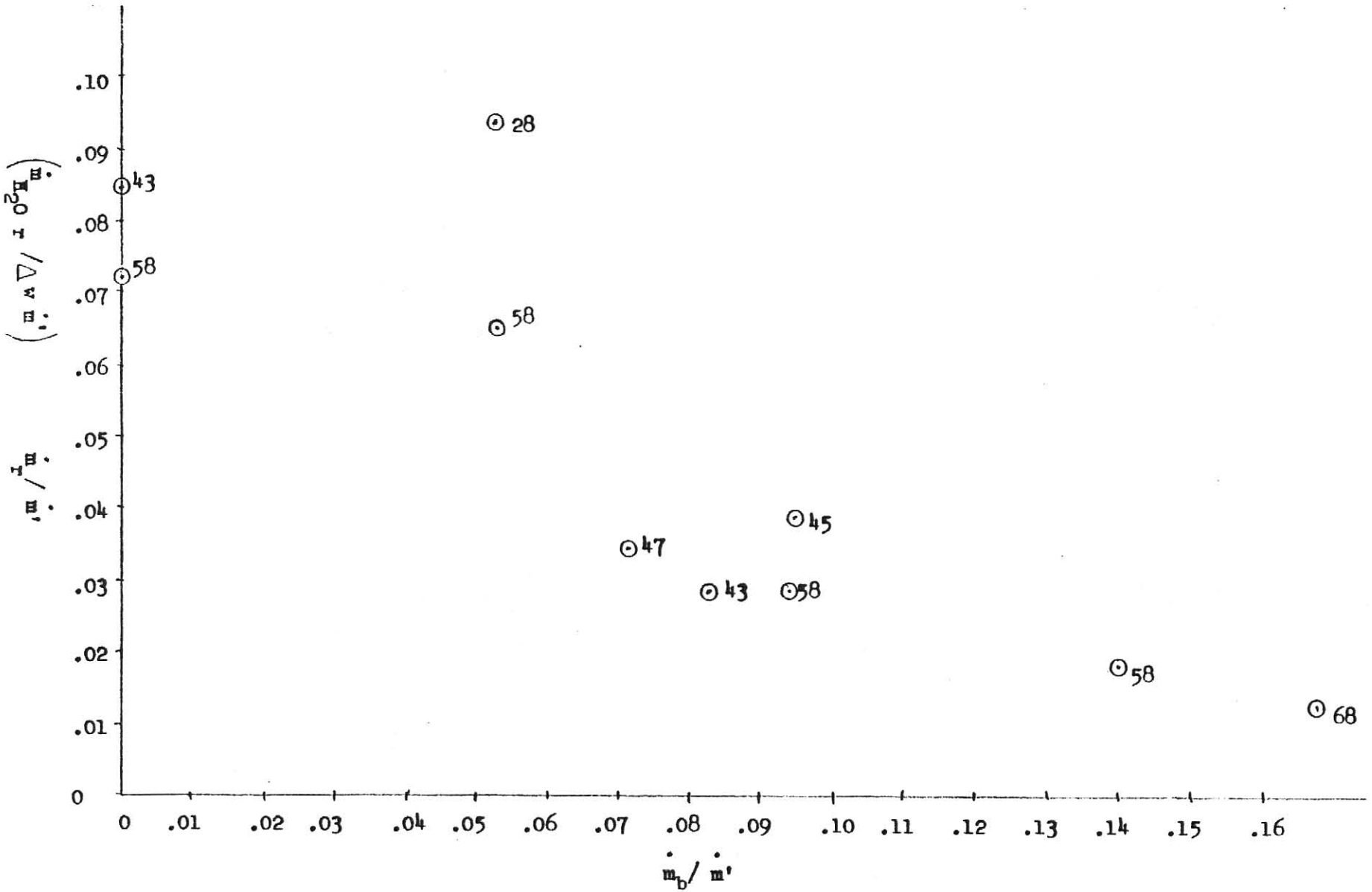

Figure 11 6x6x12 inches

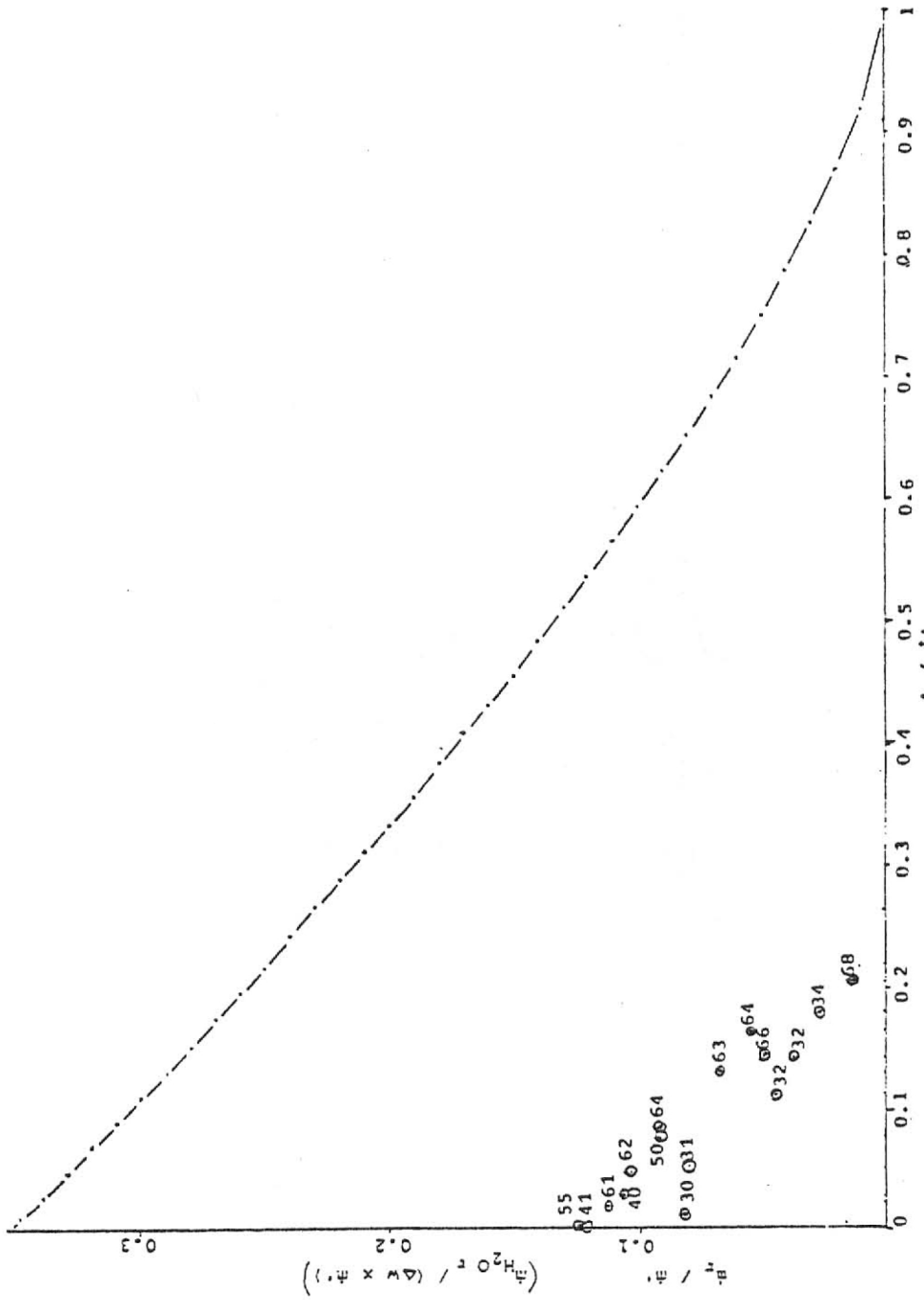

Figure 12

12x12x12 inch opening

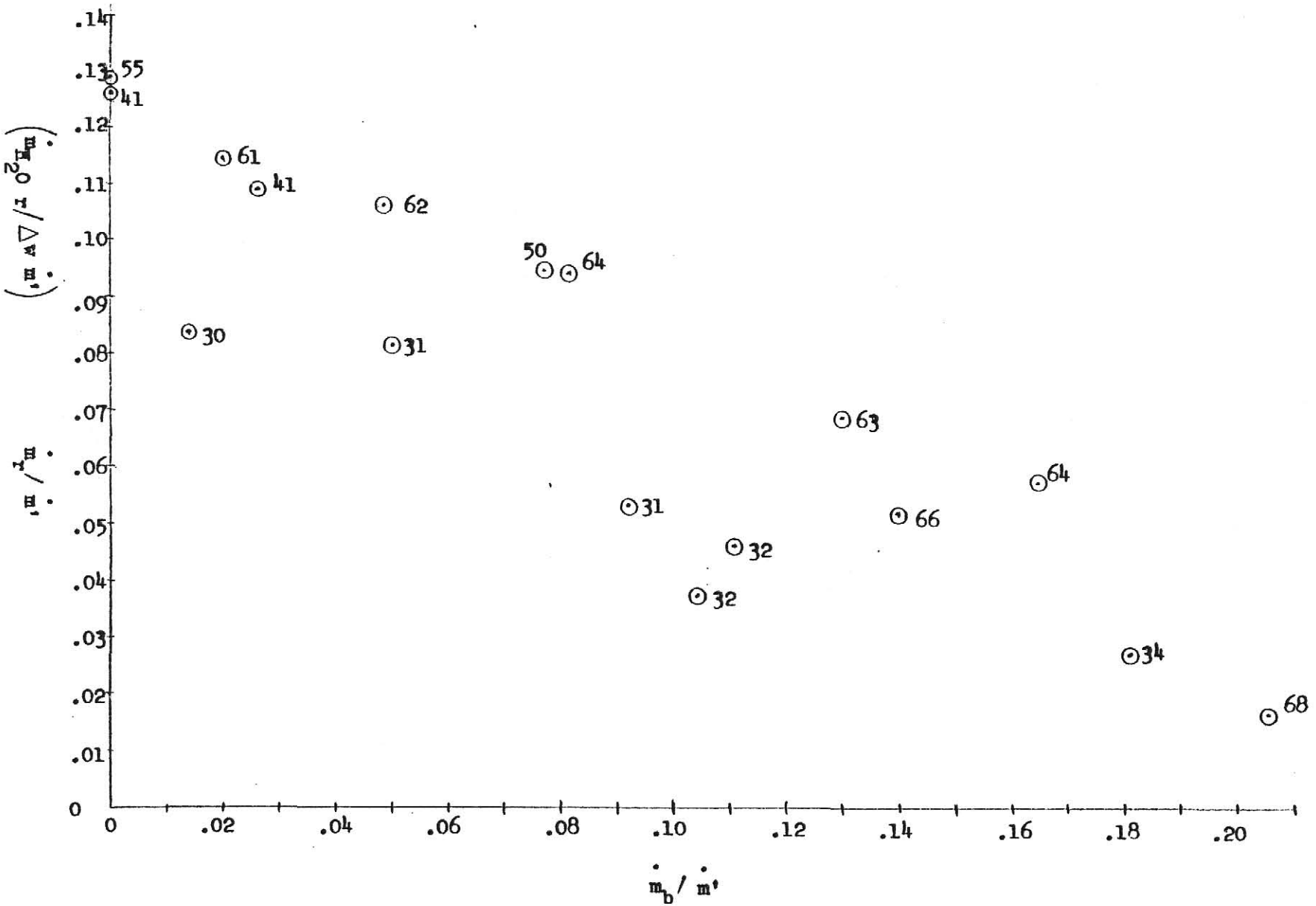

Figure 13 12x12x12 inches

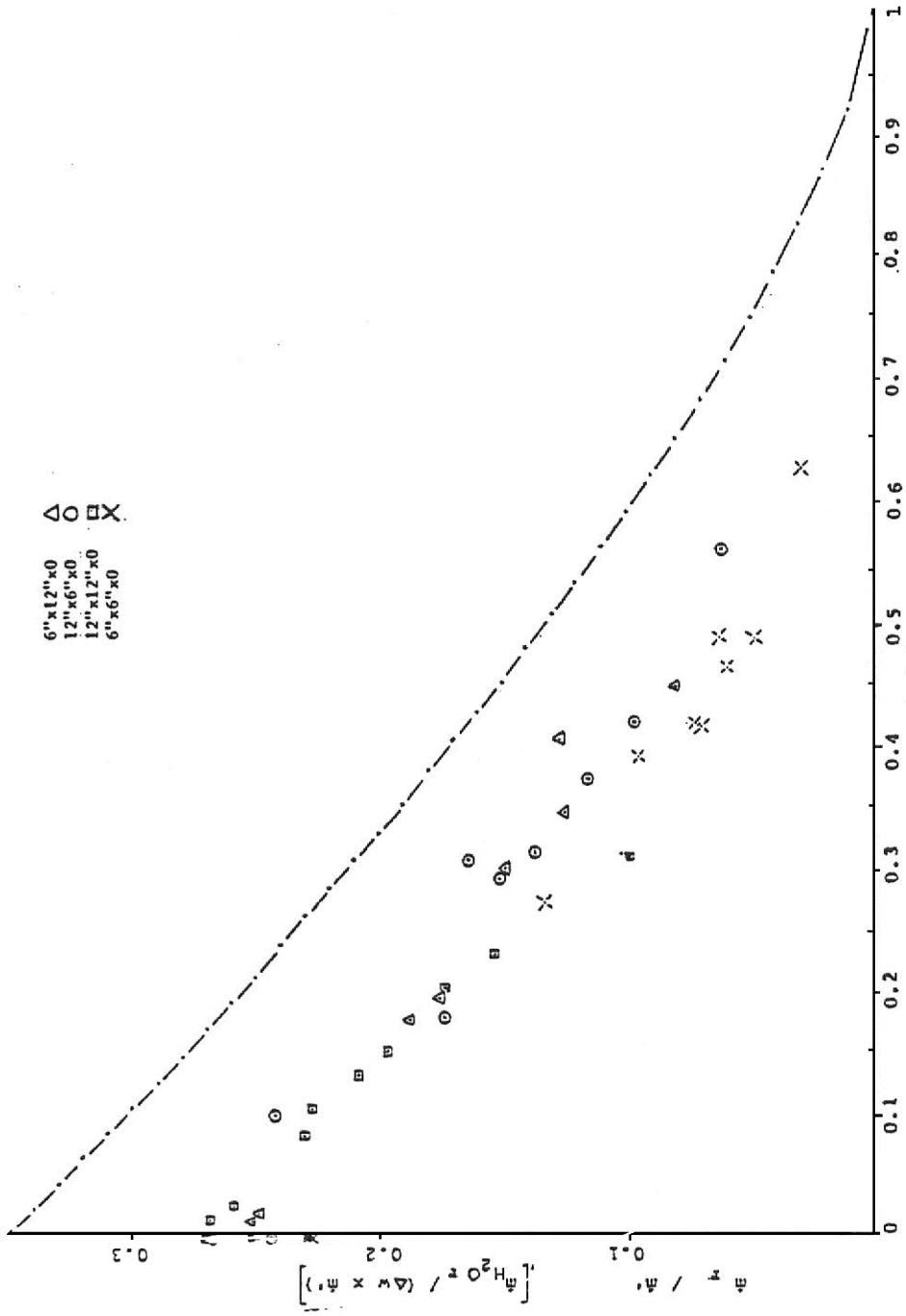

Figure 14

All Zero Length Openings

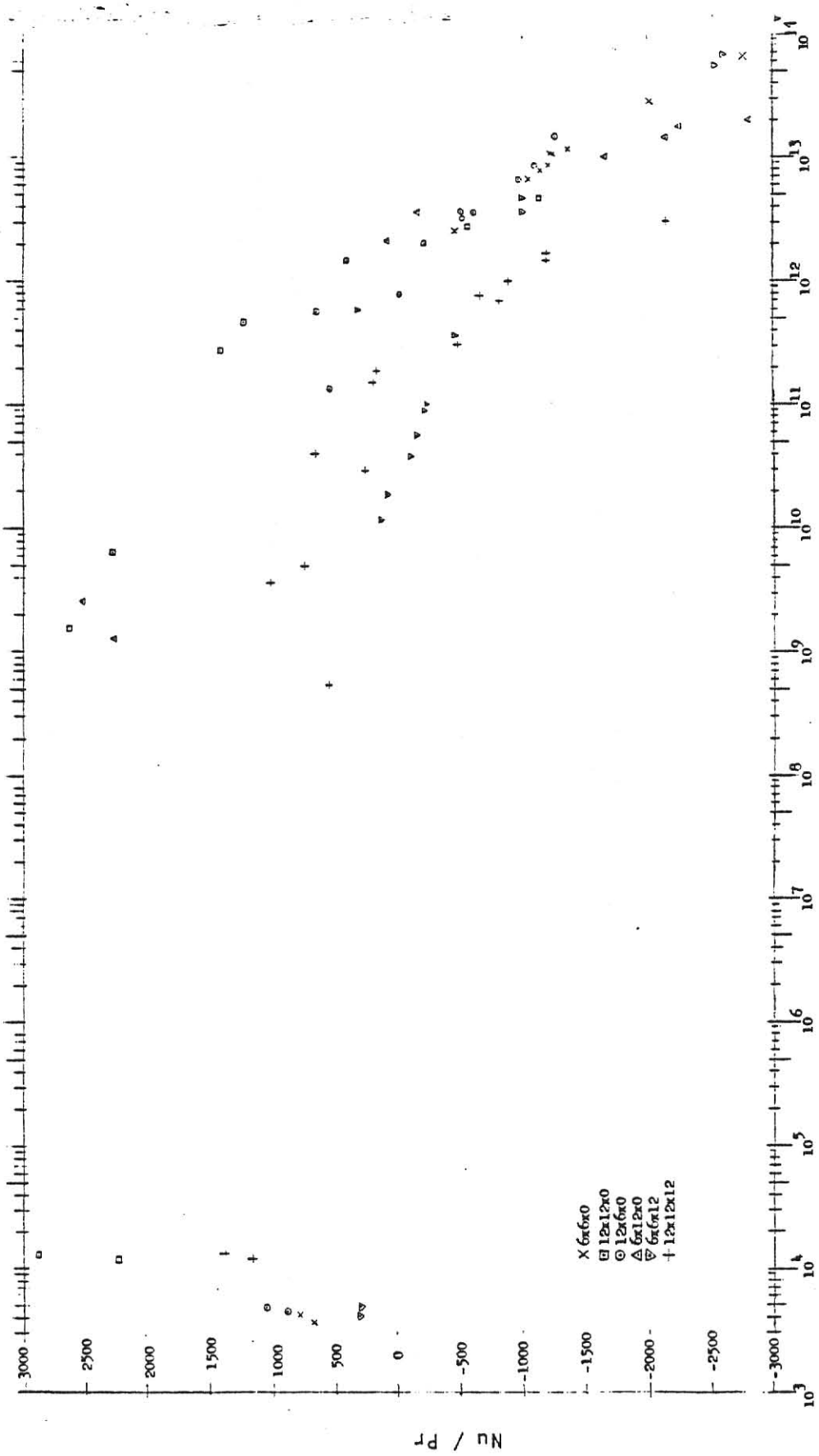

Figure 15

Presentation of Data Taken in Heat Transfer Dimensionless Group Form

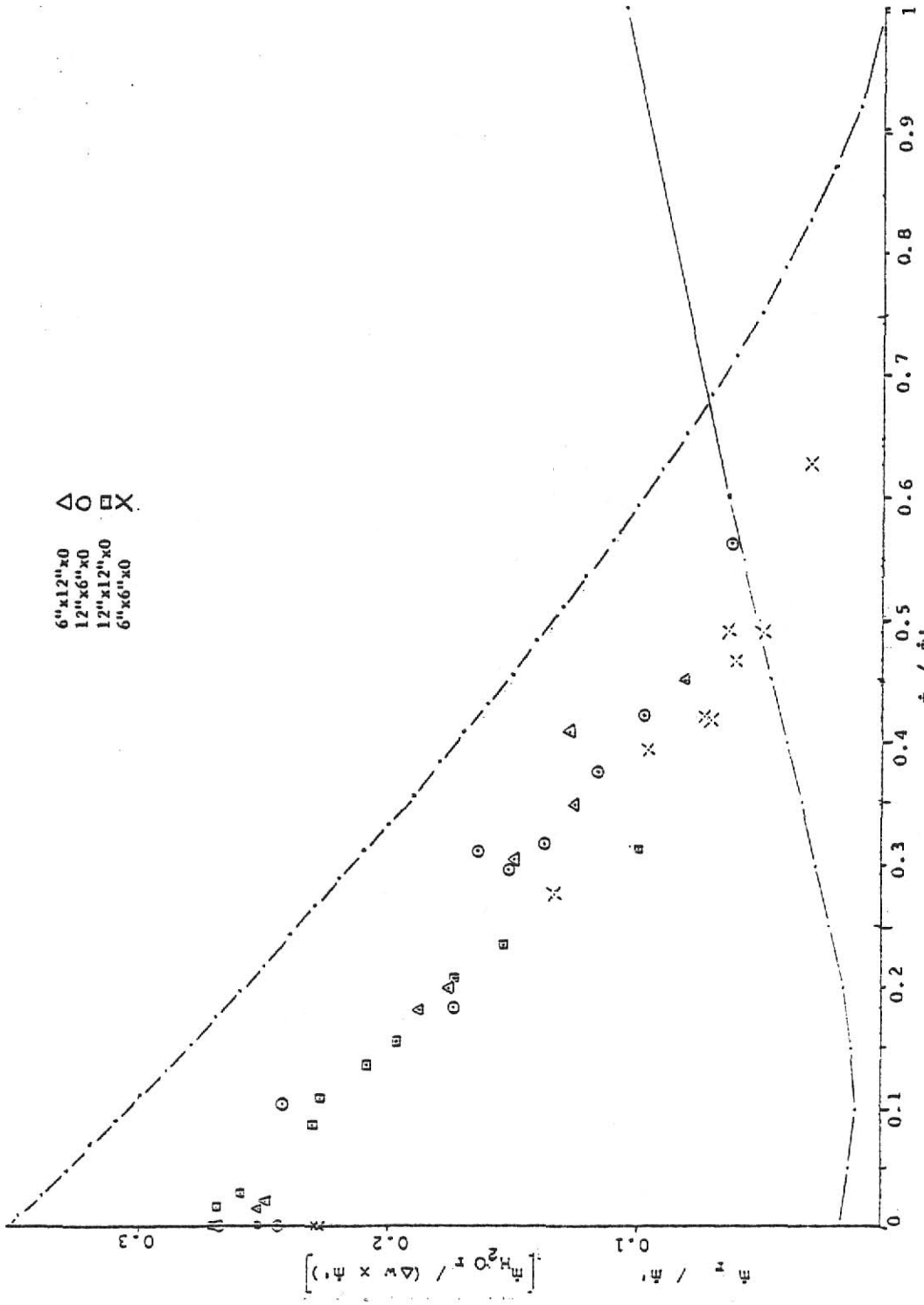

Figure 16

Zero Length Openings with Error Curve

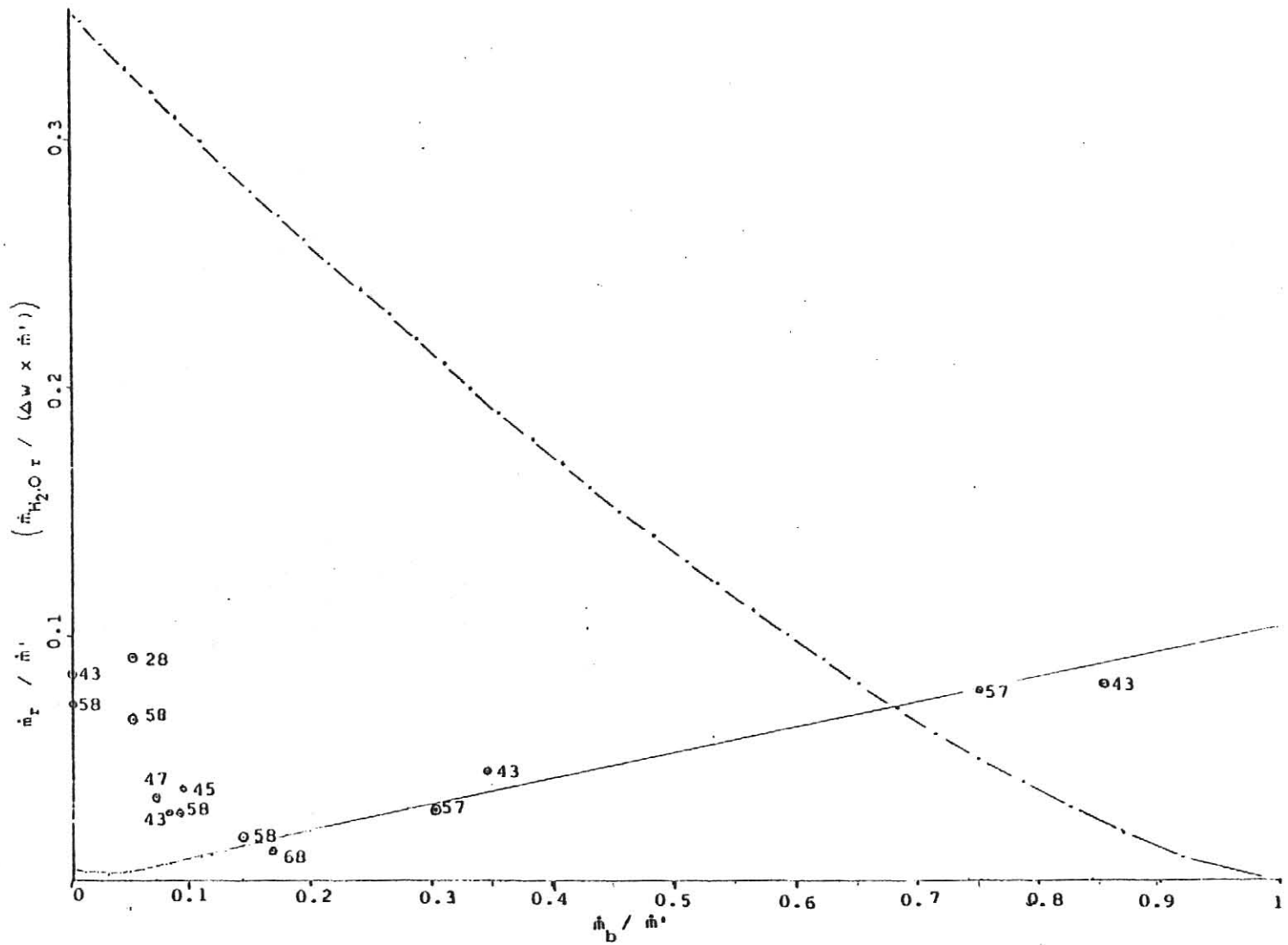

Figure 17

6x6x12 inch opening with error curve

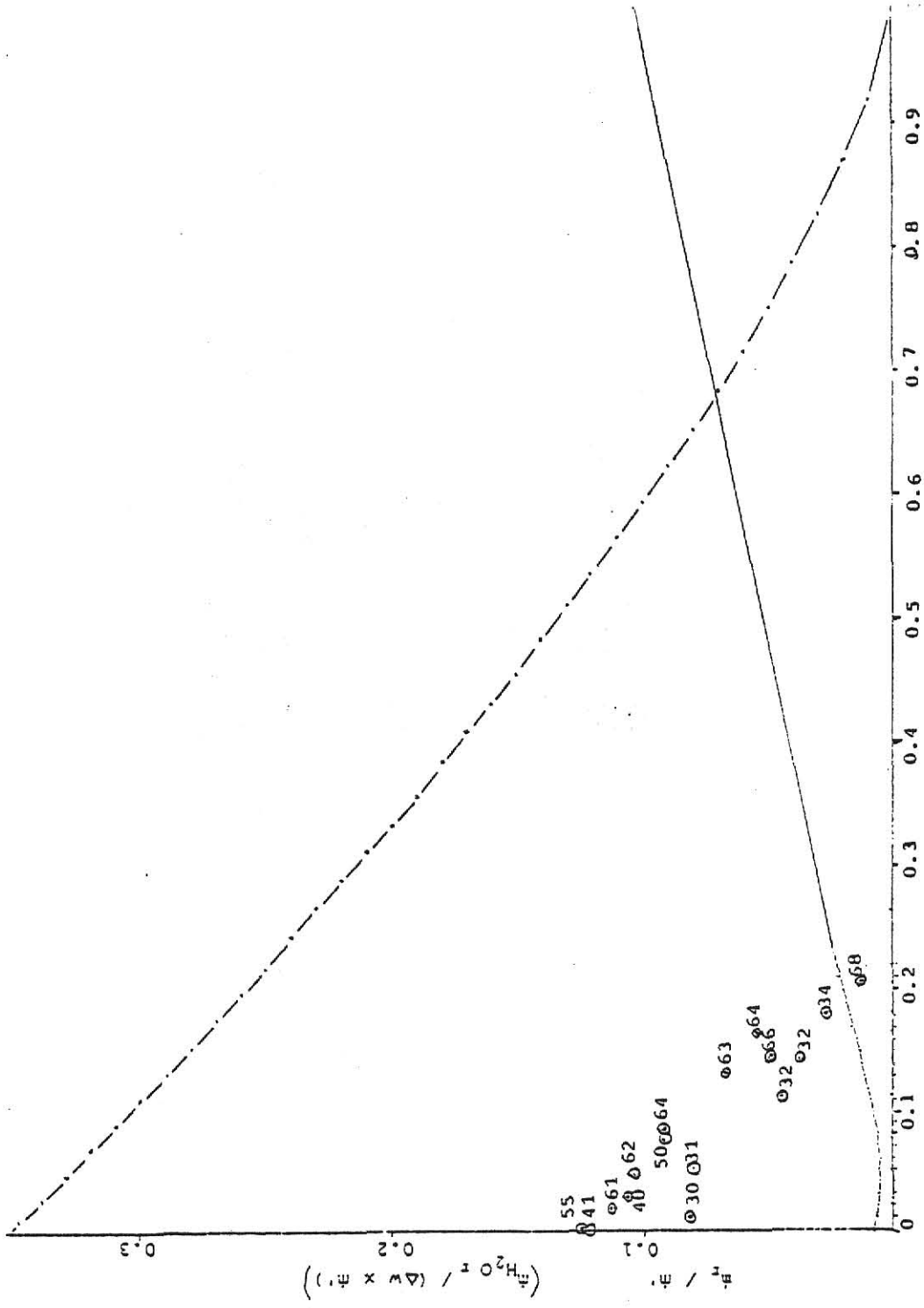

Figure 18

12x12x12 inch opening with error curve

CHAPTER V

CONCLUSIONS

Work in this thesis was based upon measured experimental test data of water vapor transfer occurring through a rectangular opening in a vertical partition. The data was taken using a specially constructed test chamber, described in Chapter 3. To facilitate the comparison of data taken under varying conditions (different temperature differences, humidity differences and opening width and height dimensions) a data reduction was designed from a model of the test situation considering the convection mass interchange occurring through the opening and the likely influence of these variables upon that interchange.

The development of the model's ideal air and water vapor mass interchange relationship was based upon an assumption of similarly shaped natural convection velocity profiles at the opening. The scales of the height and length of the velocity profile are determined by the opening's height and the air conditions associated with the driving force for natural convection, the pressure difference across the opening varying locally with vertical level. Associated with the similar convection velocity profiles are rates of mass interchange for both air and water vapor, assumed to move together the diffusion of water vapor independent of total air movement is assumed neglible.

For natural convection alone there is no net interchange of air through the opening, the forward air flow is equal to the reverse flow. For combined forced and natural convection the net mass flowrate through the opening the net mass flowrate through the opening, due to forced convection, is superimposed upon the natural convection interchange, due to air conditions, shifting the opening's similarly shaped velocity profile up or down.

The ideal air interchange equations for flow through the opening are expressed in terms of the net flowrate, forward flow, and the reverse component of flow, that in the opposite direction of the net. To directly relate these

ideal mass flowrates to the geometry of the simple convection velocity and mass flux profiles being assumed and to scale test results for comparison purposes a common normalizing factor, $\dot{m}'$ equation (9), was used on the net and reverse mass flowrates. The ideal relationship between the normalized reverse and bulk flowrates are given in equation (15) for air alone and equation (20) for the measured reverse flow of water vapor. Higher values of the normalized reverse mass flowrate, $\dot{m}_r / \dot{m}'$, indicate the line of equal pressure between the two air-spaces is approaching the opening's horizontal centerline and a greater potential for water vapor transfer, in the reverse flow direction, exists. Lower values of $\dot{m}_r / \dot{m}'$ indicated the neutral pressure line was in the vicinity of the top of the opening, for the apparatus configuration used in this study, or the bottom of the opening for forward flow from the warmer space to the cooler.

Based upon the ideal equations relating normalized flowrates to the distances from the from the line of equal pressure between the two spaces to the top and bottom of the opening when $\dot{m}_b / \dot{m}' = 0$, $\dot{m}_r / \dot{m}' = [1/2]^{3/2} = 0.354$ and when $\dot{m}_r / \dot{m}' = 0$, $\dot{m}_b / \dot{m}' = 1$.

Similar to the simplifying reduction in the development of the ideal normalized reverse and bulk flow equation the actual data taken was reduced to allow it to be graphed on a normalized reverse and net bulk mass flowrate coordinate system. The graphs of actual data collected are plotted with the ideal case curve, based on similar and superimposed similar velocity and mass flux profiles, in figures 6 - 13. Six opening configurations' graphs are presented; four zero length: 6x6, 12x12, 6x12 and 12x6 inches; and two openings with lengths other than zero: 6x6x12 and 12x12x12 inches.

Graphed data from zero length openings shows fair comparison between different geometries and appears to be parallel to, but offset from the ideal. The offset distance between the ideal and actual curve, figure 14, is believed to be due to the effects of air's viscosity or mixing of the two air streams.

The model developed using the normalizing parameter $\dot{m}'$ appears to compensate reasonably well for different temperatures, 2 dimensional geometry and bulk air flow conditions.

Plots of actual data from openings with length are shifted towards lower values of normalized reverse flow, figures 10 and 12, with some other distortion of the curve's slope also appearing. The data taken for different opening geometries with length is limited to two square openings, the 12x12x12 inch with a ratio of L/H = 1 and the 6x6x12 inch opening with a ratio of L/H = 2. At conditions where no net bulk flow exists through the opening, when $\dot{m}_b/\dot{m}' = 0$, the value of the normalized reverse flow, $\dot{m}_r/\dot{m}'$, is roughly 50 % for L/H = 1 and 40 % for L/H = 2 of the value of $\dot{m}_r/\dot{m}'$ for zero length openings.

For the zero length openings the actual values of $\dot{m}_r/\dot{m}'$ appear to be lower than the predicted ideal by a constant amount rather than a fraction of the value (the ideal and actual curves appear to have the same slopes). For the two openings with length, in addition to the reduction in $\dot{m}_r/\dot{m}'$ by a constant amount, there appears to be some changing in the slope of the actual curves. The data taken using the opening with L/H = 1 shows a decrease in (more negative) slope but the opening with L/H = 2 does not appear to support this trend. This might suggest that in adding length or imposing a bulk flow through the opening, or both, to control or reduce the value of $\dot{m}_r/\dot{m}'$ some contributing effects might come into play that have yet to be explained.

More study of the effects of length addition, especially for non square openings, is needed to determine what sort of relationship exists between $\dot{m}_r/\dot{m}'$ and $\dot{m}_b/\dot{m}'$ for $L/H \neq 0$. By studying non square openings with length some insight might be gained into what sort of friction effects are occurring at the opening's edges and how much viscous effects there are around the length of the perimeter, especially for vertical edges where the velocity changes with the vertical level. A continuation of the experimental work measuring water vapor transport through openings could be used to supplement existing theories or develop new ones.

REFERENCES

1. McDermott, P.F., "Moisture Migration, A Survey of Theory and Existing Knowledge," Refrigerating Engineering, Vol. 42, August 1941, pp. 103-111.

2. Babbit, J.D., "The Diffusion of Water Vapor Through a Slit in an Impermeable Membrane," Canadian Journal of Research, Vol. 19, March 1941, pp. 42-55.

3. Queer, E.R., E.R. McLaughlin, "What Vapor Transmission Rules Apply When Planning for Dehumidification?," Heating, Piping & Air Conditioning, January 1958, pp. 144-148.

4. Wilson, A.G. and E.S. Nowak, "Condensation Between the Panes of Double Windows," ASHRAE Transactions, Vol. 65, 1959, pp. 551-570.

5. Davis, W.J., "Moisture Flow Up a Moving Air Stream," Special Project, University of Alabama, December 1972.

6. Brown, W.G. and K.R. Solvason, "Natural Convection Through Rectangular Openings in Partitions, Part 1 - Vertical Partitions," International Journal of Heat and Mass Transfer, Vol. 5, September 1962, pp. 859-868.

7. Brown, W.G., A.G. Wilson and K.R. Solvason, "Heat and Moisture Flow Through Openings by Convection," ASHRAE Journal, Vol. 5, No. 9, September 1963, pp. 49-54; also ASHRAE Transactions, Vol. 69, 1963, pp. 351-357.

8. Solvason, K.R., "Large-Scale Wall Heat-Flow Measuring Apparatus," ASHRAE Transactions, Vol. 65, 1959, pp. 541-550.

9. Shaw, B.H., "Heat and Mass Transfer by Natural Convection and Combined Natural Convection and Forced Air Flow Through Large Rectangular Openings in a Vertical Partition," The Institution of Mechanical Engineers, 1972, pp. 31-39; Proceedings of a Symposium arranged by the Thermodynamics and Fluid Mechanics Group of IME at the University of Manchester, September 15, 1971.

10. American Soc. Heating Refrigeration and Air-Conditioning Engineers, Inc., ASHRAE Handbook 1977 Fundamentals, Ch. 21, p. 21.2, Equation (2).

Appendix A

Data Reduction Process

As a further explanation of the procedure involved in running a test and reducing the data taken a typical test sheet and the calculations necessary to reduce this data to the corresponding values of $\dot{m}_r/\dot{m}'$ and $\dot{m}_b/\dot{m}'$ to obtain a point on the graph of figure 2 are given in table 1 for a 6 x 12 x 0 inch opening. The results of tests made in this study for all opening configurations are presented in table 2 and separate graphs of the data points calculated for each opening are plotted in figures 6 through 13 where figures 11 and 13 are duplications of the data for openings graphed in figures 10 and 12 respectively, with magnified scales on each axis.

The humidity generator water consumption rate, $\dot{m}_{H_2O}$, was determined from a simple calculation using the volume of water used to maintain conditions in the sealed, humid, chamber and the interval of time, Δt, over which that volume of water was consumed.

$$\dot{m}_{H_2O} = \frac{\text{Volume of water in ml.}}{\Delta t \ (454 \ ^{ml}/_{lbm})}$$

From the effective dewpoint, or saturation, temperatures for the air in the exit section and in the spaces on the hot and cold sides of the opening; the averaged values of channels 1, 3 and 7 of the dewpoint sampling system; the vapor pressures of water in the three air spaces sampled; P_{01}, P_{03} and P_{07}; are obtained in units of pounds per square foot from the steam tables.

The total air pressure, barometric pressure in compatible units of pounds per square foot, is determined from the barometer's mercury column height.

$$P_{atm} = \frac{\text{inches Hg}}{29} \times 2051$$

The density of air moving through the flowmeter, since channel 1 of the

humidity sampling system monitored the exit air, and the humidity ratio of air at the meter are calculated using ideal gas equations.

$$\rho_{meter} = \left(\frac{P_{atm} - P_{01}}{53.35} + \frac{P_{01}}{85.76}\right) \frac{1}{T_{meter}}$$

$$w_{meter} = \frac{P_{01}}{P_{atm} - P_{01}} \; 0.6234$$

The value of the flowmeter constant, c, as a function of the pressure drop through the flowmeter, $\triangle P$, can be determined from the graphed flowmeter calibration data in figure 19 or by one of the approximating linear equations of values of c for the applicable range of $\triangle P$. Note that the abcissa of the calibration graph, figure 19, is greatly expanded and that for the range of $\triangle P$ the value of c varies by less than 10 percent.

The mass flowrate of dry air both exiting the sealed chamber through the flowmeter and entering the chamber through the opening can be calculated from conditions at the meter.

$$\dot{m}_{da} = \frac{\rho_{meter} \triangle P}{c} / (1 + w_{meter})$$

The humidity ratios, w_1 and w_2, and the densities, ρ_1 and ρ_2, of air on both sides of the opening can be calculated from partial and total pressure data.

$$w_1 = \frac{P_{07}}{P_{atm} - P_{07}} \times 0.6234$$

$$w_2 = \frac{P_{03}}{P_{atm} - P_{03}} \times 0.6234$$

$$\triangle w = w_2 - w_1$$

$$\rho_1 = \left(\frac{P_{atm} - P_{07}}{53.35} + \frac{P_{07}}{85.76}\right) \frac{1}{T_1}$$

Figure 19

Flowmeter Calibration Data Chart

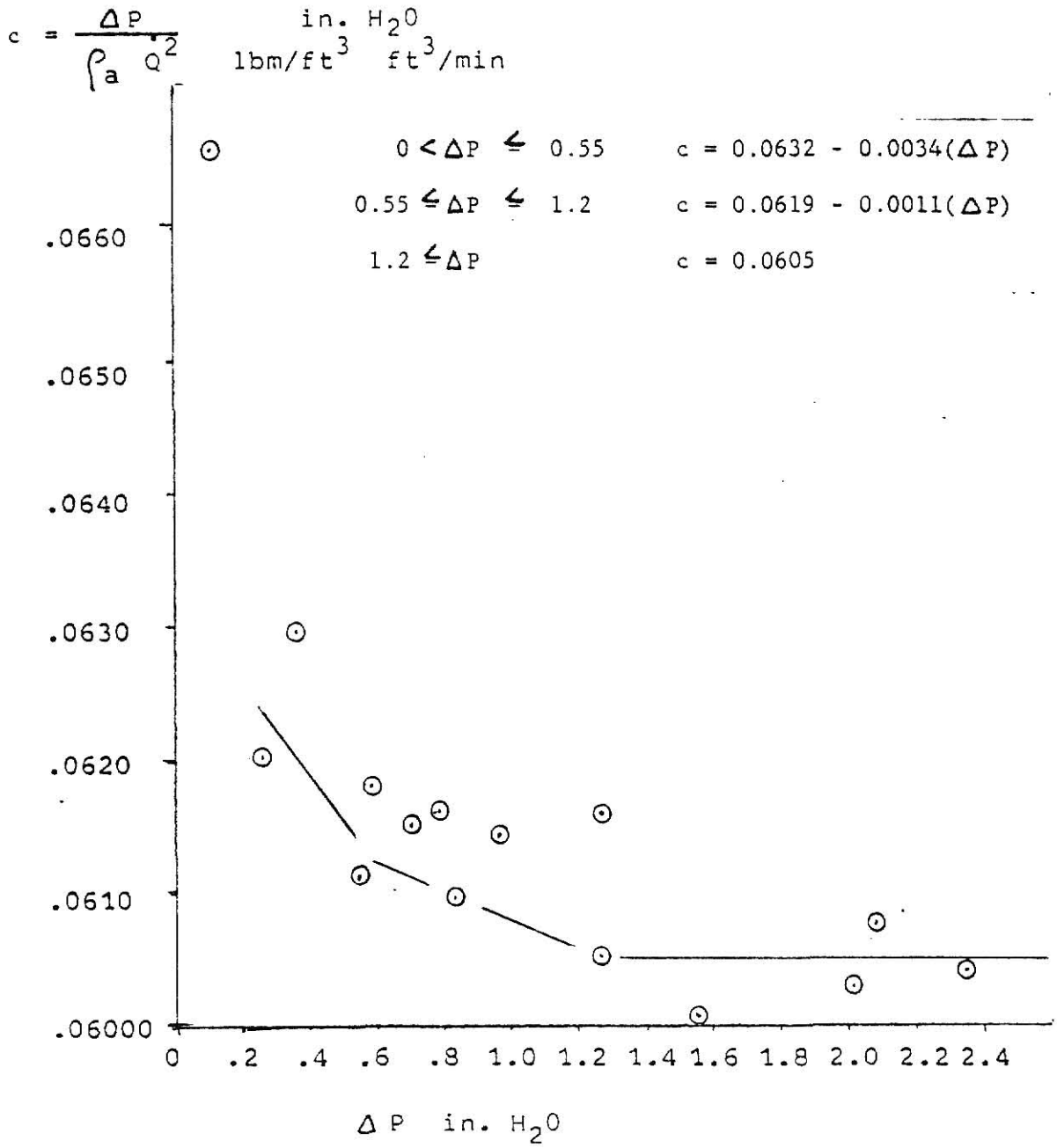

Annubar flowmeter, 1.049 in. D, the scale of c is magnified. A means of visualizing c as a function of Δ P with a curve or set of lines for greater accuracy within the flowrange desired, used in data reduction.

$$\rho_2 = \left(\frac{P_{atm} - P_{03}}{53.35} + \frac{P_{03}}{85.76}\right) \frac{1}{T_2}$$

The net bulk flow, $\dot{m}_b$ from space 1 to 2, and the reverse water vapor flow, $\dot{m}_{H_2O\ r}$ component of total flow from space 2 to 1, for the opening can be calculated.

$$\dot{m}_b = \dot{m}_{da}\ (1 + w_1)\ 60$$

$$\dot{m}_{H_2O\ r} = \dot{m}_{H_2O} - \dot{m}_{da}\ (w_{meter} - w_1)\ 60$$

The magnitude of reverse flow of vapor out the opening compared with the net flow of vapor through the opening and with the vapor flowing out the exit section give an indication of what type of accuracy can be expected in using the mass balance.

As an indication of the relative magnitude of reverse flow the ratio of reverse to bulk flow at the opening

$$\frac{\dot{m}_{H_2O\ r}}{\dot{m}_{H_2O\ b}}_{\text{open}} = \frac{\dot{m}_{H_2O\ r}}{\dot{m}_{da} \cdot w_1}$$

and the ratio of reverse to bulk flow at the meter are calculated

$$\frac{\dot{m}_{H_2O\ r}}{\dot{m}_{H_2O\ b}}_{\text{meter}} = \frac{\dot{m}_{H_2O\ r}}{\dot{m}_{da} \cdot w_{meter}}$$

where the units on $\dot{m}_{da}$ are compatible with those associated with reverse flow.

With average values of the temperature, $\bar{T}$, and vapor pressure, $\bar{P}_o$, the average density, $\bar{\rho}$, and subsequently the normalizing flow coefficient, $\dot{m}'$, can be calculated

$$\bar{P}_0 = \frac{P_{03} + P_{07}}{2}$$

$$\bar{T} = \frac{T_1 + T_2}{2}$$

$$\bar{\rho} = \left[\frac{P_{atm} - \bar{P}_0}{53.35} + \frac{\bar{P}_0}{85.76}\right] \frac{1}{\bar{T}}$$

$$\dot{m}' = \frac{2}{3} W \bar{\rho} \sqrt{2 g \bar{T} H^3 \left(\frac{1}{T_1} - \frac{1}{T_2}\right)} \quad \times 3600$$

The normalized bulk and reverse flows may not be calculated and graphed. (figure 2)

$$\frac{\dot{m}_{H_2O\ r}}{\Delta w\ \dot{m}'} = \frac{\dot{m}_r}{\dot{m}'} = \text{abcissa of graph}$$

$$\frac{\dot{m}_b}{\dot{m}'} = \text{ordinate of graph}$$

Error Analysis

Because the data taken in this study is presented graphically using the theoretical analysis from Chapter 2 the results of an error analysis, to be applicable to the data as presented, should also be graphable on the developed system of coordinates. (figure 2) The normalized mass flow terms of the opening's convection velocity profile, $\dot{m}_b / \dot{m}'$ and $\dot{m}_r / \dot{m}'$, are determined by using the measured values of the controlable variables; temperatures, dewpoint temperatures, the opening's geometry and the net flowrate through the opening; and the measured value of the observed variable, the humidity generator water consumption rate.

Relating the anticipated magnitude of errors in these measured quantities to errors on the graph, figure 2, requires a sensitivity analysis using equations in Chapter 2 and Appendix A and does not directly yield the desired magnitude of errors in $\dot{m}_r / \dot{m}'$ for specific values of $\dot{m}_b / \dot{m}'$. Determination of the sensitivity of $\dot{m}_r / \dot{m}'$ to errors in $\dot{m}_b / \dot{m}'$ is not straight forward from the ideal relationship, equation (15), but by making some linear approximations and using a sensitivity and error analysis to rule out possible errors in particular measurments that do not make a significant contribution to errors in $\dot{m}_b / \dot{m}'$ and $\dot{m}_r / \dot{m}'$, an estimation of the error relationships can be made.

For simplicity most of the root mean squared combination of contributing error sensitivity products is done using absolute errors and sensitivities rather than normalized percentage or fraction errors, since the desired result is an absolute error in the normalized reverse flowrate, $\dot{m}_r / \dot{m}'$, and expressing the result in percentage errors might lead to a confusing situation. Although in some cases the use of normalized errors lends itself to a description of the expected errors, as a percentage of the reading, or

simplifies the notation of the error sensitivity combination so that a a familiarity of what is implied in using both absolute, E, and normalized, e, errors and sensitivities, S and s, is necessary. Error magnitudes are given as the limit of error within which presumably 95 percent of all measurments will fall.

Measurment Instrumentation

Water volume measurments were made with an ASTM Pyrex 100 ml. graduated cylinder. Smallest division = 1 ml, $E = \pm 0.707$ ml. $e_{m_{H_2O}} = \frac{0.707}{100} = \pm 0.707$ % since cylinder is refilled every 100 ml.

Time measurments were made with a Micronta digital pocket stopwatch Serial # 10A9. In normal time mode smallest increment = 1 sec. $E = \pm 1$ sec. In chronometer mode smallest increment = 0.01 sec. $E = \pm 0.01$ sec.

Air temperatures inside the chamber were measured using copper constantan thermocouples. Eight junctions on the cold side and 3 junctions on the hot side were averaged to give effective air temperatures. For single junctions the limit of error is generally accepted as ± 1.5 °F. All thermocouple outputs were measured using the same Leeds and Northrup Millivolt Potentiometer Serial # 1700628 with reference junction compensation. Reference junction temperatures were determined with a mercury in glass thermometer, Western Machine Co. Serial # 92367 with a range of 20-220 °F, smallest division = 2 °F. $E_T = E_{mes} + E_{ref} = \sqrt{(1.5)^2/3 + 2} = \pm 1.66$°F.

$E_{\Delta T} = (1.5)\sqrt{1/3 + 1/8} = \pm 1$ °F

Air flow measurments were made with a 1.049 inch diameter Annubar flowmeter Serial # 183158. The pressure drop across the flowmeter was read with a Meriam Micromanometer filled with water Serial # L75571, smallest division = 0.001 inch water. The flowmeter micromanometer combination was calibrated with a bell prover and the stopwatch in the chronometer mode, calibration

data table 4. The errors in time interval measurments were probably mostly due to human reaction/anticipation. No error specifications for the prover were available although it had been previously disassembled and examined for integrity. Random flowmeter errors have been estimated using the calibration data and systematic errors in all but the bell prover, assumed to be neglible, are self canceling from calibration. $e_{\dot{q}} = \pm 0.075 = \pm 7.5\%$, $E_{\dot{q}} = \pm 0.075\ \dot{q}$

Flowmeter air temperatures were measured using a Thunder Scientific Electronic Temperature Sensor Serial # 7904201. $E = \pm 0.35^{\circ}C = \pm 0.63\ ^{\circ}F$

Dewpoint temperatures of the air on both sides of the opening and passing through the flowmeter were measured using an E G and G Digital Humidity Analyzer Serial # 00422. $E = \pm 0.3\ ^{\circ}C = \pm 0.54\ ^{\circ}F$

Atmospheric pressure was determined using a mercury filled barometer with vernier scale movement, smallest division = 0.01 inches Hg.
$E = \sqrt{2}\ (0.005)\ 2051/29 = \pm 0.52\ lbf/ft^2$

Opening dimensions were measured with a graduated rule smallest division = 1/8 inch. $E = \pm \sqrt{2}/16\ /12 = \pm 0.0074$ ft. The errors in the length, width and height are dependent.

Turbulent air velocity within the chamber, related in some way to the flow coefficient or coefficient of discharge of the opening, was measured with an Anemotherm Air Meter Serial # 14082. The published specifications list the limit of error as $\pm$ 4 fpm however the readings were observed to fluctuate quite a bit so a more realistic value would be $\pm$ 10 fpm. Ultimately no means of coordinating turbulent velocity measurments into the reduced form of data were determined anyway.

Errors in Preliminary Variables

Because of the switching of the on/off controllers that regulated

Table 4

Annubar Flowmeter Calibration

Volume of Prover (ft^3)	Average Time Span (sec)	Average $\triangle P$ (in. water)	$\dot{Q} = \frac{\text{Volume}}{\triangle t}$ (cfm)	air density (lbm/ft^3)	$\dot{m}$ actual (lbm/min)	$\dot{m}$ predicted (lbm/min)	error size m %	$\frac{\triangle P}{\dot{Q}^2 \text{ air density}}$
4	12.727	1.549	18.857	.07249	1.367	1.362	.341	.06009
4	19.125	0.7002	12.532	.07249	.9084	.9112	.310	.06150
4	14.38	1.243	16.69	.07249	1.210	1.220	.858	.05156
3	7.798	2.335	23.088	.07248	1.673	1.673	.028	.06044
4	16.343	0.960	14.685	.07248	1.064	1.069	.507	.06142
4	18.08	0.787	13.278	.07248	.9624	.9670	.479	.06159
4	11.133	2.031	21.558	.07248	1.563	1.559	.201	.06029
3	15.685	0.584	11.485	.07248	.8324	.8316	.090	.06108
3	20.23	0.361	8.896	.07248	.6448	.6497	.759	.06294
3	37.38	0.112	4.818	.07248	.3492	.3595	2.96	.06657
3	23.73	.225	7.585	.07148	.5498	.5075	7.69	.06200
3.5	9.60	2.080	21.88	.07155	1.566	1.568	.186	.06075
3.5	12.40	1.242	16.94	.07155	1.212	1.212	.008	.06049
3.5	15.285	0.823	13.74	.07155	.9831	.9862	.325	.06094
3	16.28	0.534	11.055	.07148	.8013	.7885	1.59	.06113

temperature and dewpoint temperature within the sealed chamber the measured values of the time, temperature and dewpoint temperatures could only be resolved as accurately as the cycling of the conditions within the sealed chamber allowed. A more conservative value of E has been assigned to these measurments based upon the previously stated instrument errors and commonly observed scatter conditions. Dewpoint temperatures were observed to fluctuate in regular cycles, due to long time constant effects of sampling lines and the humidity generator response time, $E_{T_{dp}} = \pm 2\ ^{o}F$. Temperatures only fluctuated slightly so the major portion of E_T is still due to measurment instrumentation, $E_T = \pm 2\ ^{o}F$. Irregularities in the length of time for full cycles of humidity conditions were not that serious considering the typical length of time for tests, Δt, was 2 hours. $E_{\Delta t} = \pm 30$ sec. $= \pm 0.0083$ hour.

To determine densities and humidity ratios a knowledge of water vapor pressures and total atmospheric pressure are necessary. The absolute sensitivities, to errors in dewpoint temperatures, of vapor pressures and humidity ratios are dependent upon the value of the saturation, dewpoint, temperature and have been determined for the anticipated range of saturation temperatures using the steam tables and ideal gas law of partial pressures.

Table 5

T_{sat}	20	25	30	40	45	50	55	60
$\frac{\partial w}{\partial T_{sat}} \times 10^4$	1.08	1.32	1.55	2.11	2.51	2.98	3.51	4.13
$\frac{\partial P_0}{\partial T_{sat}}$	.351	.428	.504	.682	.809	.958	1.12	1.31

Proceedure to Relate Errors in Variables to Errors on Graph

Equation (15) relating the ideal values of the normalized bulk and reverse flow terms is not explicitly solveable for the normalized reverse flow because of the exponentiation involved. The actual data points do not fall on the ideal curve anyway although the slope of an estimated real curve, or line, through the data points plotted for all zero length openings would nearly equal the slope of the ideal curve. The fastest means of estimating a the sensitivity of $\dot{m}_r/\dot{m}'$ to errors in $\dot{m}_b/\dot{m}'$ is a linear approximation from graphed data points.

Because the graphing scheme devised involves the normalizing parameter, $\dot{m}'$ along both axes it is desireable to demonstrate that $E_{\dot{m}'}$ makes a neglible error contribution so that errors in $\dot{m}_r/\dot{m}'$, $E_{\dot{m}_r/\dot{m}'}$, are mostly attributable to $E_{\dot{m}_r}$.

$$E_{(\dot{m}_r/\dot{m}')} = \left[\left(S^{(\dot{m}_r/\dot{m}')}_{\dot{m}_r} \; E_{\dot{m}_r}\right)^2 + \left(S^{(\dot{m}_r/\dot{m}')}_{\dot{m}'} \; E_{\dot{m}'}\right)^2\right]^{1/2}$$

$$= \left[\left(\frac{1}{\dot{m}'} \; E_{\dot{m}_r}\right)^2 + \left(\frac{-\dot{m}_r}{(\dot{m}')^2} \; E_{\dot{m}'}\right)^2\right]^{1/2}$$

If $E_{\dot{m}'}$ is of neglible value then $E_{(\dot{m}_r/\dot{m}')} = E_{\dot{m}_r} / \dot{m}'$.

Substituting the expressions for $\bar{\rho}$ and $\bar{T}$ into equation (9)

$$\dot{m}' = \frac{2}{3}\left[\frac{P_{atm} - \bar{P}_0}{53.35} + \frac{\bar{P}_0}{85.76}\right] W\sqrt{4\,g\,H^3\,\frac{T_2 - T_1}{T_1\,T_2\,(T_1+T_2)}}$$

Since T_1 and T_2 were determined using the same potentiometer and reference junction and since the primary driving force for convection is the temperature difference, $\Delta T = T_2 - T_1$, $\dot{m}'$ is reexpressed in terms of T_1 and ΔT.

$$\dot{m}' = \frac{2}{3}\left[\frac{P_{atm}-P_0}{53.35} + \frac{P_0}{85.76}\right] W\sqrt{4\,g\,H^3\,\frac{\Delta T}{T_1(T_1+\Delta T)(2T_1+\Delta T)}}$$

$$E_{\dot{m}'} = \left[\left(S^{\dot{m}'}_{P_{atm}} E_{P_{atm}}\right)^2 + \left(S^{\dot{m}'}_{P_0} E_{P_0}\right)^2 + \left(S^{\dot{m}'}_{W} E_W\right)^2 + \left(S^{\dot{m}'}_{H} E_H\right)^2 + \left(S^{\dot{m}'}_{T_1} E_{T_1}\right)^2 + \left(S^{\dot{m}'}_{\Delta T} E_{\Delta T}\right)^2\right]^{1/2}$$

To evaluate the various sensitivities typical values, for all tests made, of some variables are used; $P_{atm} = 2051$ lbm/ft^3, $\overline{P}_0 = 25$ lbm/ft^3 $T_{sat} = 49.5$, T_1 varied from 500 to 535 °R typically close to 515 °R and ΔT varied from 0 to 70 °R with a typical value of 35 °R.

$$S^{\dot{m}'}_{P_{atm}} = \frac{2}{3}\frac{1}{53.35} W\sqrt{4\,g\,H^3\,\frac{\Delta T}{T_1(T_1+\Delta T)(2T_1+\Delta T)}} \quad \text{slightly greater than} \quad \frac{\dot{m}'}{2051}$$

$$S^{\dot{m}'}_{P_0} = \frac{2}{3}\left[\frac{-1}{53.35}+\frac{1}{85.76}\right] W\sqrt{4\,g\,H^3\,\frac{\Delta T}{T_1(T_1+\Delta T)(2T_1+\Delta T)}} = -0.0001851\,\dot{m}'$$

$$S^{\dot{m}'}_{W} = \frac{\dot{m}'}{W} \qquad s^{\dot{m}'}_{W} = 1 \qquad S^{\dot{m}'}_{H} = \frac{3}{2}\frac{\dot{m}'}{H} \qquad s^{\dot{m}'}_{H} = \frac{3}{2}$$

$$S^{\dot{m}'}_{T_1} = -\dot{m}'\,\frac{3T_1^2 + 6T_1\Delta T + \Delta T^2}{T_1^3 + 3T_1^2\Delta T + T_1\Delta T^2} \qquad S^{\dot{m}'}_{\Delta T} = \dot{m}'\,\frac{T_1^2 - \Delta T^2}{T_1^2\Delta T + 3T_1\Delta T^2 + \Delta T^3}$$

$$E_{\dot{m}'} = \dot{m}'\sqrt{\left(\frac{0.52}{2051}\right)^2 + \left(.000185(2)0.958\right)^2 + \left((1+\tfrac{3}{2})0.0074\right)^2 + \left(s^{\dot{m}'}_{T_1} E_{T_1} T_1\right)^2 + \left(s^{\dot{m}'}_{\Delta T} E_{\Delta T}\Delta T\right)^2}$$

The largest contribution to $E_{\dot{m}'}$ comes from $E_{\Delta T}$.

Table 6

T_1	500	535	500	500	500	515	515	515	535	535
ΔT	0	0	1	35	70	1	35	70	1	70
$S^{\dot{m}'}_{T_1} E_{T_1}/\dot{m}'$	.012	.011	.012	.011	.011	.012	.011	.010	.011	.010
$S^{\dot{m}'}_{\Delta T} E_{\Delta T}/\dot{m}'$	∞	∞	.994	.023	.010	.994	.024	.010	.994	.010

If ΔT is greater than 10 °F then $e_{\dot{m}'}$ is less than 10 percent and for most experimental situations, where $\Delta T > 20$ °F, $e_{\dot{m}'}$ was less than 5 percent.

A comprehensive evaluation of the possible errors occuring in the measurment of the bulk flow of air passing through the meter, $\dot{m}_{meter}$, would require a sensitivity analysis of the flowmeter equation and the errors in measuring the pressure drop across the meter with the micromanometer and in determining the density of air passing through the meter. Also the deviation of the flowmeter from behavior predicted by the ideal flowmeter equation, the pressure drop being shown to the micromanometer by the flowmeter, might need to be considered. The possible errors in calibrating the flowmeter with the bell prover include the density of air in calibration, the interval of time measured and volume graduations on the bell prover.

Due to the complexity of a statistical analysis of all possible error sources a simpler estimation of the possible error occuring in measuring $\dot{m}_{meter}$ was performed by evaluating the scatter of the calibration data and its deviation from the value of $\dot{m}_{meter}$ predicted using the ideal flowmeter equation for specific values of $\rho_{meter} \Delta P$. This neglects the possibility of a systematic error in the bell prover but if some means of evaluating the accuracy of the prover is devised and systematic errors are found to exist it should be possible to retroactively correct values of $\dot{m}_{meter}$ determined. The assumption that random errors in calibration were of the same order of magnitude as the random errors in measuring flow with the meter allows a value of $e_{\dot{m}_{meter}}$ close to 7.7 percent to be selected. (see table 4) Assume that $E_{\dot{m}_{meter}} = 0.075\ \dot{m}_{meter}$

For sufficiently large ΔT, so that $E_{\dot{m}'}$ is neglible, $E_{(\dot{m}_b/\dot{m}')} = E_{\dot{m}_b} / \dot{m}'$.

$$\dot{m}_b = \frac{\dot{m}_{meter}\ (1 + w_1)}{1 + w_{meter}}$$

If ΔT is greater than 10 ^{o}F then $e_{\dot{m}'}$ is less than 10 percent and for most experimental situations, where $\Delta T > 20\ ^{o}F$, $e_{\dot{m}'}$ was less than 5 percent.

A comprehensive evaluation of the possible errors occuring in the measurment of the bulk flow of air passing through the meter, $\dot{m}_{meter}$, would require a sensitivity analysis of the flowmeter equation and the errors in measuring the pressure drop across the meter with the micromanometer and in determining the density of air passing through the meter. Also the deviation of the flowmeter from behavior predicted by the ideal flowmeter equation, the pressure drop being shown to the micromanometer by the flowmeter, might need to be considered. The possible errors in callibrating the flowmeter with the bell prover include the density of air in callibration, the interval of time measured and volume graduations on the bell prover.

Due to the complexity of a statistical analysis of all possible error sources a simpler estimation of the possible error occuring in measuring $\dot{m}_{meter}$ was performed by evaluating the scatter of the callibration data and its deviation from the value of $\dot{m}_{meter}$ predicted using the ideal flowmeter equation for specific values of $\rho_{meter}\Delta P$. This neglects the possibility of a systematic error in the bell prover but if some means of evaluating the accuracy of the prover is devised and systematic errors are found to exist it should be possible to retroactively correct values of $\dot{m}_{meter}$ determined. The assumption that random errors in callibration were of the same order of magnitude as the random errors in measuring flow with the meter allows a value of $e_{\dot{m}_{meter}}$ close to 7.7 percent to be selected. (see table 4) Assume that $E_{\dot{m}_{meter}} = 0.075\ \dot{m}_{meter}$

For sufficiently large ΔT, so that $E_{\dot{m}'}$ is neglible, $E_{(\dot{m}_b/\dot{m}')} = E_{\dot{m}_b} / \dot{m}'$.

$$\dot{m}_b = \frac{\dot{m}_{meter}\ (1 + w_1)}{1 + w_{meter}}$$

$$E_{\dot{m}_b} = \sqrt{\left(\frac{1+w_1}{1+w_{meter}} E_{\dot{m}_{meter}}\right)^2 + \left[\frac{-(1+w_1)\,\dot{m}_{meter}}{(1+w_{meter})^2} E_{w_{meter}}\right) + \left(\frac{\dot{m}_{meter}}{1+w_{meter}} E_{w_1}\right)^2\Bigg]^{-2}}$$

Typically $w_{meter} = 0.011$ and $w_1 = 0.005$. For the purpose of error analysis the dewpoint temperature and humidity ratios at the meter and on the warm side of the opening were essentially the same. $T_{dp\,meter} = T_{dp2} = 60\ ^{o}F$, $T_{dp_1} = 37\ ^{o}F$

$$E_{w_{meter}} = (0.000413)\ 2 = 0.000826 = E_{w_2} \qquad E_{w_1} = (0.000211)2 = 0.000422$$

$$E_{\dot{m}_b} = \dot{m}_{meter} \sqrt{\left(\frac{1.005}{1.011}\,0.075\right)^2 + \left(\frac{-1.005}{(1.011)^2}(.000826) + \frac{.000422}{1.011}\right)^2} = \dot{m}_{meter}\,(.0746)$$

$$= 0.746\ \frac{1 + w_1}{1 + w_{meter}}\ \dot{m}_b < 0.075\ \dot{m}_b$$

The calculation of the reverse flow of water vapor, in the direction opposite the bulk flow of air, is made using a mass balance on the sealed chamber on the warm side of the opening. The value of $\dot{m}_{H_2O\ r}$ is determined by taking the difference of two terms both of which involve differences within. The humidity generator water consumption rate term contains a time interval difference and the net water vapor carried through the exit section by the bulk flow, a humidity ratio difference.

$$\dot{m}_{H_2O\ r} = \frac{m_{H_2O}}{\Delta t} - \dot{m}_{da}(w_{meter} - w_1) \qquad (21)$$

$$\dot{m}_r = \frac{m_{H_2O}}{\Delta t(w_2 - w_1)} - \frac{\dot{m}_{da}(w_{meter} - w_1)}{w_2 - w_1}$$

$$= \frac{1}{(w_2 - w_1)} \left(\frac{m_{H_2O}}{\Delta t} - \frac{\dot{m}_b(w_{meter} - w_1)}{1 + w_1}\right) \qquad (22)$$

For use in sensitivity terms some typical values are; $w_2 - w_1 = 0.0062$ $w_{meter} - w_1 = 0.0065$, $1 + w_1 = 1.005$ and $\Delta t = 2$ hours. Also equation (21) can be rearranged to give an expression for the humidity generator water consumption rate, the observed variable, which has no typical value but appears in several sensitivity terms.

$$\dot{m}_{H_2O} = \frac{m_{H_2O}}{t} = \dot{m}_{H_2O\ r} - \dot{m}_b \frac{w_{meter} - w_1}{1 + w_1}$$

$$= \dot{m}_{H_2O\ r} - 0.00647\ \dot{m}_b$$

An error sensitivity analysis is now performed upon equation (22) for sensitivities in terms of $\dot{m}_{H_2O\ r}$ and $\dot{m}_b$ to determine $E_{\dot{m}_r}$.

$$s^{\dot{m}_r}_{w_1} = \frac{1}{w_2 - w_1} \quad \frac{1}{w_2 - w_1} \quad \dot{m}_{H_2O} - \dot{m}_b \frac{w_{meter} - w_1}{1 + w_1} \quad + \frac{\dot{m}_b}{1 + w_1} \quad 1 + \frac{w_{meter} - w_1}{1 + w_1}$$

$$= 26015\ \dot{m}_{H_2O\ r} - 175.042\ \dot{m}_b \qquad (E_{w_1} = .000422)$$

$$s^{\dot{m}_r}_{w_2} = \frac{-1}{(w_2 - w_1)^2} \quad \dot{m}_{H_2O} - \dot{m}_b \frac{w_{meter} - w_1}{1 + w_1} \quad = -26015\ \dot{m}_{H_2O\ r} + 336.57\ \dot{m}_b$$

$$(E_{w_2} = .000826)$$

$$s^{\dot{m}_r}_{w_{meter}} = \frac{1}{w_2 - w_1} \quad \frac{-\dot{m}_b}{1 + w_1} \quad = -160.5\ \dot{m}_b \qquad (E_{w_{meter}} = .000826)$$

$$s^{\dot{m}_r}_{\Delta t} = \frac{-m_{H_2O}}{(\Delta t)^2} \quad \frac{1}{w_2 - w_1} \quad = -80.65\ \dot{m}_{H_2O\ r} - 0.5218\ \dot{m}_b \qquad (E_{\Delta t} = .0083)$$

$$s^{\dot{m}_r}_{m_{H_2O}} = \frac{1}{w_2 - w_1} \quad \frac{1}{\Delta t}\ ; \quad (\dot{m}_r)\ s^{\dot{m}_r}_{m_{H_2O}} = \dot{m}_{H_2O} \frac{1}{w_2 - w_1} \quad = 161.29\ \dot{m}_{H_2O\ r} - 1.044\ \dot{m}_b$$

$$(e_{m_{H_2O}} = .00707)$$

$$s^{\dot{m}_r}_{\dot{m}_b} = \frac{-(w_{meter} - w_1)}{(1 + w_1)(w_2 - w_1)} \quad = -1.0432 \qquad (E_{\dot{m}_b} = 0.075\ \dot{m}_b)$$

The errors from humidity ratios, all determined from the same instrument, are being considered dependent.

To reduce these sensitivities further, eliminating the $\dot{m}_{H_2O\ r}$, a linear approximation of $\dot{m}_r$'s $(\dot{m}_{H_2O\ r}/(w_2 - w_1))$ relationship to $\dot{m}_b$ can be used.

From the graph of all data for zero length openings (figure 14) it is possible to visualize a linear relationship between $\dot{m}_r/\dot{m}'$ and $\dot{m}_b/\dot{m}'$. For $0 \leq \dot{m}_b/\dot{m}' \leq 0.6$;

$$\frac{\dot{m}_r}{\dot{m}'} = 0.26 - \frac{0.26}{0.6}\frac{\dot{m}_b}{\dot{m}'} = 0.26 - 0.43(\dot{m}_b/\dot{m}') .$$

For $\dot{m}_b/\dot{m}' > 0.6 \quad \dot{m}_r/\dot{m}' = 0.$

Assuming the former $0 \leq \dot{m}_b/\dot{m}' \leq 0.6$ applies

$$\dot{m}_{H_2O\ r} = (0.26\dot{m}' - 0.43\dot{m}_b)(w_2 - w_1) = .00161\dot{m}' - .00267\dot{m}_b$$

Substituting this into the various sensitivities $E_{\dot{m}_r}$ can be evaluated for the zero length opening.

$$E_{\dot{m}_r} = \Big\{\Big[\big(26015(.00161\dot{m}' - .00267\dot{m}_b) - 175.04\dot{m}_b\big).000422 + \big(-26015(.00161\dot{m}' - .00267\dot{m}_b) + 336.57\big).000826 + (-160.5\dot{m}_b).000826\Big]^2 + \Big[(.00161\dot{m}' - .00267\dot{m}_b).00707\Big]^2 + \Big[-80.65(.00161\dot{m}' - .00267\dot{m}_b).0083\Big]^2 + \Big[-1.0432(0.075\dot{m}_b)\Big]^2\Big\}^{1/2}$$

From the previously made assertion $E_{(\dot{m}_r/\dot{m}')} = E_{\dot{m}_r}/\dot{m}'$ =

$$= \Big[.0002875 - .003375(\dot{m}_b/\dot{m}') + .01605(\dot{m}_b/\dot{m}')^2\Big]^{1/2}$$

For $\dot{m}_b/\dot{m}' > 0.6$

$$E_{(\dot{m}_r/\dot{m}')} = \Big[(-175.04\,\dot{m}_b/\dot{m}').000422 + (336.57\,\dot{m}_b/\dot{m}').000826 + (-160.5\,\dot{m}_b/\dot{m}').000826^2 + -1.0432(.075\,\dot{m}_b/\dot{m}')^2\Big]^{1/2}$$

$$= 0.1060\,\dot{m}_b/\dot{m}'$$

The error curve for zero length openings is plotted on figure 16. For the 6x6x12 inch opening a linear approximation of graphed points is, from figure 11 for $0 \leq \dot{m}_b / \dot{m}' \leq 0.2$

$$\dot{m}_r / \dot{m}' = 0.08 - (0.08/0.2)\, \dot{m}_b / \dot{m}' = 0.08 - 0.4\, \dot{m}_b / \dot{m}'$$

$$\dot{m}_{H_2O\ r} = .000496\, \dot{m}' - .00248\, \dot{m}_b$$

$$E_{(\dot{m}_r/\dot{m}')} = \Big\{ \Big[\big(26015(.000496 - .00248\dot{m}_b/\dot{m}') - 175.04\dot{m}_b/\dot{m}'\big).000422 + \big(-26015(.000496 - .00248\dot{m}_b/\dot{m}') + 336.57\dot{m}_b/\dot{m}'\big).000826 + -160.5\dot{m}_b/\dot{m}'(.000826) \Big]^2 + \big[(.000496 - .00248\dot{m}_b/\dot{m}').00707\big]^2 + \big[-80.65(.000496 - .00248\dot{m}_b/\dot{m}').0083\big]^2 + \big[-1.0432(.075\dot{m}_b/\dot{m}')\big]^2 \Big\}^{1/2}$$

$$= \Big[.00002729 - .001019\dot{m}_b/\dot{m}' + .015656(\dot{m}_b/\dot{m}')^2\Big]^{1/2}$$

For $\dot{m}_b/\dot{m}' > 0.2$

$$E_{(\dot{m}_r/\dot{m}')} = 0.1060\, \dot{m}_b / \dot{m}'$$

The error curve for the 6x6x12 inch opening is plotted on figure 17. For the 12x12x12 inch opening a linear approximation of graphed points is, from figure 13 for $0 \leq \dot{m}_b / \dot{m}' \leq 0.23$

$$\dot{m}_r / \dot{m}' = 0.127 - (.127/.23)\dot{m}_b / \dot{m}' = .127 - .552\dot{m}_b / \dot{m}'$$

$$\dot{m}_{H_2O\ r} = .000787\dot{m}' - .00342\dot{m}_b$$

In an analysis similar to the previous two;

for $0 \leq \dot{m}_b / \dot{m}' \leq 0.23$

$$E_{(\dot{m}_r/\dot{m}')} = \left[.0000688 - .00178\dot{m}_b/\dot{m}' + .01769(\dot{m}_b/\dot{m}')^2\right]^{1/2}$$

For $\dot{m}_b / \dot{m}' > 0.23$

$$E_{(\dot{m}_r/\dot{m}')} = 0.1060\ \dot{m}_b / \dot{m}' .$$

The error curve for the 12x12x12 inch opening is plotted on figure 18.

The possible combined errors in determining $\dot{m}_b$ and $\dot{m}_r$ from measured values should be considered at some point although their graphical significance requires some visualization. The expected error magnitude to be encountered in $\dot{m}_r/\dot{m}'$ for various $\dot{m}_b/\dot{m}'$ can be plotted as vertical line segments on the graph relating mass flows and the errors in $\dot{m}_b/\dot{m}'$ would appear as horizontal line segments. Thus the graph's error envelope would consist of an infinite set of ellipses of uncertainty. The lengths of the ellipse's major axis, vertically, depending on the errors in $\dot{m}_r$ and the lengths of the minor axis depending on the errors in $\dot{m}_b$ an ellipse would be centered at each experimental data point and the ellipse size depending upon the data point location.

For practical purposes $E_{(\dot{m}_b/\dot{m}')}$ is insignificant compared with $E_{(\dot{m}_r/\dot{m}')}$ so that the line segment representation is sufficiently accurate.

A final consideration is now given to possible errors that could have occured by neglecting the contributing effect of water vapor in air upon the air's density. The driving force in natural convection interchange through an opening is from the difference in the density of air on both sides of the opening. The definition of $\dot{m}'$, equation (9), was evaluated for errors from variables in the definition but, in the definition, the effects of humidity in the 2 separate air masses, as far as the density difference convection driving force was concerned, were neglected. For a known range of temperature conditions

and assuming the worst case of air saturated with vapor, using the steam tables and 2 ideal gas equations one considering vapor content and one neglecting it, some rough error error estimations can be made.

$$\rho_{\text{humid air}} = \frac{1}{T}\left[\frac{P_{atm} - P_0}{53.35} + \frac{P_0}{85.76}\right] \qquad \rho_{\text{dry air}} = \frac{P_{atm}}{R\ T}$$

Table 7

Dry/Humid Air Density Errors

Temp (°F)	sat. air	dry air	%error $100 \times \frac{\rho_{s.a.} - \rho_{d.a.}}{\rho_{s.a.}}$
0	.08366	.08359	.084
40	.07675	.07690	.199
70	.07194	.07255	.848
120	.06311	.06630	5.05

Evaluating the magnitude of errors in the convection velocity of flowrate, proportional to $\sqrt{\Delta\rho}$, is somewhat more complex since 2 air density errors are involved. $\Delta\rho = \rho_2 - \rho_1$.

$$E_{\sqrt{\Delta\rho}} = \sqrt{(S_{\rho_1} E_{\rho_1})^2 + (S_{\rho_2} E_{\rho_2})^2} = \frac{1}{\sqrt{\Delta\rho}}\sqrt{(E_{\rho_1})^2 + (E_{\rho_2})^2}$$

$$e_{\sqrt{\Delta\rho}} = \frac{1}{\Delta\rho}\sqrt{(E_{\rho_1})^2 + (E_{\rho_2})^2} = \frac{1}{\Delta\rho}\sqrt{(e_{\rho_1}\rho_1)^2 + (e_{\rho_2}\rho_2)^2}$$

T_1	0	0	40	40	70	0
T_2	40	70	70	120	120	120
$e_{\sqrt{\Delta\rho}}$ %	2.43	5.24	13.1	23.4	36.7	15.5

As the temperature and or degree of saturation, relative humidity, are increased in one air space alone the potential for error in convection velocities and flowrates, by using the ideal gas density equation that neglects water vapor content, is increased. If the degree of saturation in both air spaces is similar the errors might tend to be self canceling.

Nomenclature

In the general subscripting convention used for characteristics of the two air spaces, separated by the partition containing the opening, 1 refers to the cool/dry side and 2 refers to the hot/moist side.

$\overline{\text{overbar notation}}$ - indicates an average value

Δ - prefix delta denotes a change or difference

NPL - the neutral pressure line, the vertical level where the pressure drop across the wall, between the two air spaces, is zero

P_n - the absolute pressure at the NPL

P_1 - the local pressure in air space 1

P_2 - the local pressure in air space 2

P_0 - water vapor pressure in air, depends on the air's dewpoint (saturation) temperature

H - the vertical height of a rectangular opening

W - the width of a rectangular opening

L - the length of the opening, duct, perpendicular to wall

A - area of opening = H x W

ρ - density of air, lbm/ft^3

w - humidity ratio of air, lbm water vapor/lbm dry air

t - time involved in rate of flow measurements, hours

T - temperature

$\dot{m}$ - mass flowrate, lbm/hour

$\dot{m}_{da}$ - mass flowrate of dry air

$\dot{m}_b$ - bulk mass flowrate , dry air water vapor mixture

$\dot{m}_{H_2O}$ - mass flowrate of water , liquid water into humidity generator

$\dot{m}_r$ - reverse mass flow, directed from space 2 to space 1

$\dot{m}'$ - normalizing parameter defined for opening and conditions, eq. (9)

$\dot{m}_{H_2O\ r}$ - reverse vapor mass flowrate through opening

$\dot{m}_{H_2O\ net}$ - net vapor mass flowrate through opening

$\dot{Q}$ - volumetric flowrate

D - diffusion coefficient

g - acceleration due to gravity

K - constant used in dimensionless group correlations determined experimentally

g_c - proportionality constant for units on g

D_h - hydralic diameter, 4 times the cross sectional area divided by the wetted perimeter

q - heat transfer through opening

m - vapor mass transfer through opening same as $\dot{m}_{H_2O\ net}$

h_q - convective coefficient of heat transfer, $h_q = q/W\ H\ \Delta T$

h_m - convective coefficient of water vapor mass transfer, $h_m = m/\ W\ H\ \Delta w$

V - velocity

V_b - bulk velocity through opening = $\dot{Q}/A$

V_s - velocity defined by Shaw[10] = $\left[g\ \frac{\Delta \rho}{\bar{\rho}} H - V_b^2 \right]^{\frac{1}{2}}$

C_p - specific heat of air

k - thermal conductivity

μ - dynamic viscosity

ν - kinematic viscosity

c - flowmeter constant = $\frac{\Delta P}{\dot{Q}^2 \bar{\rho}}$

C - coefficient of discharge flow through an orifice, opening

E - absolute value of expected error in a measured quantity

e - normalize fraction or percentage of error in a measurement

S - sensitivity of a quantity to an absolute errors partial derivative of dependent variable with respect to independent variable

s - sensitivity of a quantity to normalized errors partial derivative of dependent variable with respect to independent variable, times independent variable divided by dependent variable

Nomenclature (cont.)

Dimensionless Groups

Re - Reynold's number = $\bar{\rho} \frac{V_b D_h}{\mu}$

Rs - Reynold's number as defined by Shaw[10] = $\bar{\rho} \frac{V_s D_h}{\mu}$

Nu - Nusselt number = $\frac{h_q H}{k}$

Pr - Prandtl number = $\frac{\mu C_p}{k}$ a constant for air = 0.71

Gr - Grashof number = $g \Delta\rho H^3 / \bar{\rho} \nu^2$

Sh - Sherwood number = $\frac{h_m H}{D}$

Sm - Schmidt number = $\frac{\nu}{D}$

Sw - defined by Shaw = $\frac{Re^3 H^3}{Gr D_h^3} = \frac{\mu V_s^3}{\nu^2 g \Delta\rho}$

ACKNOWLEDGMENTS

I wish to express my appreciation to Dr. Byron W. Jones, my major advisor, whose ideas and planning made this thesis possible, to Dr. Herbert D. Ball, committee member, for criticism and as a source of motivation, and to Dr. Donald H. Lenhert, committee member, for his support and creative suggestions. I also thank Dr. B. Terry Beck for his assistance in reviewing literature sources.

VITA

Jean Paul Steele

Candidate for the Degree of

Master of Science

Thesis: WATER VAPOR TRANSPORT THROUGH AN OPENING IN A WALL BETWEEN TWO AIR SPACES AT DIFFERENT TEMPERATURES

Major Field: Mechanical Engineering

Biographical:

Personal Data: Born in Dodge City, Kansas, May 27, 1958, the son of Paul M. and Sharon M. Steele.

Education: Attended school in Colby, Kansas; graduated from Colby High School in January, 1976; received an Associate Arts degree from Colby Community Junior College in May, 1977; received a Bachelor of Science degree from Kansas State University, with a major in Mechanical Engineering, in December, 1979; completed requirements for a Master of Science degree, in Mechanical Engineering, in July 1981.

WATER VAPOR TRANSPORT THROUGH AN OPENING IN A WALL BETWEEN TWO AIR SPACES AT DIFFERENT TEMPERATURES

by

JEAN PAUL STEELE

B.S., Kansas State University, 1979

AN ABSTRACT OF A THESIS

submitted in partial fulfillment of the

requirements for the degree

MASTER OF SCIENCE

Department of Mechanical Engineering

KANSAS STATE UNIVERSITY
Manhattan, Kansas

1981

Abstract

The bulk of information within this thesis comes from experimental data taken using a specially constructed cubical chamber sealed air and water tight at all boundaries except for; an exit section in the ceiling through which variable measured amounts of air could be extracted, a water supply line for an air humidification system and a rectangular opening in one vertical wall. The chamber was equipped with a means to measure and control the temperature and humidity conditions of air within it and on the opposite side of the wall, containing the opening, was an equally sized cubical chamber whose air temperature and humidity conditions could also be measured and controlled independently of those within the sealed chamber.

By measuring the net flow of air leaving the sealed chamber through the exit section, and consequently the flow through the opening, as well as the temperatures and dewpoint temperatures of air on both sides of the opening and in the exit section, the water vapor carried into the sealed chamber, through the opening, and out through the exit section, by the net airflow could be determined. Using these and the flow rate of water, as liquid, into the sealed chamber to maintain humidity conditions a mass balance was used to calculate the water vapor carried out of the sealed chamber through the opening.

Temperature differences across the opening were varied from 0 to 70 F and humidity ratio difference was maintained around 0.0065 $\frac{\text{lbm}}{\text{lbm}}$. Airflows from zero to 40 cfm and openings with near zero thickness and dimensions of 6" x 6", 6" x 12", 12" x 6" and 12" x 12" were tested with subsequent tests of openings with thickness, perpendicular to plane of wall, and dimensions of 6" x 6" x 12" and 12" x 12" x 12".

A detailed description of the instrumentation and apparatus used is included and the data taken is graphed and compared with the developed theoretical ideal using a reduction scheme based on dimensionless mass flow rates.